Phenotypic analysis of *rumpshaker* mutation on two different genetic backgrounds

A thesis presented to the Faculty of Veterinary medicine, University of Glasgow

for the degree of

Doctor of Philosophy

July 2002

Khalid A. Al-Saktawi

ProQuest LLC.
789 East Eisenhower Parkway
P.O. Box 1346
Ann Arbor, MI 48106 – 1346

Abstract

rumpshaker (*rsh*) is a recessive X-linked point mutation (Ile^{186}Thr) which produces dysmyelination in the murine central nervous system. This study compared the behavioural and pathological aspects of the mutation on the C57BL/6 background (C57 *rsh*) to those on the C3H background (C3H *rsh*). C3H *rsh* is more mildly affected behaviourally and pathologically than C57 *rsh*. C3H *rsh* has normal longevity and is also able to reproduce successfully. In contrast, C57 *rsh* develops seizures at about postnatal day (P25) and dies between 4-5 weeks.

Both C3H *rsh* and C57 *rsh* fail to myelinate properly and develop dysmyelination in the CNS with the C57 *rsh* being more severely affected. This feature coincides with stages of active myelinogenesis. Western blot analyses strongly supports this finding as the levels of major myelin proteins are considerably reduced in the C57 *rsh* compared with C3H *rsh*.

There are significant differences between the mutants and their normal littermates on both genetic backgrounds and between the two mutants themselves. The total glial density is notably increased in the C57 *rsh* which is coupled with an increase in dead cells in the cervical spinal cord white matter. *In vivo* BrdU labelling shows that proliferation rates and the number of dividing cells are markedly greater in the C57 *rsh*. In spite of the differences between the two strains, C3H *rsh* and C57 *rsh* both maintain the numbers of oligodendrocytes. Nonetheless, the activated macrophage/microglial cells are more marked in C57 *rsh* CNS white matter than C3H *rsh*. Surprisingly, the actual number of astrocytes remained unchanged, however, their activation is represnted by an increase in GFAP, as shown by immunostaining and western immunoblotting.

This study suggests that there is no direct causal link between the dysmyelination and the oligodendrocyte number or even the death of oligodendrocye lineages. However, it provides evidence to support the notion that the severity of the disease correlates with the number of apoptotic cells, the reduced amount of myelin and the activation of microglia/macrophages.

While the *rsh* mutation on either genetic background is similarly heritable, the differences in phenotypes are likely attributable to differences in genetic background, thus suggesting the importance of modifying loci in determining the phenotype.

To my wife, Abdulrahman and faie

List of contents

List of tables

List of figures

Declaration

I, Khalid A. Al-Saktawi, do hereby declare that the work carried out in this thesis is original, was carried out by myself or with due acknowledgement and has not been presented for the award of a degree at any other university.

Acknowledgments

I would like to thank my supervisor, Professor Ian Griffiths, for guidance and continued support throughout this project. I would also like to thank Jennifer Barrie for her help and for having taught me various laboratory techniques; Dr Paul Montague for his advice and for having taught me molecular biological techniques and Dr Mark McLaughlin for having taught me Western blot technique. I appreciate the technical assistance and help from Malise McCulloch, Douglas Kirkham and Marie Ward. I thank Drs Christine Thompson, Demetrius Vouyiouklis, Julia Edgar and James Anderson for their advice and support.

I am very grateful to the Saudi Arabian Government for providing financial support for this study.

I would like to acknowledge Dr Mark McLaughlin who conducted the Western blots and supplied the images that have been presented in this thesis. Many of the immunostaining procedures have been performed by Jennifer Barrie.

I would also like to acknowledge the staff of the Animal House in Parasitology Unit and Veterinary Research Facility for caring for the animals used in this study.

The electron micrographs and some of the immunostaining images were taken by Professor Ian Griffiths. Some images in this thesis have also been taken by Alan May. Some images were scanned by Susan Cain. I appreciate the kind help from Professor Stuart Reid for statistical analysis.

I also thank the Professor Klaus-Armin Nave in Germany for establishing the *rumpshaker* mutation on C57BL/6NCrlBR background and donating this line of mice.

I would like to thank my wife and family for their kind and patient support as well as relatives and friends for their strong support and encouragement. Many thanks to Jaafer Falatah, Ali Ahmed, Dr. Abdulsalam Bakhsh, Jameel Gadhy, Osama and Omar Falatah; Saadiah, Kawther, Abdallah, Hamza, Baker and Mohammed Al-Saktawi for their help and support.

1. Introduction

1.1 Area of the study

The *rumpshaker* mutation causes a generalised defect of myelination throughout the CNS, although different regions show a variation in temporal change, consistent with the pattern of myelination. We chose to make the majority of our quantitative studies in the cervical spinal cord. This region was selected as it represents an area in which cell counts and myelin measurements can be performed accurately and is also a region that we have used frequently for study of normality and disease. Non-quantitative assessments of pathology were made in various brain regions.

1.2 CNS structure

The gross structure can be divided into the brain and spinal cord with the former being subdivided further. As the majority of this study is devoted to the spinal cord, this region will be emphasised. The spinal cord consists of the central grey matter and the peripheral white matter. The grey matter is subdivided into dorsal and ventral horns and intermediate regions although more complex laminar arrangements based on cytoarchitecture are also used. The grey matter contains the neuronal perikarya, glial cells and blood vessels. The white matter is classically divided into dorsal, lateral and ventral columns or funiculi. In normal mice, the white matter consists of myelinated fibres with occasional interspersed unmyelinated axons and the intervening neuropil of glial cells and blood vessels. The glial cells consist of the astrocytes and oligodendrocytes, which constitute the macroglia, and the microglia; undifferentiated glial progenitors are also present. A fine extracellular matrix also exists throughout the neuropil although this is difficult to visualise with most conventional staining methods.

1.3 Glial development

The origin of glial cells, mainly oligodendrocytes and astrocytes, has been proposed to be from a pool of neuroepithelial cells in the sub-ventricular zone of the developing spinal cord (Hirano and Goldman, 1988; Noll and Miller, 1993; Timsit

et al., 1995; Miller *et al.*, 1997; Chandross *et al.*, 1999) although the nature of the glial precursor cell(s) is still being debated. Several studies support the view that separate distinct precursors exist for oligodendrocytes and astrocytes (Phillips, 1973; Lord and Duncan, 1987; Parnavelas, 1999) although evidence for a common origin has been produced. Shortly after birth, cells can be classified into oligodendroblasts, astroblasts, and undifferentiated precursors (Prayoonwiwat and Rodriguez, 1993).

Waves of oligodendroglial progenitors migrate from the ventral zone and colonise the white matter tracts (Noll and Miller, 1993; Timsit *et al.*, 1995; Miller *et al.*, 1997). At a morphological level, light and dark oligodendrocytes have been described. The former proliferate before myelination and the later predominate at the stage of myelination (Arenella and Herndon, 1984; Lord and Duncan, 1987; Hirano and Goldman, 1988; Yoshida, 1997). Glial cell development and differentiation, however, are regulated through different factors (Scarlato *et al.*, 2000). Apoptosis which is a physiological phenomenon in normal development has been reported among these developing progenitors (Barres *et al.*, 1992).

1.4 The oligodendrocytes

1.4.1 Origin of oligodendrocytes

The issue of the origin of the founder precursor of oligodendrocytes remains controversial. It is accepted that in the spinal cord the oligodendrocyte lineage arises from the sub-ventricular zone in the ventral potion of the embryonic cord. Currently, the basic helix-loop-helix transcription factors Olig1 and Olig2 (Zhou *et al.*, 2000) together with Nkx2.2 (Xu *et al.*, 2000) define the earliest recognisable cells of the oligodendrocyte lineage (Wegner, 2001; Woodruff *et al.*, 2001). The majority of early oligodendrocyte progenitors express the alpha receptor for platelet-derived growth factor A (PDGFRα), which has been used as a marker for these cells (Pringle and Richardson, 1993; Nishiyama *et al.*, 1996; Hall *et al.*, 1996) and the myelin protein 2′3′-cyclic nucleotide 3-phosphodiestersae (CNP) (Yu *et al.*, 1994). A small, and possibly distinct, sub-population express the DM20 isoform of PLP and lack the PDGFRα (Timsit *et al.*, 1995; Dickinson *et al.*, 1996; Spassky *et al.*, 1998; Spassky *et al.*, 2000). Still later in development, progenitors express NG2 proteoglycan (Nishiyama *et al.*, 1996), a marker that also exists on adult progenitor cells.

Sonic hedgehog (shh) has been shown to specify a common precursor for oligodendrocytes (Richardson *et al.*, 1997). The use of retroviral lineage marker has

provided excellent evidence for the precursors of oligodendrocyte lineages in the brain (Small *et al.*, 1987; Leber *et al.*, 1990; Levison and Goldman, 1993; Levison *et al.*, 1993).

All these markers strongly support the notion that oligodendrocytes are descendants of genetically similar precursors.

1.4.2 Differentiation and development

Oligodendrocyte progenitors arise from the neuroectoderm in the subventricular zone, then migrate and differentiate into mature myelin-forming cells.

Considering the fact that these processes occur at specific times, a number of cell specific markers have been used to divide the lineage into distinct phenotypic stages. These stages are pre-GD3 stage, pro-oligodendroblast stage, and immature oligodendrocyte stage (Pfeiffer *et al.*, 1993). Certain mitogens such as PDGF (Miller *et al.*, 1989) or FGF (McKinnon *et al.*, 1993), and IGF(McMorris *et al.*, 1993) influence these cells, so they progressively change their morphology. It is obvious from *in vivo* and *in vitro* studies that neuronal influences play a critical role in oligodendrocyte differentiation, proliferation and survival (Barres and Raff, 1993). In addition, thyroid hormone can regulate and promote early oligodendrocyte differentiation (Rodríguez-Peña, 1999). In contrast, retinoic acid (RA) has been found to inhibit oligodendrocyte differentiation as well as proliferation (Noll and Miller, 1994). The pattern of development and differentiation in tissue culture is thought to broadly mimic that *in vivo*.

1.4.3 Morphology

Light microscopy reveals only some aspects of oligodendrocyte morphology. The oligodendrocyte nuclei appear smaller, regular and more chromophilic than astrocyte nuclei (Peters *et al.*, 1976). On the basis of ultrastructural morphology, three subtypes of differentiated oligodendrocytes have been defined in white matter, consisting of light, medium, and dark cells (Mori and Leblond, 1970). In general, oligodendrocytes possess a well developed rough endoplasmic reticulum (RER) and free ribosomes together with prominent Golgi apparatus. Microtubules are also a prominent feature. The electron density of the cytoplasm increases with maturity while the prominence and complexity of the cell's processes decreases as active myelination abates.

1.4.4 Oligodendrocyte markers

The establishment of antigenic cell type-specific surface markers facilitates the recognition of differentiated cells at different developmental stages. In other words, undifferentiated progenitor cells give rise to oligodendroblasts, which mature into oligodendrocytes and they begin a sequential expression of specific antigens, which are later inserted into myelin membranes at different times and rates.

Rapidly dividing progenitor cells stain positively by a variety of antibodies such as A2B5 (Raff *et al.*, 1983) and undergo differentiation *in vitro* into oligodendrocytes or astrocytes, depending on the medium. As these early progenitors mature, they become O4+ cells (Sommer and Schachner, 1981) and divide more slowly (Dubois-Dalcq, 1987). Before these progenitors acquire galactocerebroside (GC) and sulphatide (Bansal *et al.*, 1992; Berry *et al.*, 1992) they express coincidently O4 and proligodendroblast antigen (POA) that binds to an antibody AOO7 (Bansal *et al.*, 1992). At this stage of development, oligodendrocytes express certain antigens for instance sulphatide and seminolipids (Bansal *et al.*, 1992).

The antigenic definition of an oligodendrocyte is the expression of GC (Raff *et al.*, 1983). The traditional view, based largely on tissue culture is that expression of CNP appears concurrently with GC (Knapp *et al.*, 1988) followed by myelin-associated glycoprotein (MAG) as well as myelin basic protein (MBP) and one or two days later by PLP (Knapp *et al.*, 1987). However, more recent *in vivo* studies show that both CNP and the DM20 isoform of PLP are present in progenitors, prior to GC expression (Scherer *et al.*, 1994; Dickinson *et al.*, 1996; Spassky *et al.*, 1998).

In cultured cells diffusely distributed MBP can be seen throughout the cell bodies and processes (Dubois-Dalcq *et al.*, 1986; Konola *et al.*, 1991). A week later, fine grains of MBP staining are seen also in sheets surrounded by loops of processes (Dubois-Dalcq *et al.*, 1986; Konola *et al.*, 1991). MAG is confined to the perinuclear cytoplasm initially (Dubois-Dalcq *et al.*, 1986). PLP is initially present in the perinuclear region as granular shaped deposits (Dubois-Dalcq *et al.*, 1986; Konola *et al.*, 1991). By two weeks it is detectable in the processes (Dubois-Dalcq *et al.*, 1986; Konola *et al.*, 1991). Moreover, MBP and PLP are differentially located; MBP is present in membranous sheets of mature oligodendrocytes whereas PLP/DM20 is mainly detected along the course of the cell processes (Konola *et al.*, 1991). Finally, CNP is mainly located in the networks of processes and in the periphery of sheets (Knapp *et al.*, 1987; Konola *et al.*, 1991). Of the "O" group of antibodies, the O10 and O11 define the most mature oligodendrocytes (Kuhlmann-Krieg *et al.*, 1988). Strikingly, the "O" group of antibodies (Kuhlmann-Krieg *et al.*,

1988) is consistent with the electron microscopic study regarding light to medium oligodendrocytes (Mori and Leblond, 1970). Stages of oligodendrocyte development and differentiation are shown in (Figure 1, page 22).

1.4.5 Myelination

Myelination commences at appropriate times of development in different regions of the nervous system. The initiation of myelination, however, commences just before birth in the mouse and is completed postnatally. During myelination, oligodendrocytes, the myelinogenic cells of the CNS, elaborate numerous processes that extend to reach axons and begin to ensheath in spiral patterns (Hahn *et al.*, 1987). It has been noted that myelination first starts at cervical levels of the spinal cord and subsequently extends in a rostrocaudal direction, as well as in a caudal to rostral direction through the brain (Schwab and Schnell, 1989). In general, myelination occurs in the ventral regions of the spinal cord and brain before the more dorsal regions. Even within regions there may be considerable differences in the timing of myelination; for example, between the fasciculus gracilis and the fasciculus cuneatus.

A heterogeneous population of white matter oligodendrocytes has been described, ranging from those that myelinate a single large diameter axon in a fashion similar to Schwann cells in PNS (type IV) to those ensheathing multiple small diameter fibres (types I & II) (Del Rio Hortega, 1921; Remahl and Hildebrand, 1990). Type III cells myelinate only a few large diameter axons. Oligodendrocytes, therefore, can be classified into at least two distinct subpopulations accordingly to the number and diameter of fibres they support (Butt *et al.*, 1995). Molecular differences also exist between oligodendrocyte populations; for example with transferrin (Espinosa de los Monteros and Vellis, 1990), carbonic anhydrase II (Butt *et al.*, 1995) and small MAG (S-MAG) (Butt *et al.*, 1998). Surprisingly, it has been reported in higher vertebrates that heparan sulphate proteoglycans (HSPGs) may define the myelinogenic phenotype of oligodendrocyte populations (Szuchet *et al.*, 2000). During the active stages of myelination, immunocytochemistry has revealed that MBP appears prior to PLP. Moreover, large diameter fibres have higher MBP and less PLP than small diameter fibres and, vice versa (Hartman *et al.*, 1982). It could be concluded that molecular structure of myelin does not play a critical role in determining axonal sizes (Norton and Cammer, 1984). Nonetheless, a more recent report using transplantation supports the idea that each oligodendrocyte has the inherent potential to myelinate any calibre of axon (Fanarraga *et al.*, 1998).

1.4.6 Adult oligodendrocyte progenitors

The greatest number of oligodendrocyte progenitor cells exists during the period of normal myelination in the perinatal period. Such cells have been termed perinatal progenitors and, when cultured, were often referred to as oligodendrocyte-type 2 astrocyte (O-2A) progenitors (see 1.7, page 7). The presence of progenitors in the adult CNS is now established. They were originally identified in culture and exhibited some differences from their perinatal counterparts, such as longer cell cycle times and lower migratory capacity (Wolswijk and Noble, 1989; Wolswijk *et al.*, 1990; Wren *et al.*, 1992). More recently, NG2 has been used to identify the adult progenitor cells *in vivo* and the use of this marker has revealed a highly developed network of such cells (Nishiyama *et al.*, 1999).

Although not directly concerned with the work in this thesis, a highly topical area concerns the presence of adult neural stem cells which can be isolated and driven to differentiate into neurons and glia (Frisén *et al.*, 1998; Bjornson *et al.*, 1999; Doetsch *et al.*, 1999; Laywell *et al.*, 2000). In fact, under some circumstances the oligodendrocyte precursors can be induced to revert to multipotential stem cells (Kondo and Raff, 2000).

1.5 The astrocytes

Morphologically, there are two classical types of astrocytes, protoplasmic and fibrous, the later being more abundant in CNS white matter. However, using a variety of molecular criteria it is evident that there is marked inter- and intraregional heterogeneity of astrocytes. It is generally accepted that within the CNS glial fibrillary acidic protein (GFAP) is a specific marker for astrocytes in health and disease states (Bignami *et al.*, 1972). Astrocytes extend processes to the surface of the CNS and to the perivascular space forming a glial limiting sheath (Meier and Bischoff, 1975; Miller and Raff, 1984) and to nodes of Ranvier (ffrench-Constant *et al.*, 1986). Although originally thought of as having purely a structural role, it is now evident that astrocytes have a complex functional inter-relationship with neurons and oligodendrocytes. Ascribed functions include maintenance of ion homeostasis, uptake and recycling of neurotransmitters, modulation of synaptic activity, synthesis and release of neurotransmitters and propagation of calcium waves (Bezzi and Volterra, 2001). The proposed functions are indicative of the importance of astrocytes in the CNS.

Astrocytes are also able to secrete factors, such as PDGF-A, bFGF and IGF-1 that promote oligodendrocyte mitosis, migration and survival (Bhat and Pfeiffer, 1986; McMorris and Dubois-Dalcq, 1988; Richardson *et al.*, 1988; Noble *et al.*, 1988;

Rosen *et al.*, 1989). Astrocytes also promote adhesion of oligodendrocyte processes to axons (Meyer-Franke *et al.*, 1999).

1.6 The microglia

The microglia are the resident macrophages of the CNS. They colonise the CNS early in development, originating from the yolk sac (Alliot *et al.*, 1999). The resident microglial population is renewed from the circulating pool of monocytes. In normal CNS development, they play important roles, thereby eliminating debris (Perry and Gordon, 1988; Stoll and Jander, 1999). The density of microglia is higher in the neonate declining after birth and then increasing again in older animals. Following disease or injury there is a rapid increase in microglia/macrophage cells due to proliferation of endogenous cells and recruitment of circulating cells. The contribution played by circulating cells varies with different insults. Microglia display surface antigens common with vascular system macrophages.

1.7 Oligodendrocyte type-2 astrocyte

The O-2A progenitors derived their name from the their ability to differentiate into oligodendrocytes or type 2 astrocytes, depending on the tissue culture medium. They appear however, to be a peculiarity of *in vitro* situations and, with a few exceptions in experimental studies, are not found *in vivo*. As they are not relevant to the thesis, they will not be discussed further.

1.8 The axon

The axons are unique processes, which project from neurones. They have relatively few organelles compared with the soma or dendrites and lack a Golgi apparatus and rough endoplasmic reticulum. The axon consists of the cytoskeleton and axoplasm surrounded by the axolemma (Peters *et al.*, 1976). The neurofilaments and microtubules form the main components of the cytoskeleton but there is also a well-developed microtubular network and numerous interlinking molecules, such as spectrin. Membranous structures include mitochondria, the axoplasmic reticulum (which is an extension of the smooth ER of the cell body), vesicles and various endosomal components. The axon and its axolemma show considerable regional specialisation at the nodes, paranodes, juxtaparanodes and the internode, which forms the greatest part of the axon's length.

The axon has two main functions, the propagation of impulses and the transport of materials in both retrograde or anterograde directions (Hirokawa, 1993). Impulse conduction initiates in the initial axon and, in myelinated axons, progresses in a salutatory manner. This form of conduction is dependent on the ion channel specification at nodes and adjacent paranodes/juxtaparanodes. In unmyelinated and dysmyelinated or demyelinated axons, conduction is continuous in keeping with the more even and continuous distribution of ion channels.

1.9 The axoglial interaction

There is an intimate relationship between the axon and its associated oligodendrocyte in which the development and well-being of each depends critically upon the other. During development axons influence the proliferation, differentiation and survival of oligodendrocyte lineage cells (Barres and Raff, 1993; Barres and Raff, 1994; Barres and Raff, 1999). Several growth factors, such as PDGF-A and neuregulin, which are derived from axons, promote mitosis and/or cell survival (Yeh *et al.*, 1991; Canoll *et al.*, 1996; Flores *et al.*, 2000). Electrical activity of axons is also proposed to influence oligodendrocyte mitosis and myelination (Barres and Raff, 1993; Demerens *et al.*, 1996; Zalc and Fields, 2000). Axons guide migration of neurons and glia (Leber and Sanes, 1995) and may also secrete factors, such as jagged, that inhibit oligodendrocyte differentiation (Wang *et al.*, 1998) through notch activation. Axons influence the expression of myelin genes in oligodendrocytes (McPhilemy *et al.*, 1990; Kidd *et al.*, 1990; McPhilemy *et al.*, 1991) and have been recognised for many years as necessary for the maintenance of the myelin sheath.

The role of oligodendrocytes in promoting the differentiation of the axolemma has been known for over 20 years (Bray *et al.*, 1981; Oldfield and Bray, 1982). Recently some of the molecular mechanisms have become clearer. The organisation of axolemmal molecules at the node, paranode and juxtaparanode depends on both secreted factors and myelination (Kaplan *et al.*, 1997; Rasband *et al.*, 1999a; Rasband *et al.*, 1999b; Popko, 2000; Trapp and Kidd, 2000; Tait *et al.*, 2000; Kaplan *et al.*, 2001; Pedraza *et al.*, 2001). In some instances the specific oligodendrocyte molecules have been identified that are critical for the correct organisation of the axolemma. For example, absence of GC, the major glycolipid, results in absence of the transverse bands and a redistribution of contactin and Kv channels along the internode (Dupree *et al.*, 1998a; Dupree *et al.*, 1998b; Popko, 2000).

Oligodendrocytes also influence the formation of the cytoskeleton and axonal transport. The neurofilaments and microtubule composition and their phosphorylation status and hence the axonal diameter is dependent upon the oligodendrocyte, although there is some debate as to whether myelin formation per se is necessary (Sánchez *et al.*, 1996; Brady *et al.*, 1999; Witt and Brady, 2000; Sánchez *et al.*, 2000; Kirkpatrick *et al.*, 2001). One interesting aspect relevant to this thesis is the role that myelin mutants have played in elaborating some of the above hypotheses.

1.10 Myelin sheath

Two highly specific glial cells, the oligodendrocytes in the CNS, and the Schwann cells in the PNS, are responsible for the formation of compact myelin. The mature myelin-forming cell processes rotate around axons making up successively spiral layers from which the cytoplasm is extruded to form the compact sheath. Structurally, the myelin sheath is made up of a phospholipid bilayer that contains intrinsic and extrinsic proteins.

When viewed by conventional transmission electron microscopy, the myelin sheath shows a pattern of dark and lighter bands at a regular periodicity of approximately 11nm (This varies according to fixation and the thickness of the myelin sheath). The thicker, darker line is the major dense line (MDL) formed by fusion of the cytoplasmic surfaces of the oligodendrocyte processes. The less electron dense line is actually a double line, separated by a 2-3nm gap and is the intraperiod line (IPL). This is formed by the close apposition of the extracellular surfaces of adjacent lamellae. The thickness of sheath varies in relation to the axonal calibre. It is not unusual to have small regions of uncompacted processes within a compact sheath; while this is common in developing animals it may also be seen in mature mice.

1.11 Lipid composition in myelin

The lipid component is a major constituent making up about two thirds of solid matter of myelin (Norton and Cammer, 1984). It comprises galactosphingolipids including GC and sulphatides, cholesterol, and plasmalogen (Hildebrand *et al.*, 1993). These lipids are also not restricted to myelin. Within the CNS, GC is unique to oligodendrocytes, which makes it an excellent surface marker for these cells (Raff *et al.*, 1978).

Although myelin has minor galactolipids, half of which consist of several fatty acid esters of cerebroside, and the other half of two glycerol-based lipids,

diacylglycerylglacoside, called collectively glacosyldiglyceride. The biosynthesis of these glycerol derivatives is coincidentally related to myelination (Norton and Cammer, 1984). Myelin also contains a little phosphatidylinositol that binds tightly to myelin proteins. Ethanolamine phosphoglyceride, the most abundant phospholipid, is located exclusively in the inner half of the bilayer. Moreover, the non-significant myelin lipids include di-and tri-phosphoinositide, a series of fatty acid esters of cerebroside, at least three galactosyldiglyceride derivatives, a series of gangliosides and some alkanes.

1.12 Myelin proteins

1.12.1 Myelin-associated glycoprotein (MAG)

MAG, the major myelin glycoprotein, belongs to the immunoglobulin gene superfamily. It constitutes 1% of the total myelin protein in both central and peripheral nervous system (Quarles *et al.*, 1992). MAG has two developmentally-regulated isoforms of relative molecular mass 72 and 67 kDa, known as large and small MAG (L-MAG, S-MAG). The *Mag* gene expression is earlier in development than the major myelin protein genes, *Plp* and *Mbp*. Surprisingly, the MAG protein is absent in the compact myelin sheath but localises to the periaxonal space, paranodes and mesaxons in the CNS (Trapp and Quarles, 1984); and, additionally, Schmidt-Lanterman incisures in PNS. The functions that have been proposed for MAG include the adhesion of the myelin membrane with axon (Trapp and Quarles, 1984) and maintaining the periaxonal cytoplasmic collar of the inner Schwann cell and oligodendrocyte. MAG has also been proposed to act as a signal transducer between axon and glial cells through an interaction with an, as yet unidentified, sialoprotein (Tang *et al.*, 1997; Strenge *et al.*, 1998). Recently, MAP1B has been identified as an axonal binding partner for MAG (Franzen *et al.*, 2001). MAG is also relevant to axonal regeneration, having a repellent activity in the adult CNS (Qiu *et al.*, 2000). Surprisingly MAG null mutations show a minimal phenotype with only subtle changes in the periaxonal space and occasional double myelin sheaths in the CNS (Li *et al.*, 1994; Montag *et al.*, 1994).

1.12.2 2′,3′-cyclic nucleotide 3′-phosphodiesterase (CNP)

Two isoforms (46 and 48 kDa) have been reported for the enzyme CNP that catalyse the hydrolysis of several 2 ,3 –cyclic nucleoside monophosphates. They represent about 5% of the total myelin proteins (Lemke, 1988; Kurihara *et al.*, 1992). In CNS, CNP is localised in the oligodendrocyte plasma membrane and non-compacted parts of myelin sheath such as paranodal loops, adaxonal cytoplasm,

outer tongue processes and Schmidt-Lanterman incisures (Trapp *et al.*, 1988). These proteins are expressed at an early stage of development (Trapp, 1990), suggesting a role for CNP in myelination and myelin maintenance together with stabilising membrane components, although currently no precise function has been ascribed.

1.12.3 Myelin basic protein (MBP)

MBP denotes several differentially spliced isoforms having slightly different low molecular weights (14, 17.5, 18 and 21.5kDa) (Norton and Cammer, 1984; Ferra *et al.*, 1985; Aruga *et al.*, 1991). MBP isoforms, which account for 30% of the total myelin proteins, are hydrophilic, extrinsic membrane proteins with isoelectric points at 10.5. During myelination, *Mbp* gene expression occurs early among the other myelin genes in CNS (Kanfer *et al.*, 1989). In the CNS, antibodies stain specifically the compact myelin (Sternberger *et al.*, 1978; Hartman *et al.*, 1982). In contrast to MAG and PLP, MBP is localised mainly at the major dense line (MDL) of the compact myelin (Omlin *et al.*, 1982). The role of MBP in maintaining the MDL (Omlin *et al.*, 1982; Readhead *et al.*, 1987) is seen obviously in *Mbp* mutant *shiverer* mice in which the cytoplasmic surfaces of the lamellae fail to fuse, forming a double MDL. Furthermore, MBP is critical for elaboration of normal amounts of myelin as in its absence only small numbers of thin sheaths are formed.

1.12.4 Other CNS myelin proteins

Other proteins have been characterised and many, no doubt, are still to be defined. Examples of such proteins are myelin-oligodendrocyte glycoprotein (MOG) (Linington *et al.*, 1984), myelin-oligodendrocyte-specific protein (MOSP) (Dyer, 1993), myelin-associated oligodendrocytic basic protein (MOBP) (Yamamoto *et al.*, 1994) (Montague *et al.*, 1997), oligodendrocyte-myelin glycoprotein (OMGP) (Mikol *et al.*, 1993) and oligodendrocyte specific protein (OSP), also known as claudin-11 (Bronstein *et al.*, 1996; Morita *et al.*, 1999; Gow *et al.*, 1999).

1.12.5 The *proteolipid protein* gene: structure and function

1.12.5.1 Chromosomal locus of *PLP/DM20* gene

The single copy *PLP* gene maps on the X-chromosome (at Xq21.33-22 in man) (Willard and Riordan, 1985; Mattei *et al.*, 1986). This critical gene encodes the two classical integral membrane protein isoforms, PLP and DM20.

The murine *Plp* gene is defined by a DNA region approximately 17 kb in length which constitutes seven, possibly eight, exons and seven introns (Macklin *et al.*, 1987; Bongarzone *et al.*, 1999) (Figure 2, page 23). It also contains two

transcription units (Macklin *et al.*, 1987; Bongarzone *et al.*, 1999). Moreover, the *Plp* gene primary transcript is alternatively spliced to produce PLP and DM20 and the recently described somal-restricted isoforms (srPLP and srDM20) (Bongarzone *et al.*, 1999; Bongarzone *et al.*, 2001). "Classical" PLP is 30kDa and DM20 is 26kDa. The *Plp* gene demonstrates heterogeneity at the 5′ non-coding region of the transcription unit (Milner *et al.*, 1985; Macklin *et al.*, 1987) and also uses three alternative polyadenylation sites thus generating different message sizes (Milner *et al.*, 1985; Gardinier *et al.*, 1986; Macklin *et al.*, 1987). Heterogeneity of the transcripts as a matter of function is obscure. However, tissue specific expression would be the possibility for the multiple mRNAs.

1.12.5.2 Expression of *Plp* gene

Given the possibility for selective transcripts, it is interesting to compare spatio-temporal expression between *Plp* and *Dm20*. As early as embryonic day 10 (E10) *Dm20* mRNA is expressed in murine CNS whereas *Plp* mRNA is not detectable at this stage of development. By approximately birth, *Plp* transcripts are detectable, correlating with the onset of myelination (Verity and Campagnoni, 1988). At the stage of most active myelination the *Plp* isoform expression is reaching its peak (Verity and Campagnoni, 1988). Furthermore, *Plp* and *Dm20* mRNAs are concentrated in the oligodendrocyte cell body and expressed at relatively high levels even in the mature CNS (Amur-Umarjee *et al.*, 1990). The DM20 protein can be recognised at approximately E12 (Dickinson *et al.*, 1996) in the mouse spinal cord in cells having characteristics of oligodendrocyte progenitors. The PLP protein is localised in the compact myelin in adult CNS.

The *Plp* gene is expressed in a diverse array of tissues throughout development, rather than solely in the oligodendroglial lineage. For example, DM20 is present in both myelinating and non-myelinating Schwann cells where it is localised to cytoplasmic regions and is not generally seen in PNS myelin (Griffiths *et al.*, 1995). In addition, DM20 is detectable in the perineuronal satellite cells of spinal cord, cranial and autonomic ganglia, and in the ensheathing cells of the olfactory nerve layer of the olfactory bulb (Dickinson *et al.*, 1997). The C6 glioblastoma line (Nave and Lemke, 1991) as well as cardiac myocytes express the endogenous *Plp* gene (Campagnoni *et al.*, 1992). The significance of the *Plp* gene expression in the non-myelinating cells is not clear but its expression during gestation leads to the suggestion that the *Plp* gene may have a role in development.

1.12.5.3 Transcriptional control of *Plp* gene

Like other cellular and viral genes, *Plp* gene is transcribed by RNA polymerase II. The mRNAs encoding PLP are highly abundant in adult CNS and *Plp* gene regulation occurs predominantly at the level of transcription (Cook *et al.*, 1992). *Plp* gene modulation occurs in different ways including adjustment of *Plp*:*Dm20* mRNA ratio, stabilisation of mRNA, the turnover of mRNA, protein translation and degradation, and post-translation modification (Cambi and Kamholz, 1994). Analysis of the 5′ region of the *Plp* gene has demonstrated multiple *cis* regions capable of binding *trans* factors (Hudson *et al.*, 1996; Wegner, 2000).

Regulatory elements in the 5′ non-coding region and possibly intron 1 of the *Plp* transcription unit contain positive and negative *cis*-acting elements that are recognised by trans-acting factors (Wight and Dobretsova, 1997; Dobretsova and Wight, 1999; Dobretsova *et al.*, 2000). There is speculation that the *Plp* gene promoter modulates tissue specific expression (Nave and Lemke, 1991; Cambi and Kamholz, 1994).

Additional factors have been proposed to act either positively or negatively on *Plp* gene transcription. However, the presence of a thyroid hormone response element located in the 5′ region and exon 1 suggests transcriptional and post-transcriptional control (Gao *et al.*, 1997). Retinoic acid has also been shown to increase mRNA half-life (Zhu *et al.*, 1994). Unusually, steroids influence gene expression negatively *in vivo* (Tsuneishi *et al.*, 1991) and positively *in vitro* (Zhu *et al.*, 1994). Components of the nervous system such as axons induce signals that regulate expression of the *Plp* gene (Kidd *et al.*, 1990; Scherer *et al.*, 1992).

1.12.5.4 Post-transcriptional control

Use of two alternate splice sites, one internally in exon 3 and the other at the 3′ exon/intron boundary, generates *Dm20* and *Plp* mRNAs, respectively from the primary transcript. *Dm20* mRNA differs from the *Plp* mRNA only by deletion of 115 nucleotides that comprise exon 3B. Both sites display highly sequence similarities with U1 small nuclear ribonucleoproteins (U1snRNP) that form an RNA duplex with the 5′ splice site, an early regulatory event in the formation of the spliceosomes (Montague and Griffiths, 1997). A selectively functional site is recognised according to the relative and absolute amounts of SR proteins, possibly contributing to the cell specificity (Zahler and Roth, 1995). During early development in the murine embryo, *Dm20* mRNA is expressed predominantly although its significance at this stage is unknown.

1.12.5.5 Translation and post-translational modification

The *Plp* and *Dm20* mRNAs are translated on the RER and the proteins delivered through the secretory pathway via the Golgi apparatus, cytoplasmic vesicles, to the final destination, the plasma membrane (Gow *et al.*, 1994a). It has been suggested that developing oligodendrocytes reserve these proteins for a time prior incorporation into myelin sheath (Dubois-Dalcq *et al.*, 1986). Furthermore, the trafficking mechanism is associated with the micro-tubular apparatus and is also in partnership with other myelin components (Brown *et al.*, 1993).

Two post-translational modifications occur for PLP and Dm20; the deletion of the N-residue from both proteins (Milner *et al.*, 1985) and subsequent acylation of the cysteine residues (Weimbs and Stoffel, 1992). Like many membrane proteins, PLP and DM20 have no cleaved amino terminal signal. Strikingly, the minor srPLP and srDm20 isoforms do have a cleaved sequence encoded by exon 1.1 (Bongarzone *et al.*, 1999).

1.12.5.6 Topology of the PLP/DM20 protein

Despite other proposal models for the membrane topology of the PLP protein based on mathematical modelling, chemical labelling, limited protease digestion, and immunolabelling, the most generally accepted is the model proposed by Popot *et al.*, (1991) and Pham-Dinh *et al.*, (1991) (Figure 3, page 24). The PLP (but not DM20) protein isoform is an extremely hydrophobic and highly charged membranous protein in the CNS (Weimbs and Stoffel, 1992). It can thus be inferred that the DM20 protein may adjust a proper topological orientation to suit its function.

1.12.5.7 Conservation of the *Plp* gene

At least five mammalian species (mouse, rodent, dog, bovine, and human) display considerable amino acid sequence similarities of PLP. The similarity of amino acid sequences between human and rodent reaches 100% whereas in the dog it is 99% and in the bovine 97% (Milner *et al.*, 1985; Macklin *et al.*, 1987). Nonetheless, the sequence similarity moves to the non-coding and non-transcribed regions of the *Plp* gene. There is approximately 93% and 86 % similarities in the 5′-UTR and 3′-UTR, respectively, between human and rodent (Roth *et al.*, 1986). Again, human and rodent show highly conserved regions at the cap sites of the 5′-UTR (Macklin *et al.*, 1987). Recently, it has been shown that the similarity extends to the 5′ flanking sequence of the *Plp* gene (Montague and Griffiths, 1997). An extreme conservation of amino acid sequence (see above) suggests a very strong association between the primary structure and the function of the PLP.

1.12.5.8 The *DM* gene family

Based on the sequence similarities, other members of the so-called *DM* gene family have been identified in mammals and lower organisms. Two membrane proteins termed M6a and M6b (Yan *et al.*, 1993), are expressed in the CNS, the former being restricted to neurons (Yan *et al.*, 1996) and Muller glial cells (Mi *et al.*, 1998). M6a is also expressed in non-neural tissues such as apical surface of choroid plexus, renal tubules and olfactory epithelium. M6b is expressed in oligodendrocytes and neurons (Yan *et al.*, 1996). Both M6a and M6b are glycoprotein in nature. Moreover, three DM20-like molecules termed DMα, DMβ, and DMγ have been identified in shark and high similarities are noted between DMα and mammalian DM20 (Kitagawa *et al.*, 1993). DMα and DMγ are expressed in myelinated tracts of shark CNS. M6a is closely similar to DMβ.

1.12.5.9 Proposed functions of the *Plp* gene

The well-defined functions of PLP and DM20 are only partly resolved. The proposed functions have been derived largely from study of *Plp* gene mutants showing hypomyelination and abnormal periodicity, and, more recently, from gene knockouts. In both *Plp* null animals and those with missense mutations there are abnormalities of the IPL. This feature, therefore, suggests a structural role for PLP in maintaining the IPL of the compact myelin (Duncan *et al.*, 1987; Boison and Stoffel, 1994; Boison *et al.*, 1995; Rosenbluth *et al.*, 1996; Klugmann *et al.*, 1997; Yool *et al.*, 2002). Additionally, the formation of homophilic or heterophilic interaction between PLP and DM20 proteins at the extracellular regions of the molecules may possibly reflect adhesive peculiarities (Sinoway *et al.*, 1994).

The expression of *Dm20* mRNA early in development in the CNS and non-neural tissues suggests other functions for the *Plp* gene products apart from the structural role (Timsit *et al.*, 1992). Spontaneous mutations of the *Plp* gene result in increased numbers of dead oligodendrocytes (Knapp, 1996), leading to the suggestion that the *Plp* gene may be involved in the regulation of glial development and differentiation. *In vitro* studies demonstrate that a released *Plp* gene product may act as a mitotic factor that increases astrocyte and oligodendrocyte numbers (Yamada *et al.*, 1999). However, *Plp* null mice appear to have normal numbers of oligodendrocytes (Yool *et al.*, 2001). There is also a suggestion that PLP and DM20 may form pores in the membrane that act as proton translocation units (Helynck *et al.*, 1983). The *DM* gene family show high similarities to documented receptor proteins, strengthening the possibility for their role in permeability of the myelin membrane (Kitagawa *et al.*, 1993).

More recent studies in PLP-deficient mice and humans suggests a role for PLP/DM20 in oligodendrocyte/axon inter-relationships. In the absence of these oligodendrocyte proteins, axons develop multiple swellings, possibly reflecting defects in axonal transport. There is also a late-onset degeneration of the distal regions of long axons such as those in the fasciculus gracilis and corticospinal tracts (Griffiths *et al.*, 1998; Garbern *et al.*, 2002).

1.12.5.10 *Plp* gene mutations and disease

A range of species (mouse, rat, rabbit, dog, and human) display myelin defects as a result of spontaneous mutations of the *Plp/PLP* gene.

1.12.5.11 *PLP* gene-related disorders in man

Pelizaeus-Merzbacher Disease (PMD) and X-Linked Spastic Paraplegia Type 2 (SPG2) are two human syndromes caused by various mutations or dosage changes of the *PLP* gene.

1.12.5.12 Pelizaeus-Merzbacher Disease (PMD)

Pelizaeus and Merzbacher first described PMD in 1885 and 1910, respectively. The proposed classification of the disease into three forms is based on familial and unfamilial PMD, together with the severity. These are classical (type I), connatal or congenital (type II) and transitional forms (type III) (Seitelberger *et al.*, 1996). Clinically, the disease shows devastating symptoms and signs include nystagmus, delayed psychomotor development, spasticity, cerebellar ataxia, optic atrophy, laryngeal stridor, seizures, and mental retardation that often results in premature death of the patients (Hodes *et al.*, 1993; Seitelberger, 1995). The neuropathological criteria in PMD consist of hypomyelination of CNS especially in areas that myelinate relatively late, for instance the cerebellar and cerebral parts. The hypomyelination may be diffusely generalised or show a "tigroid" appearance where small islands of myelin are present. Oligodendroglial cells are reduced in number while astrocytes are markedly increased. In contrast to males, who mainly contract the disease, females are only sporadically affected by clinical PMD.

1.12.5.13 X-Linked Spastic Paraplegia Type 2 (SPG2)

SPG 2 is allelic to PMD. It is defined as a rare disorder that can be clinically classified into the pure form and the complicated form. In patients with the pure form, spasticity of the lower limbs is the dominant feature whereas other signs such as cerebellar ataxia, sensory loss, nystagmus, optic atrophy and mental retardation are present in the complicated form. Both PMD and SPG2 share similarities and

there is considerable overlap. Females from affected families act as asymptomatic carriers (Saugier-Veber *et al.*, 1994). The lesions of the disease are confined mainly to the CNS white matter, especially the long spinal tracts which are critically affected (Seitelberger, 1995).

In general, mutations of the *PLP* gene rarely affect the PNS. However, peripheral neuropathy has been documented in patients with null mutations of the *PLP* gene (Garbern *et al.*, 1997).

1.12.5.14 Molecular genetic basis of *PLP* gene mutations in humans

Genetic mechanisms may govern the severity of the disease phenotypes in many ways. The majority of patients with PMD/SPG2 have a duplication of a region of the X chromosome containing the *PLP* locus (Harding *et al.*, 1995; Hodes and Dlouhy, 1996; Sistermans *et al.*, 1996; Sistermans *et al.*, 1998). There is variation of the size and position of the duplicated region (Woodward *et al.*, 1999; Woodward *et al.*, 2000; Hodes *et al.*, 2000) which may account, at least in part, for the variability in phenotype.

Point mutations in the *PLP* gene mutations account for the majority of remaining PMD and SPG2 patients (Hudson *et al.*, 1989; Trofatter *et al.*, 1989; Gencic *et al.*, 1989). Genetic heterogeneity of PMD among patients is clearly noted with different families displaying a variety of point mutations leading to different amino acid substitutions (Trofatter *et al.*, 1989). Most of these point mutations are confined to the coding regions of the *PLP* gene; however, other mutations in non-coding regions are also reported. It has been suggested that some PMD families may have mutations in non-transcribed regulatory regions (Cambi *et al.*, 1996; Inoue *et al.*, 1997). Some of these mutations result in protein truncation or aberrant splicing or even conservative amino acid substitution that have little effect on protein conformation. The PLP protein seems to be intolerant to structural changes. The high conservation of the wild type PLP protein suggests a mechanism for protein-protein interaction but in most mutants this relationship is potentially altered due to the change in the amino acid sequence.

Mild PMD phenotypes have also been reported resulting from *PLP* gene deletion (Raskind *et al.*, 1991; Osaka *et al.*, 1996) or null mutations (Garbern *et al.*, 1997).

New mutations of the *PLP* gene are being described frequently; an up to date database is maintained at:- http://www.med.wayne.edu/Neurology/plp.html

1.12.5.15 *Plp* gene mutations in animals

Spontaneous mutations in the *Plp* gene are described in a wide range of species that includes mouse, rat, dog, and rabbit (Figure 4,page 25). In the *jimpy* (Plp^{jp}) mouse, a mutation at the 3′ splice site of intron 4 leads to the deletion of exon 5 from the *Plp* gene final transcript (Nave *et al.*, 1987; Hudson *et al.*, 1987). Unlike the *jimpy* mouse, various point mutations result in amino acid substitutions in *jimpy-4j* ($Plp^{jp\text{-}4j}$) (Pearsall *et al.*, 1997), *myelin synthesis deficient* ($Plp^{jp\text{-}msd}$) (Gencic and Hudson, 1990), and *rumpshaker* ($Plp^{jp\text{-}rsh}$) mice (Schneider *et al.*, 1992), the *myelin deficient* rat (Boison and Stoffel, 1989), *shaking pup* (Nadon *et al.*, 1990), and *paralytic tremor* rabbit (Tosic *et al.*, 1994).

Most mutants start to show obvious tremor between 10-12 days in mouse and the more severe phenotypes such as *jimpy* and the *myelin deficient* rat often seizure between 3 and 4 weeks of age and die prematurely at around P30. Exceptionally, the *paralytic tremor* rabbit and mild form of *rumpshaker* show less severe phenotypes and affected males are able to reproduce. As they age, both mutants show slight progression in myelination (Taraszewska, 1988; Tosic *et al.*, 1996). The interesting fact in the *Plp* gene mutants is that Schwann cells and the myelin sheaths are apparently normal.

1.12.5.16 Phenotypic characteristics of *Plp* gene mutations in animals

The common feature among these mutants is dysmyelination, which is characterised by hypomyelination and abnormal myelin. Many axons are naked or ensheathed only with one or two wraps of oligodendrocyte processes. Any myelin sheaths tend to be disproportionately thin for the calibre of axon. The severity of the myelin deficit varies considerably between different mutations.

In mice, the most affected are the *jimpy* and *jimpy-4j* which develop a severely hypomyelinated phenotype (Sidman *et al.*, 1964; Vela *et al.*, 1998) with abnormally thin myelin sheaths (Ransom *et al.*, 1985; Billings-Gagliardi *et al.*, 1995; Duncan, 1995) and poorly compacted, ultrastructurally-abnormal myelin (Duncan *et al.*, 1987; Billings-Gagliardi *et al.*, 1995). The double IPL is completely fused to a single electron-dense structure. As a result the myelin periodicity decreased from 11 nm in the wild type to 9 nm in the mutants (Duncan *et al.*, 1987).

Compared with *jimpy*, the mild form of *rumpshaker* is an example of moderate dysmyelination. As *rumpshaker* mice age, they show reduced tremor and an increased amount of myelin (Fanarraga *et al.*, 1992). A heterogeneous population of myelin sheaths is reported, some have normal periodicity and others have fused IPL (Griffiths *et al.*, 1990).

Mutations in the *Plp* gene appear to affect the oligodendroglial lineage differently. Mutants such as *jimpy*, *jimpy-4j*, *myelin synthesis deficient* mice and *myelin deficient* rat show a severe reduction in the number of mature oligodendrocytes in older mice (Billings-Gagliardi *et al.*, 1995; Knapp, 1996). Strikingly, immature oligodendrocytes are not affected in these mutants (Ghandour and Skoff, 1988; Skoff, 1995; Nadon and Duncan, 1996; Gow *et al.*, 1998; Lipsitz *et al.*, 1998; Grinspan *et al.*, 1998). An increased glial cell proliferation has also been noted in *jimpy*, the *myelin deficient* rat and the *shaking pup* (Knapp *et al.*, 1986; Jackson and Duncan, 1988; Duncan, 1990). There is no increased cell death recorded among the *shaking pup* oligodendrocytes. However, these oligodendrocytes fail to mature and further myelinate the CNS (Nadon and Duncan, 1996). The premature death of oligodendrocytes is also suggested in *jimpy* (Meier and Bischoff, 1975; Privat *et al.*, 1982; Knapp *et al.*, 1986; Knapp *et al.*, 1990; Skoff and Knapp, 1990) and the *myelin deficient* rat (Jackson and Duncan, 1988; Boison and Stoffel, 1989). Oligodendrocyte numbers are normal in the *paralytic tremor* rabbit and the mild form of *rumpshaker* (Griffiths *et al.*, 1990; Schneider *et al.*, 1992).

Distension of the RER is clearly seen in the *shaking pup* and the *myelin deficient* rat (Dentinger *et al.*, 1982; Duncan *et al.*, 1983; Jackson and Duncan, 1988). Moreover, a moderate swollen rough endoplasmic reticulum has been reported in oligodendrocytes of the *myelin synthesis deficient* mice (Billings-Gagliardi *et al.*, 1983). Using immunocytochemistry, the RER, but not the Golgi apparatus or cell surface, is positively stained for PLP/DM20 (Roussel *et al.*, 1987; Gow *et al.*, 1998). It could be concluded that the transport of PLP/DM20 is altered and may be the result of misfolding (Jung *et al.*, 1996). The absence of swollen RER, in particular in *jimpy*, suggests a quick turnover of misfolded proteins. DM20 protein levels are maintained in both *rumpshaker* and *paralytic tremor* rabbit compared with control and the protein is successively incorporated into myelin sheath (Griffiths *et al.*, 1990; Mitchell *et al.*, 1992; Karthigasan *et al.*, 1996). However, a little mutated PLP is accumulated in the RER in the rabbit mutant (Karthigasan *et al.*, 1996).

The severity of astrocytosis (Billings-Gagliardi *et al.*, 1995; Duncan, 1995) also varies between mutants.

1.12.5.17 Female carriers of *Plp* gene mutations

Males are usually affected by X-linked diseases whereas females, bearing the affected allele, seldom show the disease phenotype. The X-chromosome inactivation, which is a normal event in each somatic cell, occurs in females. For instance, female mice heterozygous for the *jimpy* gene show a mosaic population,

some of oligodendrocytes express the wild type *Plp* allele and the others express the *jimpy* allele. This could explain the premature death of some oligodendrocytes (Kagawa *et al.*, 1994), while the cells that escape this fate form considerable myelin (Skoff and Ghandour, 1995). In addition, occasional patches of dysmyelination are also seen, which are more likely to be formed by oligodendrocytes bearing the *jimpy* allele. The disappearance of dysmyelinating patches suggests a compensation role by oligodendrocytes carrying the wild type *Plp* allele (Bartlett and Skoff, 1986; Skoff and Ghandour, 1995). The early death of *jimpy* oligodendrocytes and processes of compensation may have impact in controlling apparent clinical signs in female carriers (Belmont, 1996).

Amazingly, females with an affected allele can develop clinical phenotypes based on skewing of X-inactivation phenomenon (Willard, 1995). In this context, females bearing the *shaking pup* allele may represent skewing of the X-inactivation since several phenotypes of varying degree are observed (Cuddon *et al.*, 1998). The phenotype varies not only between different mutations of the *Plp* gene but also within heterozygotes for the same mutation. Dysmyelinated patches are seen frequently in the optic nerves of *jimpy* mice, *myelin-deficient* rat and *shaking pup* but only in the last mutant are spinal cord patches a regular feature.

Two phenotypes, juvenile-onset (Hodes *et al.*, 1995; Hodes *et al.*, 1997) and adult-onset (Nance *et al.*, 1996), are described in female carriers of PMD.

1.12.5.18 *Plp* null mice (gene knockout)

Null mice, lacking PLP and DM20, provide a useful model to test the normal cellular function of PLP. Two lines of mice have been generated using different targeting strategies (Boison and Stoffel, 1994; Klugmann *et al.*, 1997). *Plp* null mutants develop normally without any of the clinical signs of naturally occurring dysmyelinated mice, for example *jimpy*. Oligodendrocytes appear normal and produce thick myelin sheaths. However, the structure of the myelin sheath is abnormal with regions of "loose" myelin and areas of compacted myelin. Abnormally condensed IPL are noted in these mice (Rosenbluth *et al.*, 1996; Klugmann *et al.*, 1997) and also regions in which no IPL is evident (Yool *et al.*, 2002). Demyelination is not detected, even at the age of two years. Both PLP and DM20 appear unnecessary for oligodendrocyte survival and myelin formation; however the presence of these proteins does confer an advantage when *Plp* null oligodendrocytes are in competition with wild type cells (Yool *et al.*, 2001). Axonal swellings, containing mainly membranous organelles and mitochondria, are associated with small axons. The swellings are found from about P40 in the optic nerve. These swellings, therefore, suggest defects in axonal transport. Late-onset

degeneration of long spinal tracts occurs from the age of about 8 months onward and exhibits a length-dependent progression (Griffiths *et al.*, 1997; Garbern *et al.*, 2002). It has been speculated that the axonal swellings are specific to the absence of PLP/DM20 (Griffiths *et al.*, 1998).

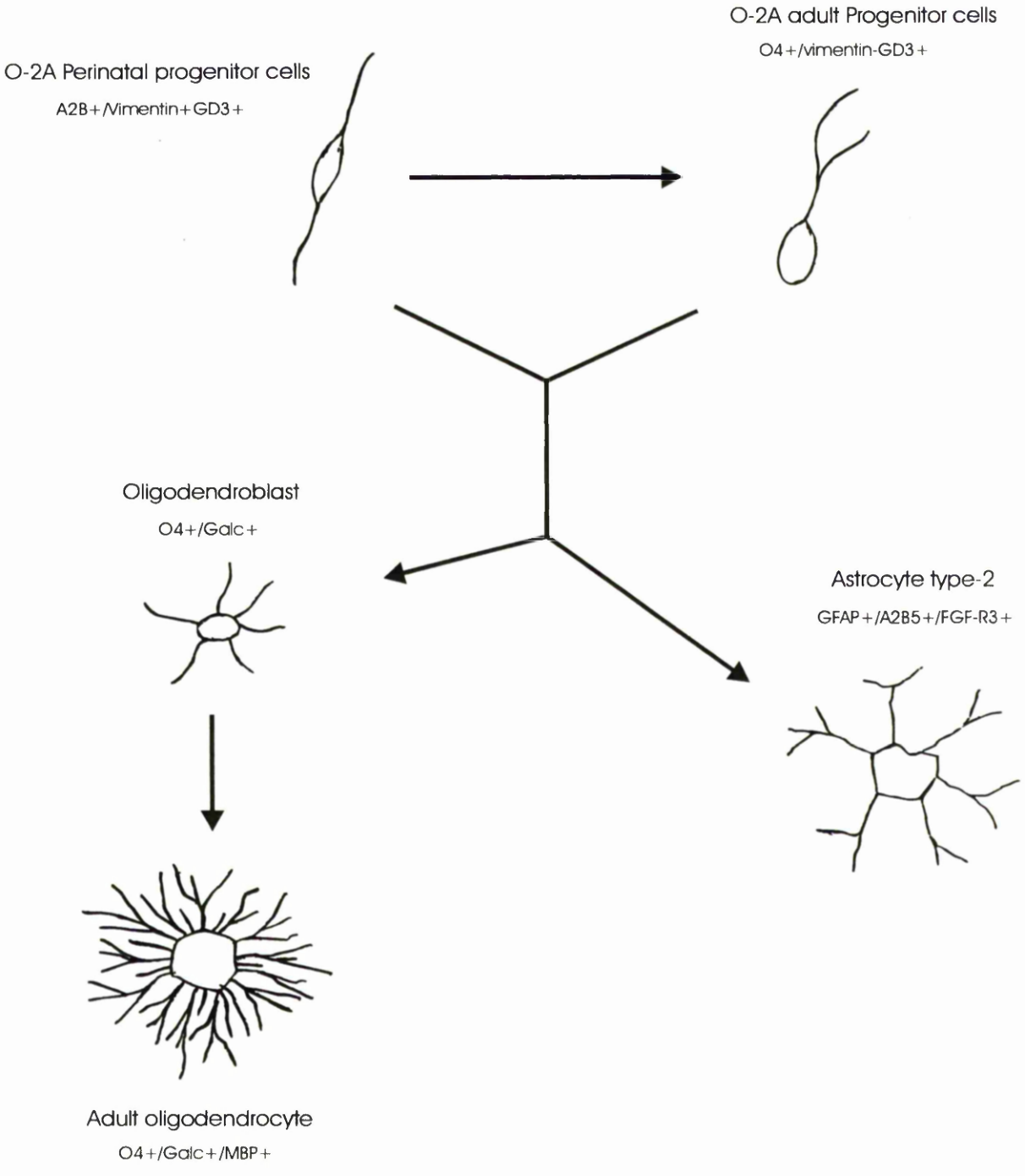

Fig. 1. Oligodendrocyte development and differentiation in the murine CNS (modified from Lee J. C. et al., 2000). O-2A cells develop into oligodendrocytes and astrocyte type-2. O-2A ^{perinatal} progenitors derive into either a differentiated progeny or different precursor cells present in the adult. The differentiation into adult oligodendrocytes is a process represented by expression of specific marker(s). Some of these markers are given beside each stage of differentiation.

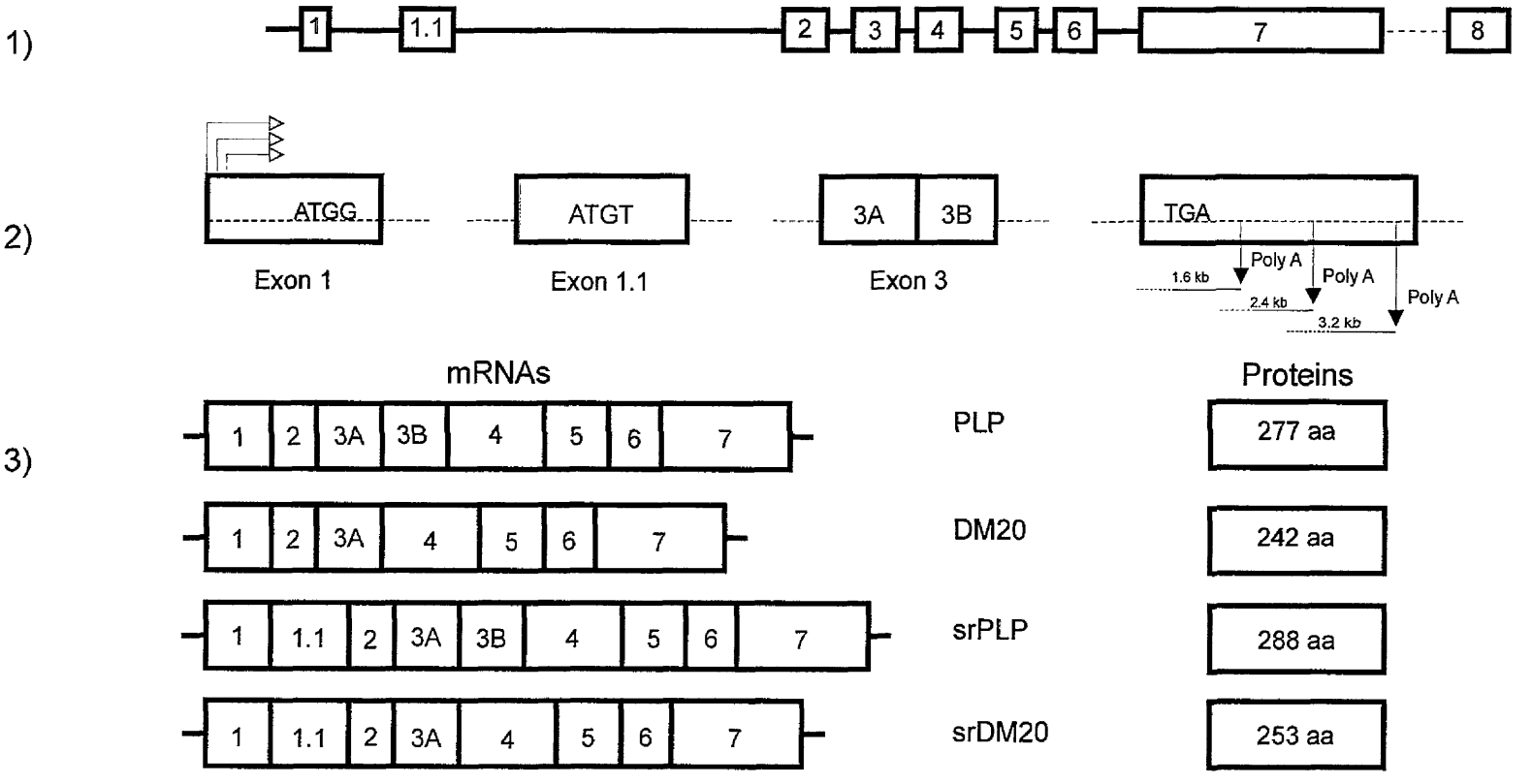

Fig. 2. Physical map of the murine *Plp* gene and its transcripts (adapted from Griffiths *et al.*, 1995 and Bongarzone *et al.*, 1999).
1) Gene structure showing seven exons or possibly eight, 17 kb in length, (hatched boxes).
2) There are 3 transcription start sites (red arrows), one alternative splice site within exon 3 giving rise to synthesis of *DM20* and three Polyadenylation sites are shown in exon 7 (Blue arrows), giving rise to the 3 sizes of mRNA.
3) On the left, the exonic compositions of the *PLP* mRNAs are shown. To the right of mRNAs are diagrams of the protein products corresponding to each of the mRNAs and the number of amino acids (aa) in the protein.

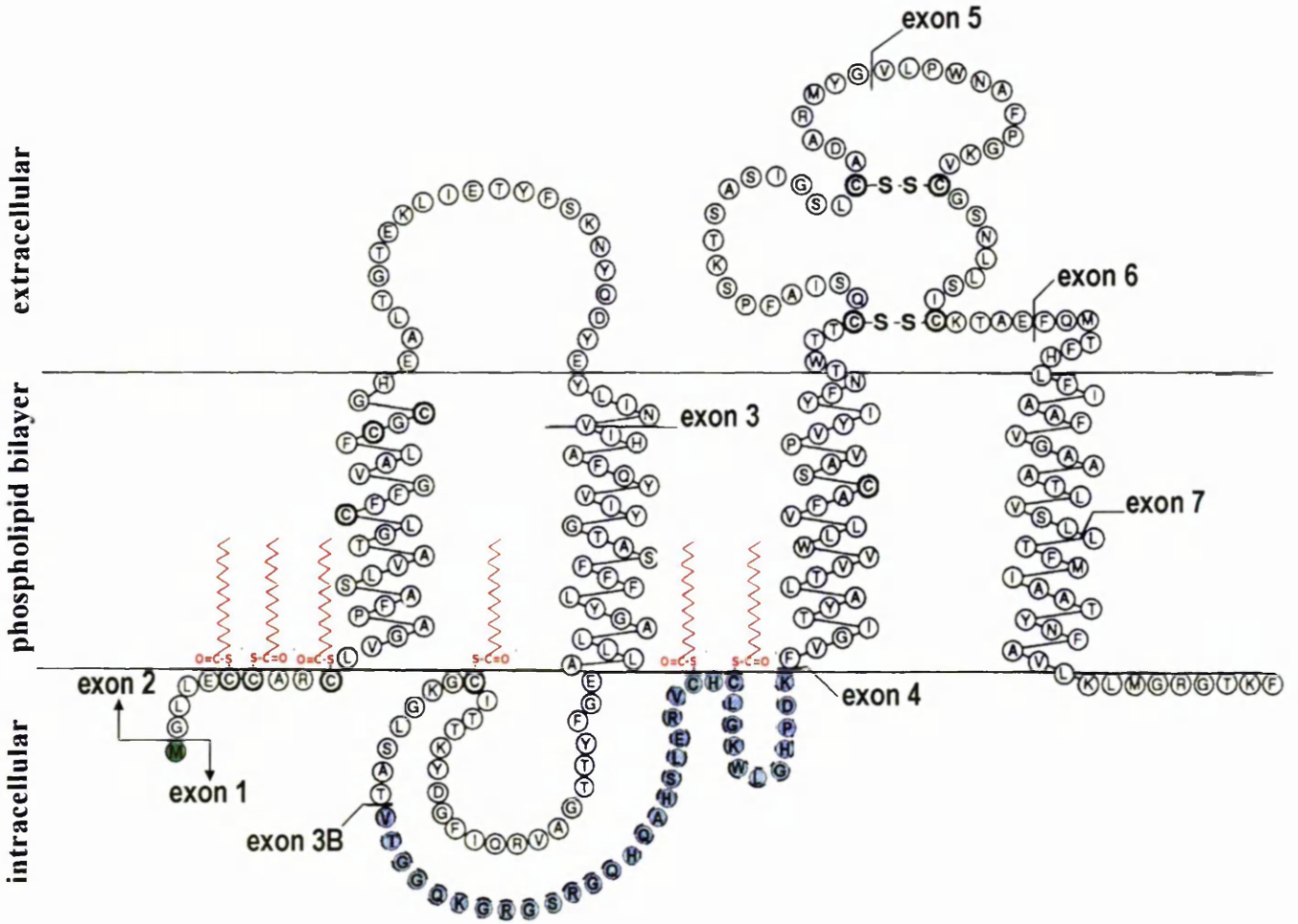

Fig. 3. Amino acid sequence of the murine PLP in the myelin membrane (adapted from Weimbs and Stoffel 1992). Within the protein, six cysteine residues act as acylation sites for long chain fatty acids (shaded red) and two disulphide bonds in the third extramembranous loop place marked constraints on protein topology. The 35 amino acid sequence deleted in DM20 is indicated by bars (shaded blue). The first methionine residue of the amino terminus (shaded green) is cleaved before protein incorporated into myelin.

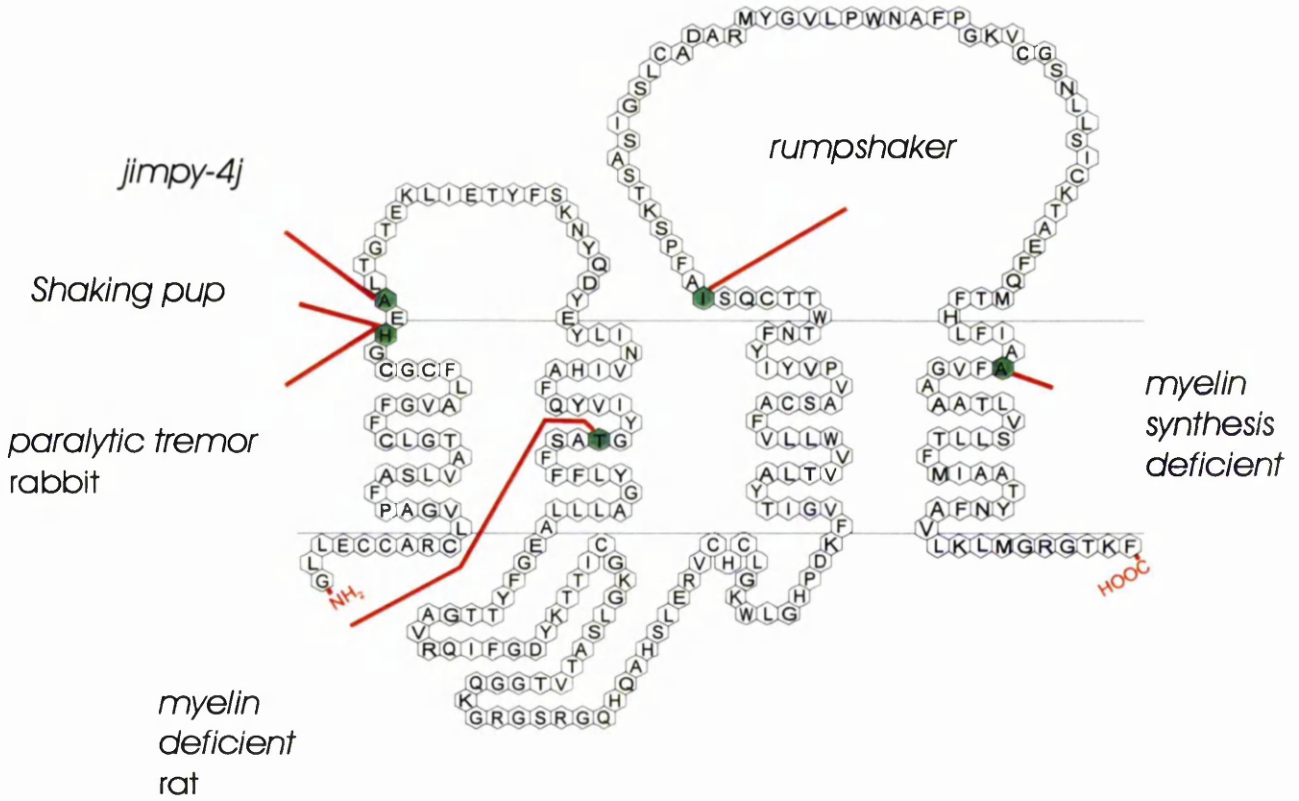

Fig. 4. Regions of point mutations in the animal PLP. Amino acid transitions resulting in neurological disorders are highlighted green.

2. Aims

Mutations of the *PLP* gene have heterogeneous phenotypes. The severity can range from early lethal forms of Pelizaeus-Merzbacher Disease to the mildly affected form "spastic paraplegia type 2".

Likewise, the *rumpshaker* mutation on C3H/101 and C57BL/6NCrlBR backgrounds shows mild and severe phenotypes, respectively, which hopefully, provide an authentic model for PMD and SPG2. The focus of this study was to compare the phenotypes of *rumpshaker* on the two different genetic backgrounds. The approach work was designed to cover the life-span of the severe phenotype of the mutation, which is about 30 days. The mutant and the littermate control animals from both genetic backgrounds were investigated histopathologically at various ages to quantify various parameters linked to the development and the progression of the neurological manifestation. These included myelin status and behaviour of the glial population. Immunohistochemistry was used to confirm the results obtained from examining resin sections and finally, levels of selected myelin proteins and GFAP were quantified on Western blotting. Comparing the two mutants may provide new fundamental information that allows a better understanding of diverse phenotypes in PMD and SPG2.

3. Material and methods

3.1.1 Mouse breeding and gene nomenclature

Mice were maintained at Glasgow Parasitology Unit and Veterinary Research Facility, University of Glasgow Veterinary School. The mice were housed with free access to regular laboratory diet, at constant temperature and humidity, during the entire experiment. All experimentation reported in this thesis was conducted on neural tissues obtained from only male mice.

Two strains (C57BL/6NCrlBR (abbreviated to C57) and C3H/101 (abbreviated to C3H)) of mice were used for the current work. C57 mice were obtained from a colony maintained at Zentrum fur Molekulare Biologie (ZMBH), Universitat Heidelberg, Im Neuenheimer Feld 282, D-69120 Heidelberg, Germany and established from the original C3H *rumpshaker* mice which were discovered and maintained at Glasgow University Veterinary School. A genetic nomenclature of normal and some mutant alleles are illustrated in Table 1, page 27.

All studies were perfomed under licence from the Home Office (project # 60/2077).

Table 1. Genetic nomenclature of normal and mutant alleles

Alelle	**Gene symbol**
wild type (WT)	*Plp*
rumpshaker	$Plp^{jp\text{-}rsh}$
rumpshaker male	$Plp^{jp\text{-}rsh}$/y
rumpshaker heterozygote	$Plp^{jp\text{-}rsh}$/+
rumpshaker homozygote	$Plp^{jp\text{-}rsh}/Plp^{jp\text{-}rsh}$
jimpy	Plp^{jp}
jimpy male	Plp^{jp}/y
jimpy heterozygote	Plp^{jp}/+

3.1.2 Rotarod

Mice were placed, facing the opposite direction to the operator, on the Rotarod (UGO BASILE) with the speed at rest. When the drive is activated, the rod slowly accelerates to reach the maximum speed (30rpm). At first the mice were given 2-3 conditional trials to familiarise them with the rod and then four actual tests followed. After each task, the mice were rested for 10-15 minutes. The mean was calculated for the four readings.

3.1.3 Growth/Weight of mice

After killing, the mice were immediately weighed and then perfused or dissected for fresh cryopreservation. The weight gain is, in general, an indicator of development.

The two basic factors responsible for the pattern of growth and adult size of animals are its inherited characteristics and the environment. Some of these factors may have significant effects on weight gain such as age, size of litter, etc.

3.1.4 5-bromo-2′-deoxyuridine (BrdU) labelling

Mice were injected intraperitoneally with BrdU in 0.9% sterile saline (50 μg/g of mouse body weight, Sigma) at midday. After one hour, the mice were sacrificed and then perfused or the neural tissues were deeply frozen for cryopreservation.

3.2 Isolation and quantification of nucleic acids

3.2.1 Tail biopsy

1 cm of the tip of the tail was removed from mice anaesthetised with halothane (Rhone-Poulenc Chemicals Ltd) in aseptic manner and the wound was cauterised. The part of the tail was cut into 2 mm pieces before placing in a labelled Nunc Cryotube (GibcoBRL) and rapidly frozen in liquid nitrogen and stored at –20°C.

3.2.2 Extraction of genomic DNA (gDNA) from mouse tails

3.2.2.1 Use of Wizard Genomic DNA Purification Kit

For each sample, 120 μl of 0.5M EDTA solution (pH 8.0) was added to 500 μl of Nuclei Lysis Solution (Promega) in a universal tube and chilled on ice. Tissue samples were lysed overnight at 55°C in 600 μl 0.5M EDTA/ Nuclei Lysis Solution containing 58 $\mu g.ml^{-1}$ proteinase K (see 3.2.2.2, page 29). The samples were centrifuged and transferred to clean tubes. A volume of 200 μl Protein Precipitation Solution were added to the samples, vortexed and chilled on ice for 5 minutes. The

mixtures were centrifuged at high speed for 4 minutes. The supernatants containing the DNA (leaving the protein pellets behind) were carefully transferred to clean tubes containing 600 µl of isopropanol (Sigma) at room temperature. These solutions were gently mixed by inversion until the white thread-like strands of DNA formed a visible mass. The solutions were centrifuged at high speed for 1 minute and small white DNA pellets were formed. The supernatants were decanted and 600 µl of 70% ethanol, room temperature, were added to wash the DNA by inverting the tubes several times and centrifuged at high speed for 1 minute. The ethanol was aspirated and the DNA pellets were left in the tubes. The tubes were inverted on clean absorbent paper and air-dried for 30 minutes. The DNA pellets were rehydrated by addition of 200 µl DNA Rehydration Solution (Promega) overnight at 4°C. The DNA was stored at 4°C.

3.2.2.2 Preparation of Proteinase K

Proteinase K was supplied as a lyophilised powder (Promega). It was reconstituted in 50mM Tris-HCl, pH 8.0, 10mM $CaCl_2$ and stored at –20°C in 20 µl aliquots.

3.2.3 Quantification and standardisation of nucleic acids

3.2.3.1 Quantification of nucleic acids

Samples of gDNA were quantified with a GeneQuant RNA/DNA calculator (Pharmacia Biotech) using a 100 µl spectrophotometer cell.

3.2.3.2 Dilution of nucleic acids

Nucleic acid samples were diluted to working concentration with sterilised dH_2O. A concentration of 50 ng μl^{-1} was used to dilute gDNA for PCR analysis.

3.2.4 Nucleic acid electrophoresis

3.2.4.1 Agarose gels

DNA analysis was performed on 0.7-3% agarose gels in a Tris acetate ethylene-di-amine-tetra-acetate (TAE) buffer (see 6.1.7.5, page 120). The gDNA was electrophoresed through a 0.7% agarose gel (Figure 5, page 47) and the PCR products on 2-3%.

Gels were cast from ultrapure electrophoresis grade agarose (GibcoBRL) and melted in TAE buffer. Ethidium bromide (from a stock of 1 $mg.ml^{-1}$) was added to cool gel to give a final concentration of 0.5 $\mu g.\ ml^{-1}$. Samples were loaded with a 6x gel-loading buffer. Gels were electrophoresed in TAE buffer.

3.2.4.2 Imaging and photography of Gels

Gels were visualised using a "Fotoprep I" ultraviolet (UV) transilluminator (Fotodyne Inc.) and Photographed with a Polaroid MP4 land camera (Polaroid) on Polaroid 667 (ASA 3000) film through a Wratten 22A filter (Kodak) or a Kaiser RA1 CCD camera and UP-890CE Video graphic thermal printer (Sony).

3.3 PCR genotyping

3.3.1 PCR programme

Reaction tubes were submitted to initial cycle (3 min denaturing at 94°C, 1 min annealing at 55°C, 4 min extension at 72°C), 35 core cycles (40 sec at 93°C, 1 min at 55°C, 2 min at 72°C) and final cycle (40 sec at 93°C, 1 min at 55°C, 5 min at 72°C) in a Techne PHC-3 thermocycler.

3.3.2 PCR conditions and *Acc*I restriction

The DNA fragment including the *rumpshaker* region was amplified by PCR, using primers α-intron 3 and α-intron 4 sequenced C (5-CATCACCTATGCCCTGA-3) and D (5-TACATTCTGGCATCAGCGCCAGAGACTGC-3), respectively (Schneider *et al.*, 1992). The reaction was performed in 25 µl containing 0.4 µM of each primer, 0.2 mM dNTPs, 2.5 units of *Taq* polymerase (Promega) with the manufacturer's ammonium buffer, 1.5 mM $Mgcl_2$ and 50 ng of DNA extract. This was overlaid with 50 µl of molecular biology grade mineral oil (Sigma) to prevent evaporation. The digested gDNA samples were stored at 4°C until further analysis. PCR products were pipetted beneath the oil layer and run on 2% agarose gels.

For the *Acc*I restriction (Schneider *et al.*, 1992), 9 µl of PCR product were added to 6 µl of sterile dH_2O containing 10 units restriction enzyme *Acc*I and 10x buffer, and this mix was incubated at 37°C for 2-3 hours. Restricted DNA fragments and control (undigested PCR products) were run on 3% agarose gel (Figure 5, page 47).

Positive and negative controls were included with each set of samples. A control reaction was also included with the sample omitted and replaced by sterilised dH_2O to ensure that there were no contaminating nucleic acids.

3.4 Tissue fixation

3.4.1 Fixatives

3.4.1.1 Karnovsky's modified fixative (Paraformaldehyde/Glutaraldehyde 2%/5%)

This fixative (Griffiths *et al.*, 1981) was used for the preservation of tissues prepared for resin embedding for the light and electron microscopy. Fixed tissues were stored at 4°C until processed. (For preparation see 6.1.3.1, page 110).

3.4.1.2 4% Paraformaldehyde

4% paraformaldehyde in phosphate buffered saline (PBS) was used for the preservation of tissues intended for immunohistochemistry. After fixation, tissues were post-fixed in the same fixative for 3-6 hours and then transferred to 20% sucrose in PBS for 24 hours and rapidly frozen. (For preparation see 6.1.3.2, page 111).

3.4.1.3 Periodate-lysine-paraformaldehyde (PLP) fixative

P-L-P fixative (McLean and Nakane, 1974) was used for the preservation of tissues destined for immunohistochemistry, especially for staining microglia. After fixation, tissues were post-fixed in the same fixative for 3-6 hours and then transferred to 20% sucrose in 0.1 M phosphate buffer for 24 hours and rapidly frozen. (For preparation see 6.1.3.3, page 111).

3.4.1.4 Buffered neutral formaldehyde (4%BNF)

BNF fixative was used for the preservation of tissues for paraffin embedding and subsequently used for immunohistochemistry and routine haematoxylin and eosin (H&E) staining. BNF fixed tissues were stored at room temperature until processed. (For preparation see 6.1.3.4, page 111).

3.4.2 Fixation techniques

Mice were humanely euthanased using an overdose of carbon dioxide or halothane in a closed chamber. The carcass was then pinned on a wooden board. The chest was also opened and the pericardium was removed. To flush the vasculature, the right atrium was punctured to allow drainage; a needle was inserted into the left ventricle and PBS was injected under moderate pressure. Once the effluent was clear, the fixative was injected. Between 100 ml and 200 ml of fixative was injected, depending on the age of the mouse. After fixation the animal was left in

fixative for up to 3 hours before dissection. The brain, optic nerves and spinal cord were removed, cut into appropriate blocks, placed in fixative and stored until processing.

3.5 Tissue processing and sectioning

3.5.1 Paraffin wax processing and sectioning

BNF-fixed tissues for paraffin wax embedding were processed using a Shandon Elliot automatic tissue processor (Histokinette). These tissues were passed through different graded dehydrating solutions (see 6.1.4.1, page 112) and blocked out with wax at 60°C. 8μm sections were cut on a Biocut 2035 microtome (Leica), mounted onto APES-coated slides (see 6.1.1, page 110) and placed in the oven at 56°C overnight.

3.5.2 Resin processing and sectioning

Tissues for Araldite resin embedding were processed using a Lynx *el* microscopy tissue processor (Leica). The tissues were passed through different graded alcohols (see 6.1.4.2, page 113) and infiltrated with resin. For blocking out, the tissues were oriented in resin-filled rubber moulds and placed in the oven at 60°C overnight for polymerisation. Using an Ultracut-E ultratome (Reichert-Jung), 1μm sections were cut with a glass knife from resin blocks and mounted on glass slides for light microscopy while 70nm sections were cut with a diamond knife and mounted on 200-mesh 3.06mm-diameter copper grids for electron microscopy.

3.5.3 Cryopreservation and sectioning

Freshly dissected tissues and tissues fixed with P-L-P fixative or 4% paraformaldehyde were suspended in Tissue-Tec O.C.T compound (Miles Inc) and frozen in isopentane cooled in liquid nitrogen. The frozen blocks were wrapped with NescoFilm (Bando Chemical Ind. Ltd.) and stored at -20°C. 15μm sections were cut using an OTF cryostat (Bright Instrument Company) and mounted onto APES-coated slides (see 6.1.1, page 110) and stored at -20°C.

3.6 Staining techniques

3.6.1 Light microscopy

3.6.1.1 Haematoxylin and Eosin (H&E)

8μm paraffin sections and 15μm cryopreserved sections were stained with H & E (see 6.1.5.3, page 116) and mounted in DPX (BDH).

3.6.1.2 Haematoxylin

To counterstain, paraffin and cryopreserved sections were stained with haematoxylin (see 6.1.5.4, page 117).

3.6.1.3 Methylene blue/ azure II

1μm resin sections were stained with methylene blue/azure II (see 6.1.6.1, page 118). The slides mounted with sections were placed on a 60°C hot plate, flooded with stain for 30-60 sec and rinsed in running water. After drying, slides were mounted in DPX.

3.6.2 Electron microscopy (EM)

For electron microscopy, the 70nm resin sections were stained using uranyl acetate and lead citrate (see 6.1.5.5, page 117).

3.7 Quantitatlve studles (classical methods)

3.7.1 Quantification of glial cells

Transverse 1μm resin sections of the second segment of the cervical cord (C2), post-fixed in osmium tetroxide and stained with methylene blue/azureII, were used for quantification of glial cell nuclei. Quantification was performed using a 100x oil immersion lens with 6.3x eyepieces, one of which contained a 100 square graticule (Graticules Ltd). The white matter areas subjected to counting were the ventral columns immediately adjacent to the ventromedian fissure and its continuation onto the ventral surface of the cord. Two sections, 15 μm apart were examined. On each section, two fields, one on each half of the cord, were counted. Thus a total 300-400 squares were estimated. Endothelial nuclei were ignored. Only nuclei having morphological criteria of glia were considered.

The mean and the maximum nuclear lengths were measured in longitudinal sections of the caudal segments of cervical cord using a calibrated eyepiece. The mean

length of 50 nuclei (oligodendrocytes, astrocytes and microglia) was calculated. Areas of white matter were calculated from Polaroid light microscopy images using Sigma Scan/Image measurement software (Jandel Scientific Software) and SummaSketch III graphics tablet (Summagraphics). Corrected total glial cell counts and corrected glial cell densities were calculated using Abercrombie's correction (Sturrock, 1983).

3.7.2 Differential glial cell count

Based on nuclear morphology, the glial nuclei (oligodendrocytes, astrocytes and microglia) were counted as previously described for quantification of glial cells.

3.7.3 Dead cell numbers

The same two sections used for quantification of glial nuclei were considered for estimating the dead cell numbers. Pyknotic nuclei were counted in the total white matter using a 100x oil immersion lens. Pyknotic nuclei for the two sections were averaged and used to represent the counts for that particular animal. Due to the lack of any morphological characteristics of a particular population, the pyknotic nuclei arising from a particular glial cell type are indistinguishable.

3.7.4 Myelin volume

The same blocks used for the glial cell quantification were trimmed and 70 nm ultrathin sections were cut for electron microscopy. Random fields from the ventral columns were photographed with AEI EM6B electron microscope at approximately 5000x magnification and printed at approximately 2x magnification. Calibration was achieved by photographing a diffraction grating of known size for each set of prints.

These measurements were performed on the electron micrographs masked with transparent ruled squares of 2.25 cm^2. The myelin volume was calculated by counting of the number of intercepts hitting the myelin lamellae in each micrograph relative to the total intercepts (Williams, 1977). Ten-12 photographs were counted per animal.

3.8 Immunohistochemistry

Resin and paraffin sections were stained with PAP technique and cryostat sections were stained either with indirect immunofluorescent techniques, PAP or ABC. Buffers were applied to sections to block non-specific binding and increase tissue permeability. Sections were not allowed to dry throughout sequence procedures of

staining, therefore, all incubation with antibodies and links were performed in a humid chamber at room temperature, unless stated. Control sections were also included, with the primary antibodies omitted. Immunostained sections were stored in the dark at 4°C.

3.8.1 Labelling markers

Commercially available and other antibodies were used and their sources and dilution are illustrated in Table 2, page 37.

Anti-BrdU antibody (Sigma) was applied to detect the BrdU incorporated into DNA of dividing cells. Anti-Caspase-3 antibody (R&D systems) was used to recognise apoptotic cells. Anti-NG2 chondroitin sulphate proteoglycan antibody (Chemicon International Inc.) was used to selectively stain oligodendrocyte progenitors. Anti-adenomatous polyposis coli (APC) antibody (Oncogene) was employed to distinguish mature oligodendrocytes (Fernandez *et al.*, 2000; McTigue *et al.*, 2001). Anti-CD45 antibody (Serotec) and F4/80 hybridoma supernatant (Serotec) recognise pan-leukocyte and microglial/macrophage-specific epitopes, respectively, and were used to identify microglia. For staining astrocytes anti-glial fibrillary acidic protein (GFAP) antibody (Dako) was applied (Bignami *et al.*, 1972). Anti-MBP antibody (NP. Groome, Oxford, UK) was used to stain central compact myelin. Anti-PLP C-terminal antibody (NP Groome, Oxford, UK) recognises the carboxy terminus (amino acids 271 to 276) of both PLP and DM20 protein isoforms (Fanarraga *et al.*, 1993).

3.8.2 Immunofluorescence

Secondary antibodies were labelled with fluorescein isothiocyanate (FITC) and Texas red (TxR) (Table 3, page 37) and sections were examined by epifluorescence. FITC absorbs light with a wavelength 495 nm and emits it at 525 nm, which can be visualised as green light using a blue filter. TxR absorbs light at 596 nm and emits it at 620 nm, which can be visualised as red light using a green filter. 4,6-diamidino-2-phenylindole (DAPI) provides a fluorescent light with excitation of 345 nm and emission of 455.

3.8.3 Cryostat sections

Sections at –20°C were allowed to warm to room temperature and then washed in PBS (see 6.1.7.1, page 119), twice for 10 minutes. Between steps, sections were washed two changes with PBS for 10 minutes if required. Unfixed sections were fixed in 4% PF for 20 minutes and then washed with PBS. At this stage the sections are ready for different treatments. After completion of staining, sections were

mounted in Citifluor antifade medium (UCK Chem Lab) and the coverslips sealed with nail varnish.

Table 2. Primary antibodies

Primary antibody	**Host**	**Isotype**	**Dilution**	**Source**
Anti-PLP C-terminal	Rabbit polyclonal	IgG	1:600	Groome
Anti-MBP	Rat monoclonal	IgG	1:500	Groome
F4/80	Rat monoclonal	IgG2b	1:1000	Serotec
Anti-GFAP	Rabbit polyclonal	IgG	1:1000	DAKO
Anti-BrdU	Mouse monoclonal	IgG1	1:2500	Sigma
Anti-APC	Mouse monoclonal	$IgG_{2b}k$	1:100	Oncogene
Anti-CD45	Rat monoclonal	IgG	1:600	Serotec
Anti-NG2	Rabbit polyclonal	IgG1	1:150	Chemicon
Anti-caspase-3	Rabbit polyclonal	IgG	1:5000	R&D

Table 3. Secondary antibodies

Secondary antibody	**Dilution**
Goat-anti-mouse IgG1 TxR	1:80
Goat anti-rabbit IgG FITC	1:80
Goat anti-rat IgG FITC	1:50
Goat anti-mouse IgG2b FITC	1:100

(Sourced from Southern Biotech)

3.8.4 Peroxidase anti-peroxidase (PAP)

3.8.4.1 Preparation of Slides

3.8.4.1.1 Resin sections

Resin was removed by immersion of slides, with rotation, in sodium ethoxide (50% ripened sodium ethoxide in 50% absolute alcohol) for 30 minutes. Slides were washed, 6 changes, in absolute alcohol for 30 minutes. Endogenous peroxidase activity was quenched using 3% hydrogen peroxide in water for 30 minutes. Sections were again washed in running water for 30 minutes.

3.8.4.1.2 Paraffin sections

Paraffin sections dewaxed in xylene and hydrated through alcohols. Endogenous peroxidase activity was quenched using 3% hydrogen peroxide in water for 30 minutes. Sections were again washed in running water for 30 minutes.

3.8.4.2 PAP staining

After washing with running water, sections were coated with 10% normal goat serum (NGS) in PBS for about 2 hours at room temperature. Excess NGS was removed and the primary antibody, diluted in 1% NGS/PBS, was immediately applied and sections were incubated overnight at 4°C. The following day sections were allowed to warm to room temperature and were washed in PBS, 6 changes, for 30 minutes. The appropriate link antibody diluted in 1% NGS was applied for 1 hour at room temperature and washed in PBS 6 changes for 30 minutes. Sections were incubated with PAP complex (Table 4, page 39) for 30 minutes at room temperature and washed in PBS, 6 changes, for 30 minutes. The chromogen reaction was developed in filtered PBS containing 0.5 $mg.ml^{-1}$ 3,4,3,4-tetraminobipheyl hydrochloride (DAB) and 0.003% hydrogen peroxide until the required colour change was seen (30 seconds to 5 minutes). DAB was removed by washing in PBS for 2 minutes and running water for 5 minutes. Sections were immersed in 1% Osmium/Caccodylate buffer for 2 minutes before washing.

Sections were dehydrated through alcohols, cleared and mounted in DPX.

Table 4. Link antibody and PAP complexes

Link antibody	Dilution	PAP complex	Dilution	Source
Goat-anti-rabbit	1:10	Rabbit	1:40	ICN

3.8.5 Avidin biotin complex (ABC)

3.8.5.1 Preparation of Slides

3.8.5.1.1 Paraffin sections

Paraffin sections were prepared as described for PAP.

3.8.5.1.2 Cryostat sections

Cryostat sections post-fixed with P-L-P fixative were washed in PBS, 6 changes, for 20 minutes.

3.8.5.2 ABC staining

Sections were washed in PBS, 6 changes, for 20 minutes between steps and all reagents were diluted in PBS. Endogenous peroxidase activity was quenched by immersing the slides in 0.3% hydrogen peroxide in ethanol for 20 minutes. Washed PBS sections were blocked in 10% NGS for 30 minutes. Excess NGS was removed and the primary antibody diluted in 1% NGS was applied for 1 hour. The sections were washed and the appropriate link antibody was applied for 45 minutes. The sections were then washed in PBS and incubated in avidin-biotin complex (Elite ABC) (Table 5, page 40) for 45 minutes. The chromogen reaction was developed in filtered PBS containing 0.5 $mg.ml^{-1}$ DAB and 0.003% hydrogen peroxide until required colour change was seen (30 seconds to 5 minutes) and then washed. The sections were exposed to 0.01% osmium tetroxide for 30 seconds to increase the chromogen intensity. The sections were washed, counterstained with haematoxylin (see appendix 6.1.5.4 , page 117), dehydrated through alcohol (see appendix 6.1.5.2, page 115), cleared and mounted in DPX.

The paraffin sections were stained for MPB and the cryostat sections were stained for microglial epitopes F4/80 as well as CD45.

Table 5. Link antibody and Avidin biotin Complex (ABC)

Link antibody	Dilution	ABC Dilution	Source
Rabbit-anti-rat IgG	1:100	10 µl of A and B in 625 µl PBS	Vector labs

3.8.6 BrdU staining of proliferating cells

A combination of fresh cryopreserved and 4% PF cryopreserved sections were used for BrdU staining. Slides were immersed in 6 M HCl, 1% triton x-100 for 10 minutes. The sections were washed in 0.2% triton x-100 in PBS. Anti-BrdU antibody, 1:2500, diluted in 0.2% triton x-100 was applied to the sections for 3 hours and then washed in PBS. The sections were incubated with goat anti-mouse IgG1 TXR secondary antibody at 1:80 for 30 minutes. The sections were then washed and mounted.

3.8.7 NG2 staining of oligodendrocytes

Cryostat sections post-fixed with P-L-P fixative were permeabilised in methanol at –20°C for 10 minutes and washed in PBS. The sections were then incubated with anti-NG2 at 1:150 in PBS at 4°C overnight and washed. Goat anti-rabbit IgG FITC secondary antibody was applied to the sections at 1:80 in PBS for 30 minutes and washed. The sections were counterstained with DAPI, washed and mounted.

3.8.8 APC staining of oligodendrocytes

Sections were immersed in 0.5% triton x-100 for 30 minutes and non-specific binding was blocked with 0.1% triton x-100, 0.2% pig skin gelatin in PBS for 30 minutes. Excess blocking solution was removed and anti-APC antibody at 1:100 diluted in blocking solution was applied to the sections at 4°C overnight. The sections were washed and incubated with goat anti-mouse IgG2b FITC secondary antibody, 1:100, diluted in blocking solution for 30 minutes. The sections were washed, stained with DAPI, washed and mounted. APC has been used to label mature oligodendrocytes (Mays, 1999; Fernandez *et al.*, 2000; McTigue *et al.*, 2001). As it has been reported to label some astrocytes in certain situations (Leroy *et al.*, 2001) we double labelled spinal cords for APC Figure and for GFAP, a marker for astrocytes; no double labelled cells were seen (Figure 6,page 48) suggesting that in our hands we are not detecting astrocytes with the APC antibody.

3.8.9 GFAP staining of astrocytes

Sections were permeabilised in methanol at –20°C for 10 minutes and washed in PBS. The sections were then coated with anti-GFAP antibody at 1:1000 overnight at 4°C and washed in PBS. The sections were again coated with goat anti-rabbit FITC secondary antibody at 1:80 for 30 minutes. Finally, the sections were stained with DAPI, washed and mounted.

3.8.10 CD45 staining of microglial

Sections were permeabilised in methanol at –20°C for 10 minutes and washed in PBS. The sections were then incubated with anti-CD45, 1:600, in PBS at 4°C overnight and washed. Goat anti-rat IgG FITC secondary antibody was applied to the sections at 1:50 for 30 minutes and washed. The sections were counterstained with DAPI, washed and mounted.

3.8.11 Caspase-3 staining of apoptotic cells

Sections were coated with blocking solution containing 0.1% triton x-100, 0.2% pig skin gelatin in PBS for 30 minutes. Excess blocking solution was removed and anti-caspase-3 antibody, 1:4000, diluted in blocking solution was applied to the sections at 4°C overnight and washed. The sections were washed and incubated with goat anti-rabbit IgG FITC secondary antibody, 1:80, diluted in blocking solution for 30 minutes. The section were washed, stained with DAPI, again washed and mounted.

3.8.12 DAPI Staining

Following immunostaining, cell nuclei were visualised with $1\mu g.lm^{-1}$ 4,6-diamidino-2-phenylindole (DAPI), the fluorescent dye, for 30-60 seconds. Non-immunostained sections were also stained with DAPI.

3.8.13 Double staining of BrdU-labelled sections

Sections were first immunostained with appropriate primary antibody, as described for each single immunostaining method, and then the procedures for BrdU were followed. The sections were washed and mounted.

3.8.14 Double staining of Caspase-3 Cells

Sections were first immunostained with appropriate primary antibody, as described for each single immunostaining method, and then immunostaining for caspase-3 was followed. The sections were washed and mounted.

3.9 Quantitative studies (immunolabelled methods)

3.9.1 Quantification of MBP-labelled myelin

Resin sections (1μm) were immunolabelled for MBP using the PAP technique. Using a x40 dry objective four areas of ventral column, two each side of the ventromedian fissure, were imaged using the CCD camera and stored in the computer. Images were converted to grey scale and adjusted to give optimum contrast and brightness. Using the segmentation software (Image Pro Plus v4, Media Cybernetics) the dark areas (MBP staining) were separated from the remaining background. This was accomplished initially using a black image on a translucent background so that any false staining of non-myelinated tissue could be removed. In the majority of cases no manual adjustment was necessary. The image was then converted to a black on white format. For each image, a square area of interest (AOI) of 2500μm^2 was placed at one side and the area of black (MBP-stained myelin) within the AOI was measured. The AOI was then moved to the other side of the image and the process repeated. For each animal a total of eight AOI were measured. From these data the density of MBP-stained myelin (μm^2)/mm^2 of white matter was calculated. As the white matter area had been determined previously for the glial cell quantification, we could determine the total area of MBP-stained myelin in white matter of a transverse section of spinal cord.

3.9.2 Quantification of BrdU-labelled cells

Cell counts were performed on cryosections (15μm) of the ventral columns, adjacent to the ventromedian fissure, from rostral cervical spinal cord. Images of BrdU-labelled or DAPI-labelled nuclei were collected at x20 objective using a CCD camera system (Photonic Science Colour Coolview) and stored in the computer. Approximately 20 images of BrdU nuclei and 6 of DAPI nuclei were obtained from each animal. For each BrdU-labelled image a frame (35804 μm^2) outlining the AOI was placed on the screen. Counting parameters were set to include bright objects of area between 4 and 200μm^2 within the AOI or touching the top or left side but excluding those touching the bottom or right sides. Automated counts were made with adjustments for any touching objects or false images due to dirt or debris. DAPI-labelled nuclei were counted in a similar manner with an AOI of 10,000μm^2. The density of BrdU-labelled nuclei and DAPI-stained nuclei (nuclei/mm^2) and the labelling index (LI) (BrdU nuclei/DAPI nuclei x 100) were calculated.

3.9.3 Quantification of APC+ cells

Cell counts were performed on cryosections (15μm) of the ventral columns, adjacent to the ventromedian fissure, from rostral cervical spinal cord. Images of APC-labelled cells (green channel) and DAPI-labelled nuclei (blue channel) from the same sampling area were collected at x20 objective using a CCD camera system (Photonic Science Colour Coolview) and stored in the computer. The green and blue channels were merged using Adobe Photoshop (Adobe systems Inc., San Jose) and the image quality adjusted. For each combined image, a frame (35804μm^2) outlining the AOI was placed on the screen. The number of APC+ cell bodies containing a DAPI-stained nucleus was counted within the AOI or touching the top or left side but excluding those touching the bottom or right sides. The density of DAPI-labelled nuclei was counted automatically with an AOI of 10,000μm^2. The density of APC-labelled cells and DAPI-stained nuclei (nuclei/mm^2) and the percentage of APC+ cells (APC cells/DAPI nuclei x 100) was calculated.

3.9.4 Quantification of NG2+ and CD45+ cells

These cells were quantified as described for the APC+ cells.

3.9.5 Quantification of caspase-3+ cells

Cell counts were performed on cryosections (15μm) of the ventral columns, adjacent to the ventromedian fissure, from rostral cervical spinal cord. Images of caspase-3-labelled cells were collected at x20 objective using a CCD camera system (Photonic Science Colour Coolview) and stored in the computer. For each image, a frame (35804 μm^2) outlining the AOI was placed on the screen. The number of caspase-3+ cell bodies was counted within the AOI or touching the top or left side but excluding those touching the bottom or right sides. The density of DAPI-stained nuclei was taken from the sections stained for APC/DAPI. The density of caspase-3-labelled cells and the percentage of caspase-3+ cells (Caspase-3+ cells/DAPI nuclei x 100) was calculated.

3.9.6 Calculation of cell numbers

Quantification of cells or nuclei was determined by their density in the ventral funiculi. As the area of the white matter varied between different genotypes we calculated the total number of cells/nuclei in the white matter of a transverse section. This calculation assumes that the density is equally distributed throughout the white matter when there is variation between tracts and at different ages. In fact the nuclear density alters across the width of the ventral column, being greater in the central region adjacent to the grey matter. The alternative strategy is to define a

precise sub-region of the ventral column in which to calculate total numbers, a task that would be problematic to ensure consistent identification of the same region. The calculation based on the total white matter area therefore offers an acceptable way of comparing cell numbers between different genotypes and ages.

3.10 Statistical analysis

3.10.1 Group sizes

The number of animals included in a group varied between ages, genotype and techniques. In general, 4 or more animals were included in a group. When a developmental profile was followed, for example, cell counts between P10 and P30, the number of animals was increased to 6 or even 10 or more at key ages (e.g. P20 and P30) with sizes of 4 at P15 and P25. If only a single analysis point was used, group sizes were always 6 or more.

3.10.2 Data presentation

Graphs are presented as mean ± SEM.

3.10.3 Statistical tests

As group sizes were always relatively small no assumptions were made that the data was distributed normally. Groups were first compared using one-way Analysis Of VAriation (ANOVA). If a significant difference ($p<0.05$) was detected, individual groups were compared using the Bonferroni multiple comparison test. P was taken at < 0.05.

Further details of group sizes, numerical values and P values for all analyses are presented in (7. Appendix 2. Details of statistical analyses, page 121).

3.11 Western blotting

3.11.1 Protein extraction

Protein was extracted from mouse spinal cord and brain that had been freshly dissected, rapidly frozen in liquid nitrogen and stored at –80°C until required. All solutions were chilled on ice before use. The tissue samples were homogenised in an extraction buffer containing (0.85 M sucrose, 10 mM Hepes (pH 7.4), 2 mM DDT and 1 mM TLCK) for 10 seconds using a polytron homogeniser set at maximum speed. Aliquots of the homogenates were removed to represent total

homogenate fractions. The remaining homogenates were transferred to the Beckman SW41 rotor tubes and 0.25 M sucrose/ 10 mM Hepes (pH 7.4) solution was gently added until the volume was about 1cm from the top of the ultracentrifuge tubes. The homogenates were centrifuged at 70,000g for 90 minutes at 4°C. This produced a biphasic solution with cellular debris left in the lower phase (0.85 M sucrose), lipid floating on top of the upper phase (0.25 M sucrose) and myelin protein trapped at the interface between two phases. The myelin protein was transferred to clean tubes and hypotonically lysed for any remaining cellular organelles by adding chilled dH_2O. This was centrifuged at 23,000g for 30 minutes at 4°C. The supernatant was discarded and the process was repeated 3 times with the final centrifugation at 17,000g for 30 minutes. The myelin pellets were resuspended in 10 mM Hepes (pH 7.4) containing protease inhibitor (0.5 mM PMSF, 10 $\mu g.ml^{-1}$ leupeptin, 10 $\mu g.ml^{-1}$ aprotinin, 10 $\mu g.ml^{-1}$ trypsin inhibitor and 1 mM benzamidine). The protein concentration was measured using the BCA assay (Pierce Ltd). The myelin protein and homogenate fractions were stored at -80°C until required.

3.11.2 Precipitation of protein

For GFAP immunoblotting the total homogenate was precipitated. 150 µl aliquot of each sample was made up to 900 µl by adding chilled dH_2O and 100 µl of a 50% (wt/vm) of TCA. The samples were then incubated on ice for 30 minutes and centrifuged at 13,000g for 15 minutes at 4 °C. Pellets were resuspended with 100 mM Tris base pH 10.4 and proteins concentration was measured as previously mentioned.

3.11.3 SDS-Polyacrylamide gel electrophoresis

3.11.3.1 SDS-Polyacrylamide gel preparation

Proteins were resolved on a vertical SDS-polyacrylamide mini-gel produced by polymerisation of acrylamide cross-linked with N,N′-methylene bisacrylamide at a ratio of 30:8. The catalyst for the reaction was ammonium persulphate and the accelerator was N,N,N,N′,-tetramethylethylenediamine (TEMED). Routinely, proteins were separated on a 12.5% acrylamide resolving gel and a 4% stacking gel.

3.11.3.2 Protein electrophoresis

Aliquots of samples (myelin and homogenates) were made up to 20 µl with dH_2O and then to 30 µl final volume with denaturing buffer containing (25 mM Tris, 192 mM glycine, 0.1% SDS). The samples were denatured at water bath 90°C for 4 minutes and loaded onto the gel with size markers as controls.

The samples were electrophoresed at room temperature in a mini-PAGE-rig (ATTO Corp.) in a buffer containing 25 mM Tris 192 mM glycine, 0.1% SDS) at 20mA constant current per gel for 90 minutes until the dye front reach the gel bottom.

3.11.3.3 Electrophoresis protein transfer

The separated proteins were transferred onto a polyvinylidene fluoride (PVDF) microporous membrane (Millipore) in a semi-dry blotter (The W.E.P. Company). Layers were arranged from the bottom to the top, a 3MM paper sheet (Whatman) soaked in Anode 1 buffer (0.3 M Tris (pH10.4), 7.5% MeOH), 2 sheets soaked in Anode 2 buffer (0.025 M Tris (pH 10.4), 7.5% MeOH), PVDF membrane treated with 100% methanol, rehydrated in dH_2O and equilibrated in Anode 2 buffer, the gel equilibrated in cathode buffer (0.025 M tris/40 mM glycine (pH 9.4), 7.5% MeOH and 3 sheets soaked in cathode buffer. The transfer was performed at 100 mA constant current for 1 hour. The membrane was stained with Ponceau stain to check for equal loading and efficiency of transfer.

3.11.3.4 Immunostaining

The membrane was blocked by immersing in TBS blocking buffer containing 5% dried semi-skimmed milk and 0.1% Tween-20 (T-TBS) for 1 hour at room temperature. The primary antibodies (see below) were diluted in blocking buffer and applied for 2-3 hours at room temperature. The membrane was then washed 3 times in T-TBS for 10 minutes. The link secondary antibody (see below), diluted in blocking buffer, was applied for 1 hour at room temperature. The membrane was washed again in T-TBS (pH 7.6) 3 times for 10 minutes. The membrane was incubated in equal volumes of luminal enhancer solution and stable peroxide solution (Pierce Ltd) for 1-2 minutes at room temperature. The membrane was wrapped in Saran wrap and exposed to X-omat imaging film (Kodak) in a radiography cassette for 1-5 minutes. The film was finally developed in an automatic processor (Dupont Cronex CX-130).

Membranes were incubated with 1:50000 diluted anti-PLP C-terminal rabbit polyclonal antibody (NP. Groome, Oxford, UK), 1:10000 diluted anti-MBP rat monoclonal antibody (NP. Groome, Oxford, UK), 1:2000 diluted anti-MAG polyclonal antibody (NP. Groome, Oxford, UK), 1:10000 diluted anti-CNP polyclonal antibody (PJ. Brophy, Edinburgh, UK), and 1:200000 diluted anti-GFAP rabbit monoclonal antibody (Sigma). The immunocomplexes were detected with anti-rabbit HRP-linked IgG (SAPU) or anti-rat HRP-linked IgG (Sigma) secondary antibody.

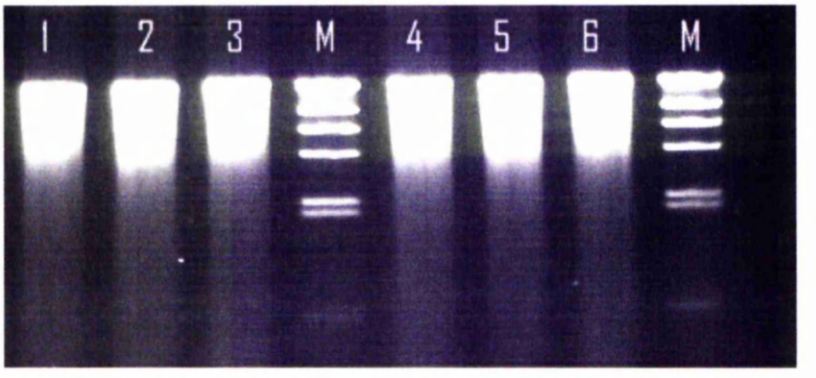

Fig. 5A. Examples of gDNA extracted from mouse tails and electrophoresed on 0.7% agrose gel (size marker: λ-DNA/*Hind*III).

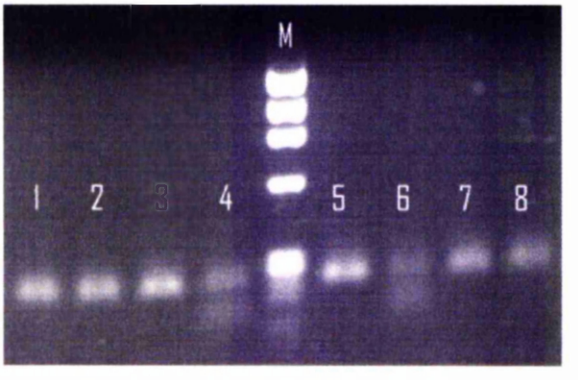

Fig. 5B. Products of PCR and PCR products digested using *AccI,* used for identification of rsh mutant animals. Lane 1, 3, 5 and 7 are the PCR products. Lane 2, 4, 6 and 8 are PCR products digested with *AccI* enzyme at 37 °C. Only lane 4 and 6 are successfully digested, therefore, they represent *rsh* mutation. (size marker (M): ϕX174-DNA/*Hae*III).

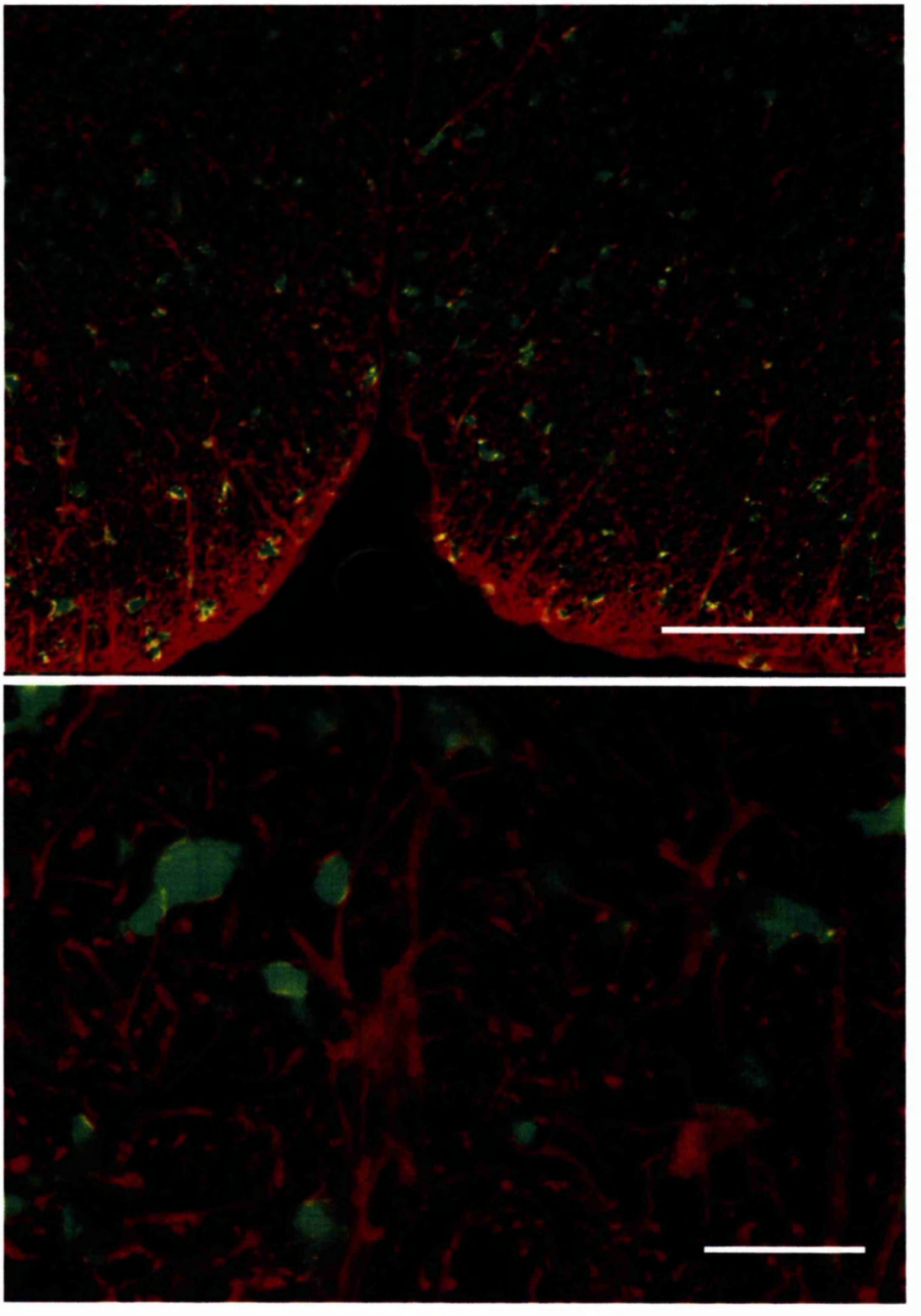

Fig. 6. Double immunofluorescence for APC and GFAP. Sections from ventral white matter of C3H *rsh* at P20. No double labelled cells are evident. Bars top = 100um; bottom = 20um

4. Results

4.1 Clinical manifestations of *rumpshaker*

4.1.1 Introduction

The *rumpshaker* (*rsh*) mutation arose spontaneously in C3H mice at the MRC Radiobiology Unit in 1988. These mutant mice were crossed with the 101 strain to improve breeding (the usual practice at that time in the unit) and donated to Glasgow University Veterinary School for further study and maintenance. The mice on the C3H/101 background showed a generalised tremor related with hypomyelination in the CNS and an X-linked mode of inheritance suggesting possible role of *Plp* gene (Griffiths *et al.*, 1990). Importantly, they live a normal length of time and affected animals reproduce. The *rumpshaker* mutation was identified as a recessive point mutation causing an amino acid transition ($Ile^{186}Thr$) in the murine *Plp* gene (Schneider *et al.*, 1992). *jimpy* mutant mice and *rumpshaker* have been indicated to be allelic to each other (Cattanach and Beechey, 1991).

4.1.2 Materials and Methods

4.1.2.1 Mouse breeding

The animals used in all experiments are described in mouse breeding (see 3.1.1, page 27). Mutant male mice from the two genetic backgrounds and their normal littermate males as controls were used for the current work. PCR (see 3.3, page 30) was used to confirm the genotype of 10 day postnatal (P10) or younger mice as well as female carriers for the mutated allele, which were used for breeding.

4.1.2.2 Rotarod

Mice were assessed on the Rotarod, as described in (4.1.2.2, page 49) at P20 and P30.

4.1.3 Results

4.1.3.1 Clinical presentation

Physically *rumpshaker* mutants from the two backgrounds develop a generalised tremor at 10-13 days. This neurological abnormality is clearly noted during

movement of animals while it ceases at rest or during sleep. As animals age, the tremor is confined to the hindquarters and peaks at approximately 20-25 days. Compared with C3H *rsh*, which survive to reproduce, C57 *rsh* develop seizures after 25 days and die at about 4-5 weeks.

4.1.3.2 Rotarod

Animals were placed on a suspended horizontal rotating rod, which gradually accelerated from 3 to 30 rpm and the time until falling was recorded. Since many wild type mice do not fall off the rod and generally remain on it for a long periods of time, a maximum reading (500 sec) was set. In the actual experiment there was variability between individual mice scoring.

The C57 WT and C3H WT groups stayed on the rod for a significantly longer time than did the mutants. The C3H *rsh* also stayed for a significantly longer time than the C57 *rsh*. The time of staying on the rod was slightly decreased at P30 (Figure 7, page 52).

4.1.3.3 Body weight

Growth is normally closely linked with chronological age. The *rumpshaker* mutation is likely to influence the weight gain of the mutant animals. All groups studied showed steady increase in weight up to P30. The C57 wild types weighed significantly less than their C3H counterparts. The mutant animals were relatively smaller than normal littermates. The four groups of animals, on the basis of weight gain, were represented in the order C3H WT>C3H *rsh*>C57 WT>C57 *rsh* (Figure 8, page 52).

4.1.4 Discussion

The severity of the *Plp* gene mutant phenotypes is highly dependent on the nature of mutation and the genetic background. Characteristic features are common among the *Plp* gene mutants including man. Generalised body tremors, the first clinical sign which identify the mutant animals, are noted early during the first postnatal weeks. The tremors are usually obvious at P10-13 in mutant mice and before 10 years of age in human. The severe phenotype of the C57 *rsh* mutation is closely similar to *jimpy* mutant mice (Duncan, 1990) as both of the mutants develop seizures at about P25 and die around P30. As the frequency and intensity of the seizures increase the condition causes the death of the mutant animals between 4-5 weeks (in general during seizures). In contrast to the above severe phenotypes, C3H *rsh* is the mild form of the mutation and manifests no seizures. Additionally, the tremor gradually disappears as the animals age. Moreover, mutations in the *Plp*

gene appear to influence gaining of body weight. This criterion is remarkable in the *rsh* mutants which weigh less than their normal littermates on either genetic background. Consistent with this finding, *jimpy* mutants are also lesser in their weight when compared to their wild type littermates (Bolivar and Brown, 1994).When assessing locomotor activities on the Rotarod, the *rumpshaker* mutant mice also spend less time than their respective wild type animals.

Patients with PMD/SPG2 due to amino acid substitutions also show considerable heterogeneity of clinical presentation and signs. Much of this has been ascribed to the different mutations and to some extent this may well be true. However, variation within families has been noted (for review see Hodes *et al.*, 1993; Baron *et al.*, 1994) and some of the heterogeneity may be due to non-*PLP* gene-related polymorphisms within the human genome.

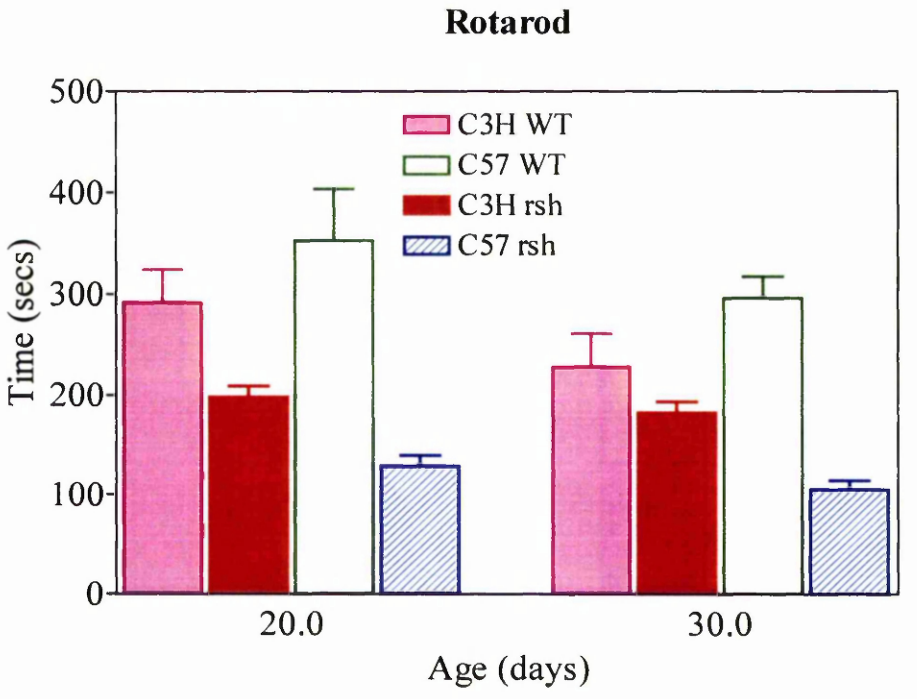

Fig. 7. Time on Rotarod for groups of mice. There is no difference between wild type mice at either age. The C57 *rsh* values are lower than wild type at both ages while the C3H *rsh* are lower only at P20. The two mutants differ from each other at P30.

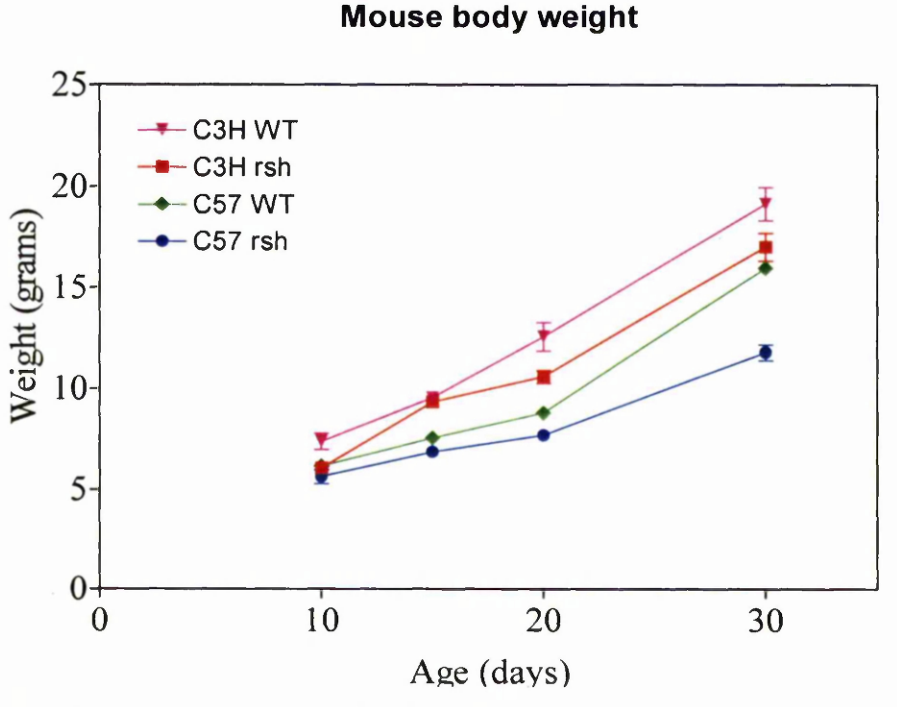

Fig. 8. Mouse body weights. The C57 wild type is less heavy than its C3H counterpart after P10. The C3H wild type and mutant have similar weights between P10 and P30. The C57 mutant differs from both its wild type and the C3H *rsh* after P10.

4.2 Neuropathology of *rumpshaker*

4.2.1 Introduction

Neuropathologically, the CNS (but not PNS) of C3H *rumpshaker* mice shows generalised hypomyelination. The appearance of myelin sheaths can vary from poorly compacted oligodendrocyte processes to the thin sheaths, which may be compacted or occasionally vacuolated. Sheaths of many smaller axons are of a similar thickness to those of equivalent axons in normal mice. The total number of glial cells and in particular the oligodendrocytes, appears increased even at one year of age (Griffiths *et al.*, 1990). Many of these oligodendrocytes are likely to be metabolically active with prominent RER and Golgi apparatus (Griffiths *et al.*, 1990). Unlike many *Plp* gene mutant animals, cell death was not thought to be a prominent feature in *rumpshaker* (Schneider *et al.*, 1992). In separate projects to attempt to rescue mutant phenotypes by transgenic complementation it was necessary to move the *rsh* mutation to a C57BL/6 background. However, as the proportion of C57 alleles increased with successive backcrosses it was noted that the phenotype worsened and mice started to seizure and die prematurely. In this thesis the appearance of the C57 mutants is compared with the C3H *rsh*, using the spinal cord as a representative tissue. The intention is not to provide a detailed description of the *rumpshaker*, as this has been published previously, but to highlight the new or different features of the mutation on the C57 background.

4.2.2 Materials and methods

4.2.2.1 Tissue preparation

The preparation of neural tissues for various purposes is described in (3.4. Tissue fixation, page 31 and 3.5. Tissue processing and sectioning, page 32). An investigation of the CNS materials was achieved on resin sections (1μm) stained with methylene blue/azure II (see 3.6.1.3, page 33) and paraffin sections stained with H&E (see 3.6.1.1, page 33).

4.2.2.2 Immunohistochemistry

Immunostaining was performed for PLP/DM20, MBP and GFAP as described for each individual marker in (3.8, page 34).

4.2.3 Results

4.2.3.1 Morphology

The general appearance of the C57 mutants was similar to that of the C3H mutants with obvious dysmyelination (Figure 9, page 57) characterised by naked axons surrounded by astrocyte processes or uncompacted oligodendrocyte processes (Figure 10, page 58). Any myelin sheaths present were thin for the axonal diameter and the myelin tended to be loose and undulating, sometimes containing vacuoles (Figure 11, page 59). Astrocyte processes were sometimes present between the axon and surrounding myelin or oligodendrocyte process (Figure 12, page 59). Overall, the amount of myelin appeared less in the C57 *rsh* with more naked axons and thinner sheaths. Pyknotic glial nuclei were evident in both mutants (Figure 9, page 57) but clearly more frequent in the C57 mice. The number of microglial nuclei was increased in the C57 *rsh* and many microglia/macrophages had foamy or vacuolated cytoplasm due to lipid droplets and/or membranous inclusions (Figure 13, page 60;).

4.2.3.2 Immunostaining

MBP immunostained collars were visible around many axons of varying sizes in both mutants. However, intense immunostaining was seen in ventral column of C3H *rsh* spinal cord compared with the C57 mutant. Many axons in C57 *rsh* appeared unassociated with MBP, due to the lack of myelin sheath or presence of very thin myelin sheaths in C57 *rsh*. In contrast, the normal mice contained many MBP immunostained myelin sheaths. The difference between the mutants and age-matched normal animals in MBP immunostained sections is evident (Figure 14, page 61). Immunostaining of sagittal brain and transverse spinal cord sections of C3H *rsh* and C57 *rsh* with PLP/DM20 and MBP showed variation between the mutants (Figure 15, page 62) with the intensity of staining for both proteins being greater in the C3H *rsh*.

Immunostaining for GFAP was performed to provide an indication of the distribution and reactivity of astrocytes in brain and spinal cord. The intensity of GFAP staining was moderately increased in the white matter of both mutants relative to their wild types (data not shown); however there was no consistent difference between the two *rumpshaker* strains (Figure 16, page 63).

4.2.4 Discussion

Myelination occurs predominantly in the postnatal period in rodents, coinciding with the period of major expression of the *Plp* gene. Thus, mutations in the *Plp* gene

result in varying degrees of myelin deficit in neurological mutants although the lethality of these mutations does not correlate with the beginning or even the stage of active myelination. Analysis of the pathology of mutant animals revealed that *jimpy*, the classic *Plp* mutant, has severely reduced amounts of myelin in the CNS white matter and the myelinated axons are found in low numbers (Sidman *et al.*, 1964; Duncan, 1990). The C3H r*sh* has a much less severe phenotype than *jimpy* with considerably more myelin, a lack of seizures and normal longevity. Some findings from the current study suggest that C57 *rsh* is not closely similar to *jimpy* but at other levels, it is closer to *jimpy* than to the original C3H *rsh*. It is possible that C57 *rsh* could be positioned between the more severe *jimpy* and the mild C3H *rsh* phenotypes. In *jimpy*, many axons are, in fact, surrounded by a single layer of myelin sheath (Hirano *et al.*, 1969). This feature is also seen in C57 *rsh*, although many of the sheaths are thicker than those found in *jimpy*. Furthermore, myelin lamellae wrap loosely around the axon with fewer turns than normal and are vacuolated in both C57 *rsh* and *jimpy* (Nagara and Suzuki, 1982). In areas where the compacted myelin sheaths are found in *rumpshaker*, the IPL may appear normal regardless of dysmyelination, or its spacing may be reduced (Griffiths *et al.*, 1990). This contrasts with *jimpy* where, if myelinated areas are found, the IPL is fused to a single electron dense line (Duncan *et al.*, 1987; Duncan *et al.*, 1989). Overall, the C57 *rsh* has more myelin than the *jimpy* and *jimpy-msd* mutant mice although the clinical presentation is very similar. Interestingly, the C57 *rsh* also has more myelin than the *shiverer* mouse, an *Mbp*-deletion mutant, which die at approximately 4-5 months of age (Chernoff, 1981). The amount of myelin, therefore, does not necessarily correlate closely with the longevity of the animal (Billings-Gagliardi *et al.*, 1999; Wolf *et al.*, 1999). The exact pathological basis for both seizures and death is not well understood in any of the myelin mutants.

Immunostaining results of PLP and MBP in the C3H *rsh* in this thesis agree with the previous findings (Griffiths *et al.*, 1990; Fanarraga *et al.*, 1992) and extend this to demonstrate the further marked reduction in the C57 *rsh*. Myelin sheaths from both strains of *rumpshaker* immunostain for PLP/DM20 in contrast to the *jimpy* mouse in which there is an absence of staining (Sorg *et al.*, 1986). The results of the GFAP immunostaining were somewhat surprising. In general terms, the intensity of reaction correlates with the severity of phenotype; thus, in the *jimpy* mouse there is intense astrocytosis and GFAP staining (Skoff, 1976; Vela *et al.*, 1998). In the case of the *rumpshaker*, the intensity of GFAP stain appears similar in the white matter of both mutants and this is supported by the western blotting studies (see 4.4.3.2, page 97). However, there is not necessarily a direct link between dysmyelination and astrocytosis; in the severely dysmyelinated *shiverer* mouse there is little increase in astrocyte markers (Jacque *et al.*, 1986; Chen *et al.*, 1993). The role of the

astrocyte reaction in *Plp* mutants is still unclear. While the astrocyte changes may be purely a reaction to the myelin changes and apoptosis there are also suggestions that this cell may be more intimately involved in the pathogenesis (Skoff, 1976; Knapp *et al.*, 1993; Knapp and Skoff, 1993), despite the lack of *Plp* gene expression in the astrocyte. The astrocyte has also been implicated as the source of the GRO-1 chemokine, involved in stimulating the proliferation of oligodendrocyte progenitors, and whose levels are markedly elevated in the *jimpy* spinal cord (Wu *et al.*, 2000).

The number and morphology of microglia/macrophages also differs between the two strains of *rumpshaker*. The morphological features do not allow us to determine whether the cells are derived from resting microglia or from monocytes of haematogenous origin. We found no evidence for "typical macrophages" within the myelin sheath, as found in classic inflammatory demyelinating disorders and little evidence of such cells in a perivascular location. We suspect that most of these cells are derived from endogenous microglia. Although the absolute number is greater in the white matter of the C57 mutant it is the morphological difference that is more striking. The frequency of cells with foamy cytoplasm and lipid and membranous inclusions is considerably higher in the C57 *rumpshaker*. Occasional cells also appear to have an additional pyknotic nucleus, suggesting they may have ingested an apoptotic cell. Similar microglia are also found in the *jimpy* mouse. The microglia/macrophage in the *Plp* mutants may fulfil more than one role. There is evidence for phagocytosis of apoptotic cells, probably oligodendrocytes (Vela *et al.*, 1996). The lipid and membranous inclusions may indicate that they are involved in catabolism of myelin lipids. Microglia are also a rich source of pro-inflammatory cytokines and, although this aspect has not been investigated in *Plp* mutants, it is possible they may contribute to the dysmyelination rather than just respond to it.

In summary, the general neuropathology suggests that the C57 *rsh* has few if any unique features compared with its C3H counterpart; rather, the common parameters differ quantitatively and qualitatively between the two mutants. However, the dissimilarity does not, at first impression, appear sufficient to explain the very marked difference in clinical features and outcome. For example, the exact pathological basis for both seizures and death in the C57 *rsh* is difficult to explain and indeed, the reasons for these features in any of the *Plp* mutant animals have not been adequately described.

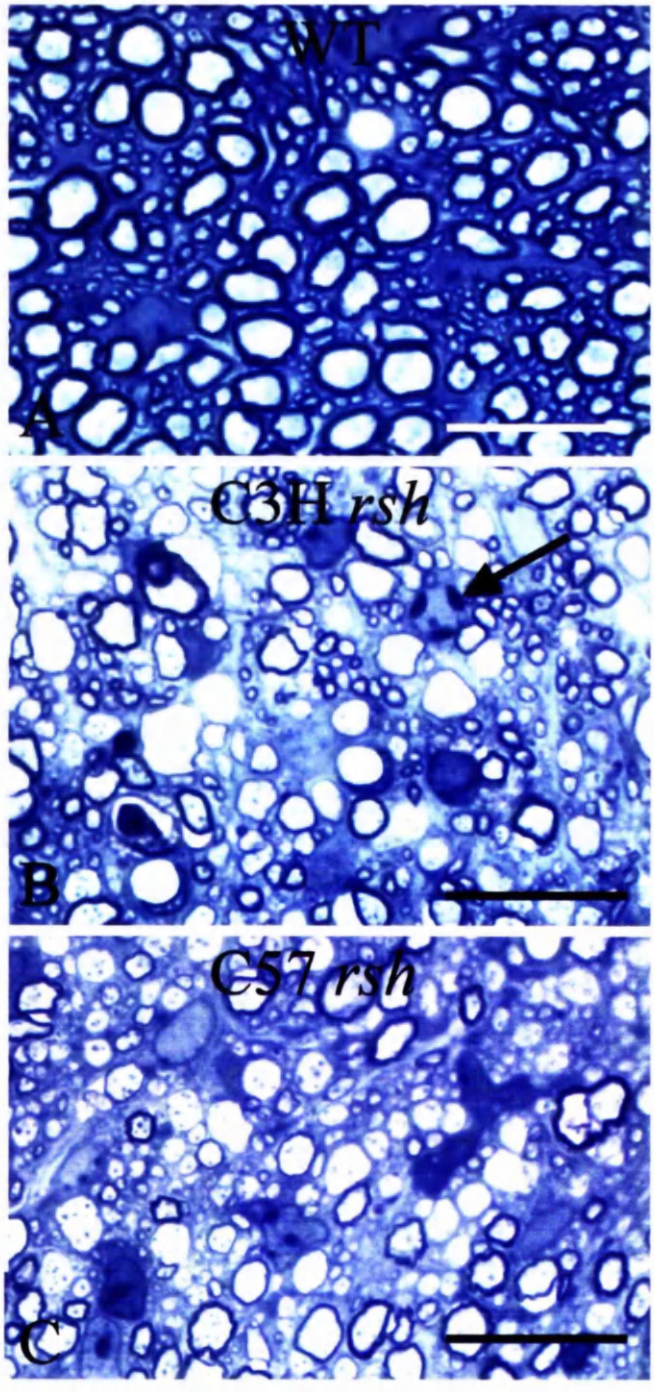

Fig. 9. Dysmyelination in mutant mice. Ventral column of spinal cord from wild type (A), C3H *rsh* (B) and C57 *rsh* (C). There appears to be marginally more myelin in the C3H mutant. A pyknotic nucleus is shown (arrow). Resin section (1um), Bar = 20um.

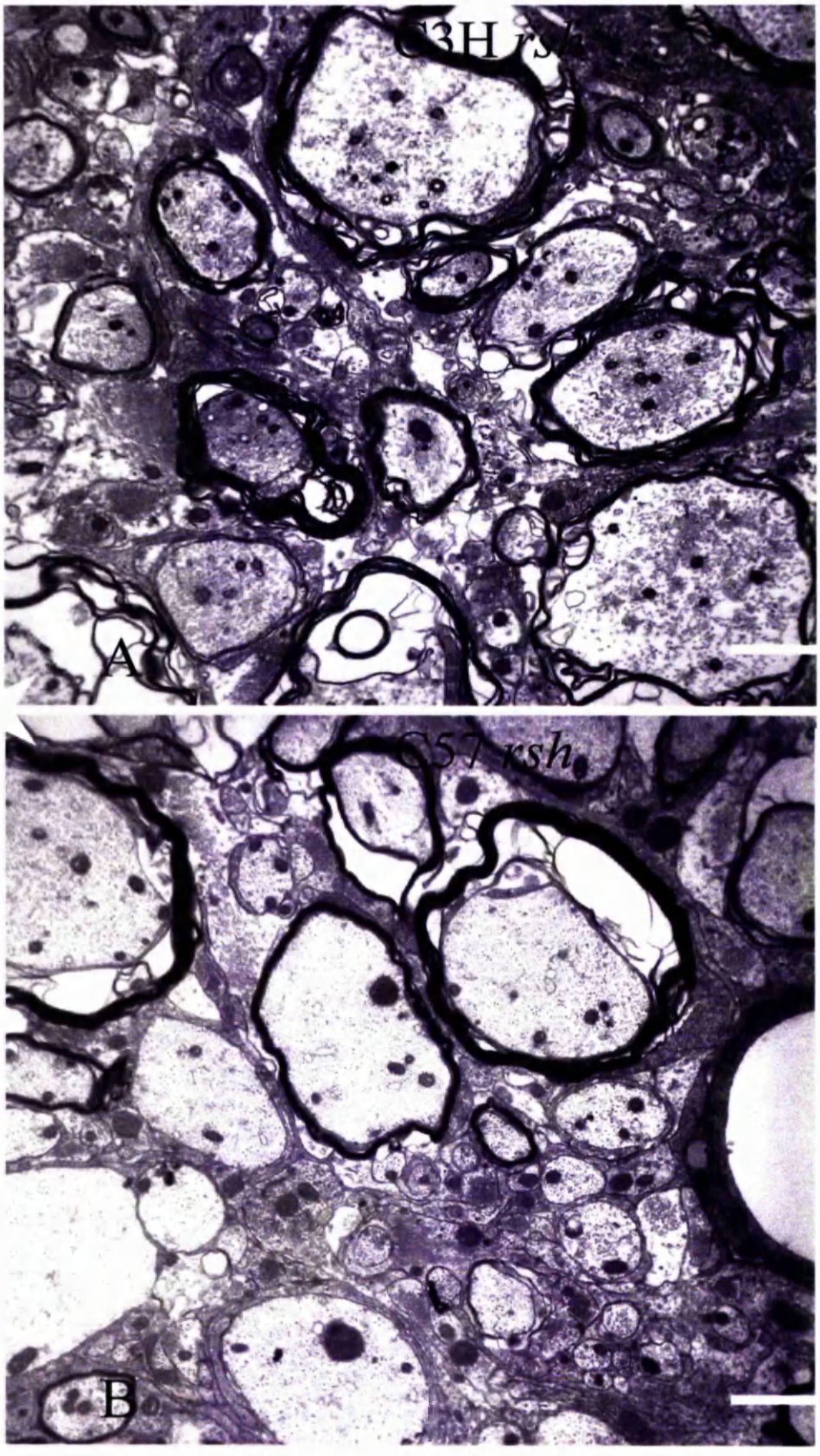

Fig. 10A, B. Electron micrographs of spinal cord from C3H and C57 *rsh*. Numerous naked or thinly sheathed axons are present. Bars = 2um.

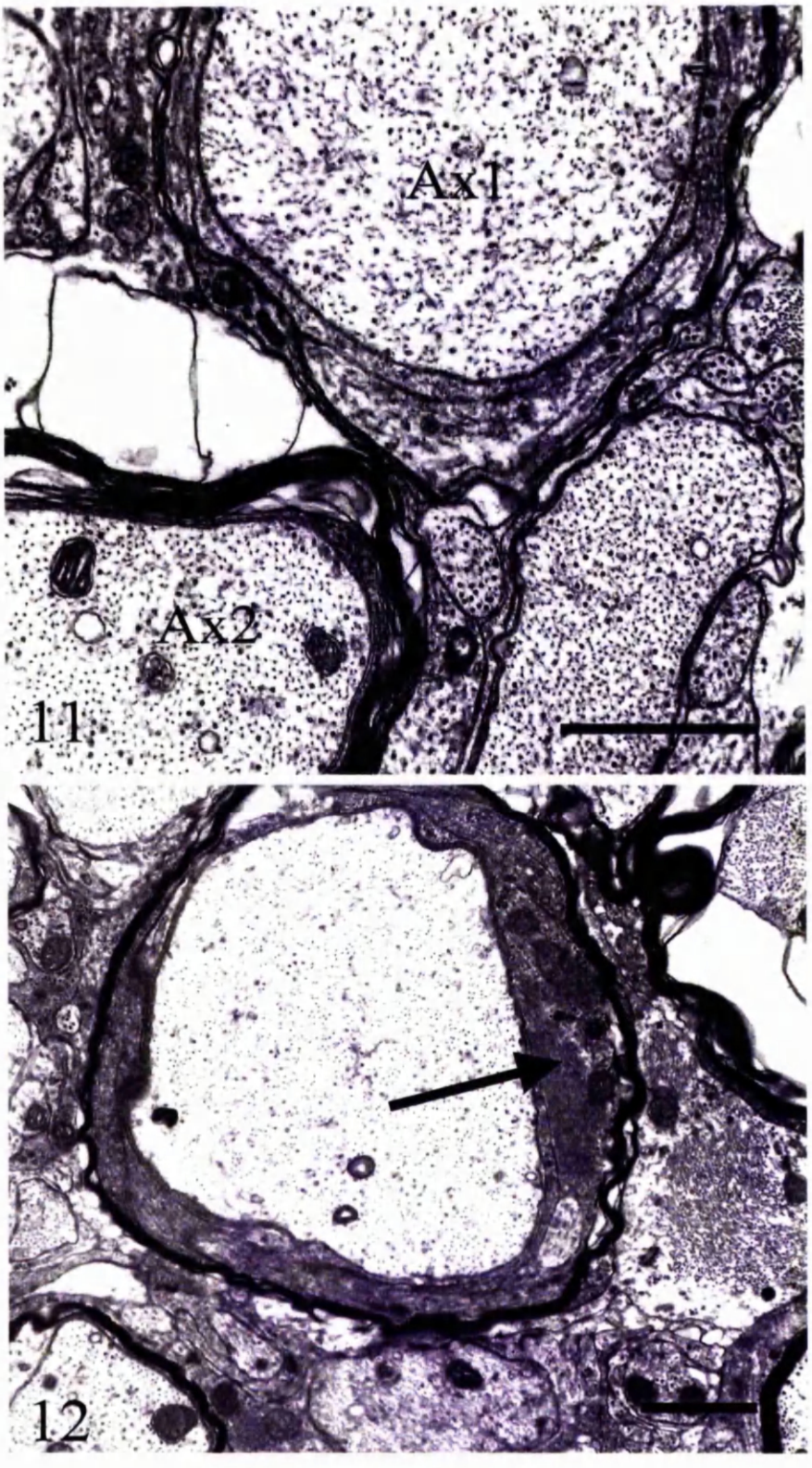

Fig. 11. Electron micrograph of C57 *rsh* spinal cord at P20. Axon (A1) is surrounded by uncompacted oligodendrocyte prcesses and axon (A2) by a thin undulating myelin sheath.

Fig. 12. Electron micrograph of C57 *rsh* spinal cord at P20. The axon is surrounded by oligodendrocyte processes and a thin sheath. An astrocye process (arrow) is present within the sheath. Bars = 1um.

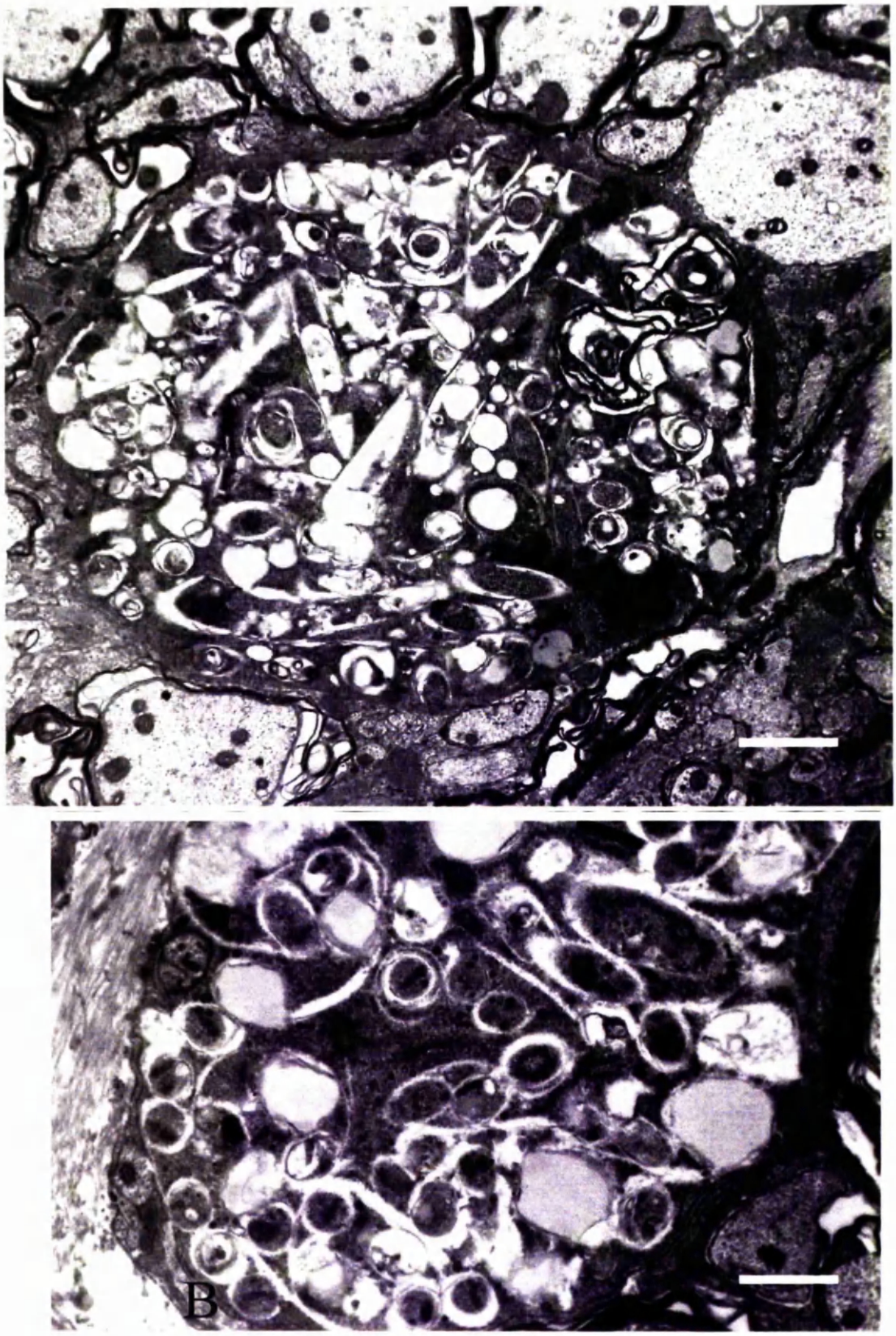

Fig. 13A. Electron micrographs of microglial cell. The cytoplasm contains numerous lipid and membranous inclusions. Bar = 1um;
Fig. 13B. Cytoplasm of microglial cell. The various inclusions are shown at higher magnification. Bar = 2um.

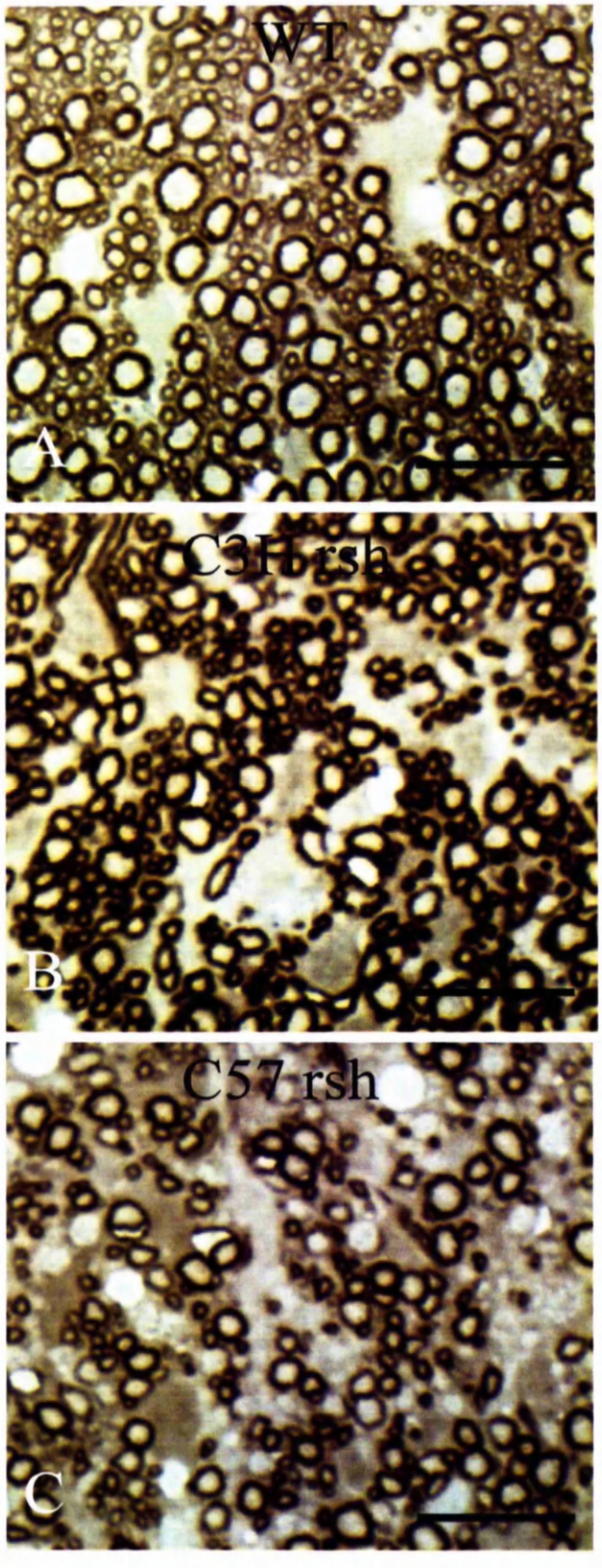

Fig. 14. MBP immunostaining. Resin sections of ventral column of spinal cord immunostained for MBP. Bars = 20um

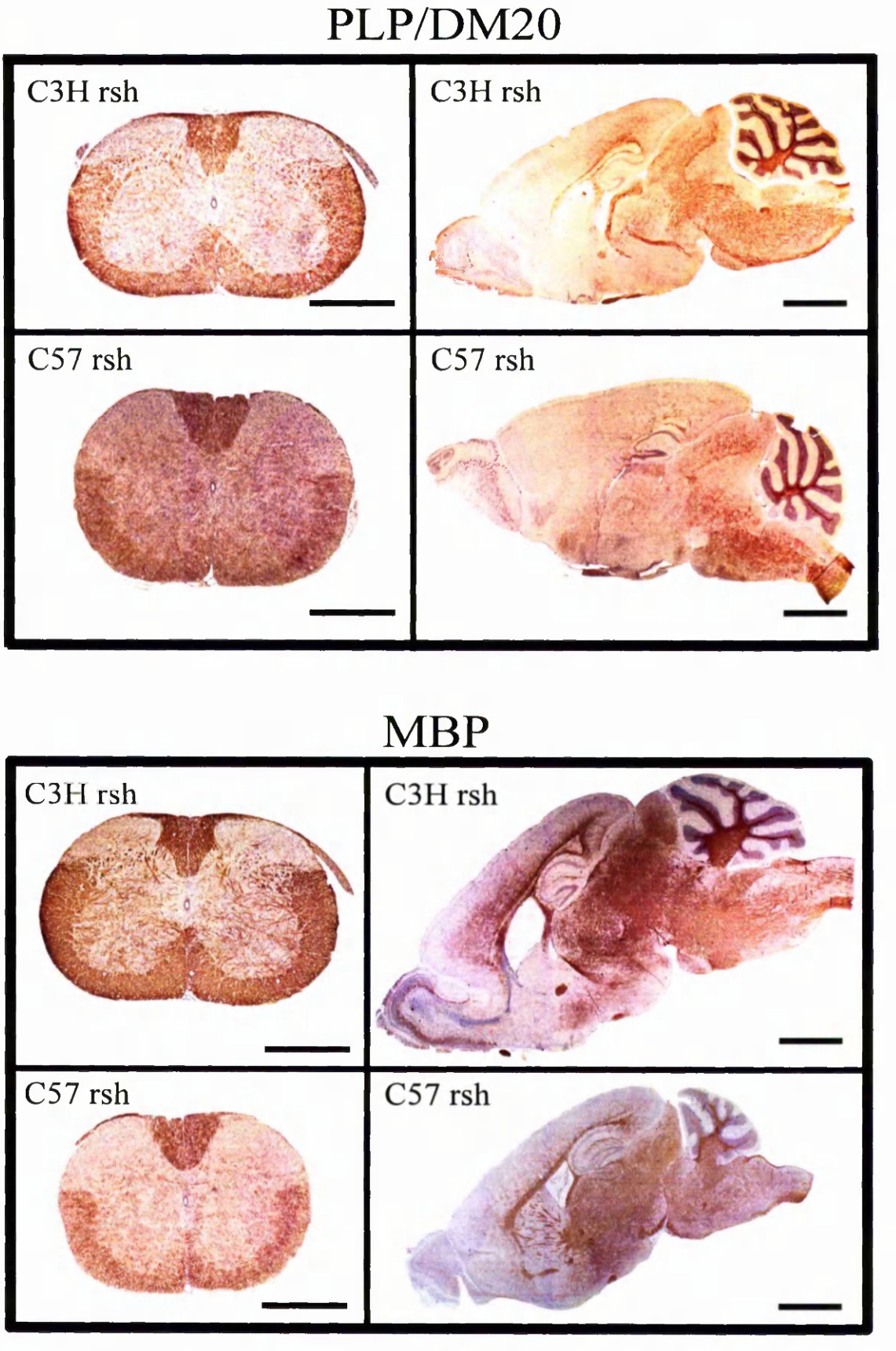

Fig. 15. Immunostaining for PLP/DM20 and MBP. Saggital brain and transverse spinal cord sections of C3H and C57 *rsh* at P20. Bars cord = 0.5mm; brain = 2mm.

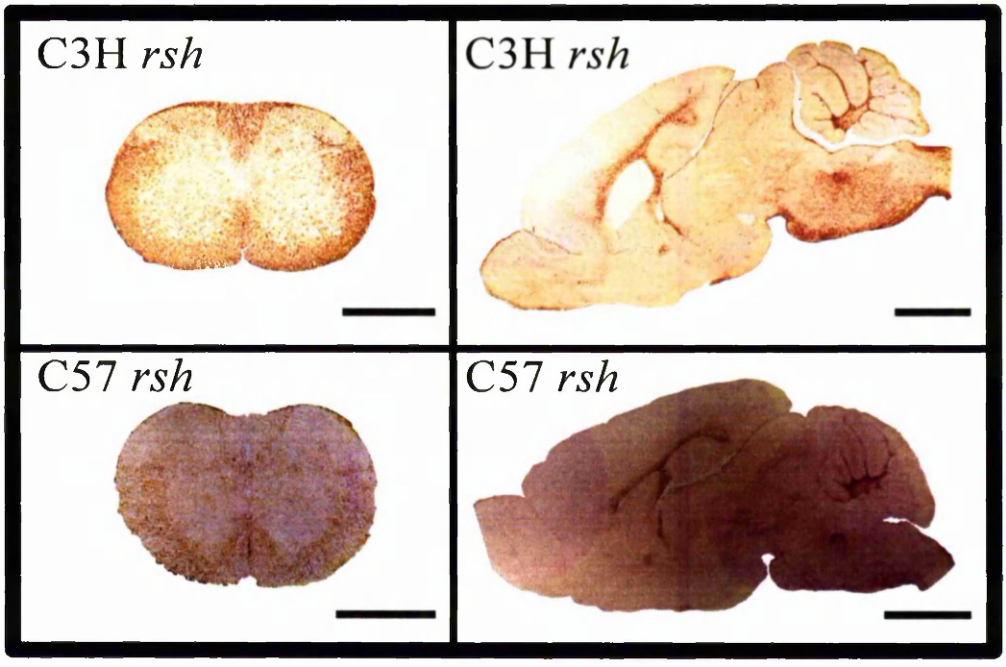

Fig. 16. Immunostaining for GFAP in spinal cord and brain of C3H and C57 mutants. The intensity and extent of staining is greater in the C3H *rsh*. Bar cord = 0.5mm; brain = 2mm.

4.3 Quantitative studies in *rumpshaker*

4.3.1.1 Introduction

Myelination is a feature of both CNS and PNS. Within the former, there is a very definite spatiotemporal pattern of myelination in which the spinal cord, particularly the cervical region, is one of the earliest sites. Most mammalian CNS axons are myelinated and the functions and structure of myelin have been described previously (see 1.8 The axon, page 7 and 1.10 Myelin sheath, page 9). Myelin is made up of lipids and proteins, of which PLP is the major component; thus, abnormalities in its molecular structure could result in phenotypic deficits. As defects in myelination or loss of formed myelin are associated with clinical deficits the differences between C3H and C57 *rumpshaker* mice might be reflected in differences in the amount of myelin. To evaluate the amount of myelin, myelin volume and myelin areas were measured in the ventral cervical spinal cord of both strains of wild type and mutant mice.

4.3.1.2 Materials and Methods

4.3.1.2.1 Myelin volume and myelin area

The estimation of myelin areas was made at P15, P20, P25 and P30 as described in (3.9.1, page 42). Myelin volume was calculated only in the mutant mice at P20 and P30 as described in (3.7.4, page 34).

4.3.1.3 Results

4.3.1.3.1 Myelin areas

The myelin areas were estimated in resin sections immunostained for MBP at P15, P20, P25 and P30. The two strains of wild types showed an identical profile. An obvious difference was noted between the mutant animals and their normal littermates at all ages examined. A significant reduction was noted between C57 *rsh* and C3H *rsh* (Figure 17, page 67).

4.3.1.3.2 Myelin volume

The volume of myelin present in the ventral column of cervical spinal cord of the two mutants at P20 and P30 was estimated by point counting of compact myelin using electron micrographs. The myelin volume was significantly reduced by approximately 50% in C57 *rsh* over C3H *rsh* (Figure 18, page 67).

4.3.1.3.3 Percentage of myelinated axons

Using the same EM micrographs used for myelin volume quantification, the percentage of myelinated axons was considered. It was 38 ± 3.2%; (M ± SEM, n = 4) in C3H *rsh* whereas this was significantly decreased in C57 *rsh* 19.77 ± 2.6%, (M ± SEM, n = 4).

4.3.1.4 Discussion

Mutations of the *Plp* gene result in severe myelin deficits. The degree of dysmyelination varies between mutants and although the C3H *rsh* represents one of the least severe phenotypes, there is still a significant myelin deficit. The C57 *rsh* was more severely affected than C3H *rsh* with approximately half the amount of myelin of the C3H *rsh*. A heterogeneous population of myelinated axons was found in *rumpshaker*. In C3H *rsh*, the majority of axons were myelinated whereas in C57 *rsh* a smaller percentage were surrounded by myelin and naked axons were seen frequently in the spinal cord white matter. In both mutants the majority of sheaths were disproportionately thin for the axonal diameter although in smaller axons the deficit appeared less obvious; the sheath thickness was not quantified.

The *jimpy*, *jimpy-msd* and *jimpy-4j* represent the most severely affected *Plp* mutant animals, showing little myelin in the CNS (Duncan *et al.*, 1989; Duncan, 1990; Billings-Gagliardi *et al.*, 1995). In contrast, the C57 *rsh* has more myelin than any of these mutants although the clinical presentation is very similar. Interestingly, the C57 *rsh* also has more myelin than the *shiverer* mouse, an *Mbp*-deletion mutant, which die at approximately 4-5 months of age (Chernoff, 1981). It seems probable that the presence of lengths of naked axon interspersed with thinly sheathed areas is responsible for some of the clinical signs, for example the tremor. However, whether the difference in amounts of myelin is enough to explain the seizures in one strain of *rumpshaker* is more debateable. The amount of myelin does not necessarily correlate closely with the longevity of the animal and several mutants with extended lifespan and virtually no myelin, have been described (Billings-Gagliardi *et al.*, 1999; Wolf *et al.*, 1999).

Myelin mutant animals have been used to explore the role of oligodendrocytes and compact myelin in determining the structure of axons, particularly in relation to the nodal/paranodal area or the axonal cytoskeleton. Many instances have employed *shiverer* (Sánchez *et al.*, 1996; Brady *et al.*, 1999; Rasband *et al.*, 1999a; Rasband *et al.*, 1999b; Tait *et al.*, 2000; Sánchez *et al.*, 2000; Boiko *et al.*, 2001) although the *jimpy* mutant has also been used (Baba *et al.*, 1999; Jenkins and Bennett, 2002). Some diversity of opinion has resulted as to the necessity of compact myelin and/or oligodendrocyte processes in defining the molecular architecture of the

nodal/paranodal area; one possible reason is that without ultrastructural studies in combination with the immunostaining procedure, it is very difficult to decide if a single layer of oligodendrocyte process is present. The aspect of nodal organisation and molecular composition in *rumpshaker* has not been investigated in the present thesis, but is an aspect worthy of future study.

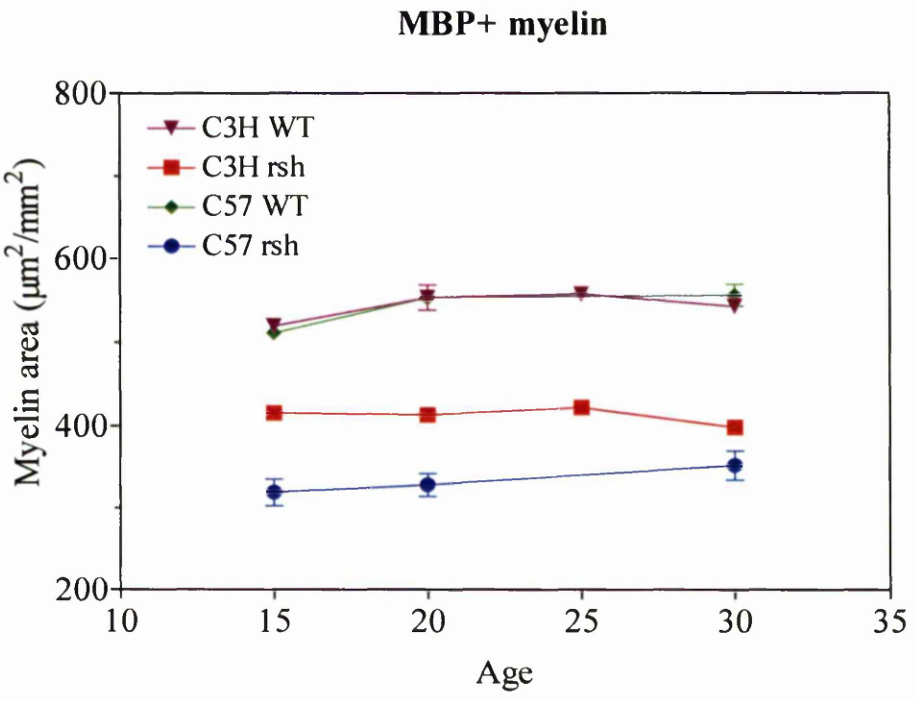

Fig. 17. Myelin area (defined as the area of MBP-stained myelin per mm^2 of ventral white matter) between P15 and P30. The two wild types are identical and different from their respective mutants. The C3H *rsh* has more myelin at all ages.

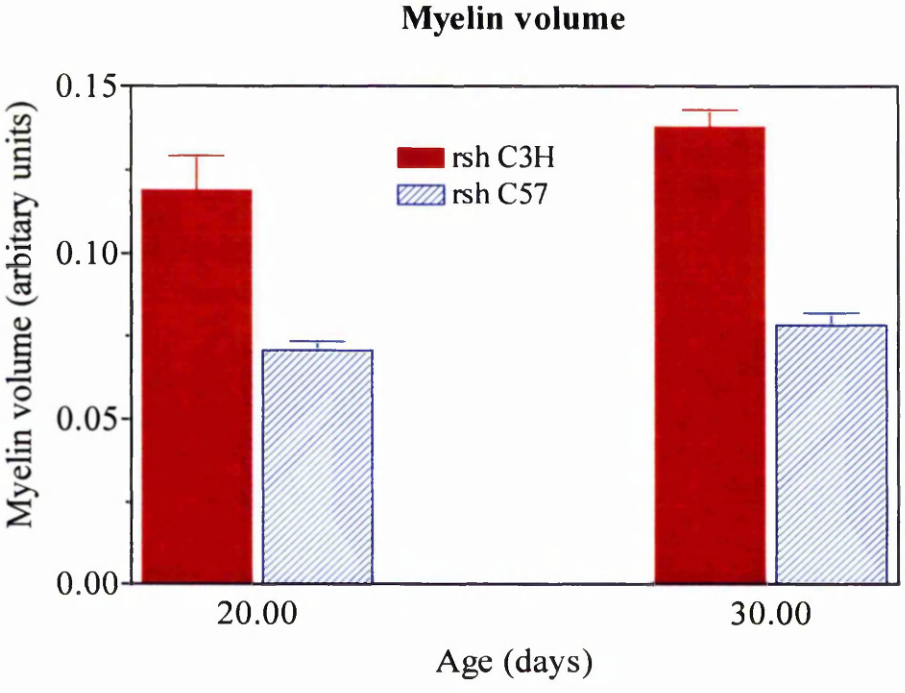

Fig. 18. Myelin volume, derived by point counting from electron micrographs. There is significantly more myelin in the C3H *rsh* compared with the C57 mutant at both ages.

4.3.2 Evaluation of total glial cell and oligodendrocyte numbers

4.3.2.1 Introduction

Diseases of the CNS, of various aetiologies, may selectively produce changes in the numbers of neurons and glia. Spontaneous *Plp* gene mutations generally result in diffuse pathology affecting myelin-producing cells, the myelin itself and the supporting environment. There has been a long-standing debate as to whether the dysmyelination in *Plp* mutants is a direct result of apoptosis of oligodendrocytes and therefore a reduction in their numbers or whether the oligodendrocytes death and myelin deficit are not a direct cause and effect (Knapp *et al.*, 1986; Thomson *et al.*, 1999). In previous studies no reduction in oligodendrocyte numbers was detected in the C3H *rsh* (Griffiths *et al.*, 1990; Mitchell *et al.*, 1992; Fanarraga *et al.*, 1993). To re-evaluate this and to determine if the same was true for the C57 mutant the glial cell population was quantified in resin sections at various ages. Total glial cells and differential counts were considered in *rumpshaker* and wild types in both genetic backgrounds of mice. Additionally, the population of NG2+ oligodendrocyte progenitors was quantified.

4.3.2.2 Material and methods

4.3.2.2.1 Glial cell quantification in resin sections

Total glial cell numbers and densities were estimated at P10, P15, P20, P25 and P30 as described in (3.7.1, page 33). The areas of the whole spinal cord and white matter, in transverse section were determined as described in (3.7.1, page 33).

4.3.2.2.2 Differential count of glial cells in resin sections

Oligodendrocytes, astrocytes and microglia were counted differentially at P20 as described in (3.7.2, page 34).

4.3.2.2.3 Quantification of APC-positive mature oligodendrocytes

Quantification of APC-positive mature oligodendrocytes was performed as described in (3.9.3, page 43).

4.3.2.2.4 Quantification of NG2-positive oligodendrocyte progenitors

Quantification of NG2-positive oligodendrocyte progenitors was performed as described in (3.9.4, page 43).

4.3.2.3 Results

4.3.2.3.1 Glial cell population (resin sections)

The areas of the whole spinal cord and the white matter were measured in transverse section at the different ages studied. The white matter area increased steadily as the animal aged. After P15, the differences in white matter area between wild type and mutant were significant (Figure 19, page 73).

Total glial cell density was evaluated between P10 and P30. There was no difference between the C3H WT and the C57 WT at any age. The values in both mutants were significantly greater than their respective wild types at all ages. The values in the two mutants were similar at P10; thereafter the density in the C57 *rsh* was elevated at P15 and P20, similar at P25 and reduced at P30 compared with the C3H mutant (Figure 20, page 73).

Using the glial cell density in the ventral column and the white matter area the approximate total numbers of glial cells in the white matter per transverse section could be calculated. Total glial cell numbers were similar in both wild type strains and elevated in both mutants. The values in the C57 *rsh* were elevated at P20 and P25 compared with the C3H mutant (Figure 21, page 74).

4.3.2.3.2 Differential count of glial cells in resin sections

A differential count of the glial population, based on cell morphology, was performed at P20. The specific interest at this stage was the number of oligodendrocytes present in the various genotypes. At this single time point, there was no difference in oligodendrocyte or astrocyte numbers between any of the genotypes. The number of microglia was elevated in both mutants relative to wild type (Figure 22,page 74).

4.3.2.3.3 APC-positive mature oligodendrocytes

To provide a further independent marker for oligodendrocytes we used the APC antigen to quantify cells in the ventral columns between P15 and P30. Again, we determined cell density and total cell numbers. APC density (and total cells) was similar between both groups of wild type and stayed relatively constant between P15 and P30. In the C3H mutants the values were significantly elevated at P20 and P30 compared with their wild type. The C57 values were similar to the respective wild type at all ages but not different from the C3H *rsh* (Figure 23, page 75 and Figure 24, page 76).

4.3.2.3.4 NG2-positive oligodendrocyte progenitors

NG2+ cell density in the ventral white matter was similar in both groups of wild type, declining steadily between P15 and P30. The values in the C3H mutant were elevated over its wild type only at P30 whereas the C57 *rsh* was higher at all ages compared with wild type and with the C3H mutant (Figure 25, page 77).

4.3.2.4 Discussion

Quantification of the total glial cell population in the spinal cord indicated that the mutant animals were significantly different from their respective normal littermates on both genetic backgrounds. Total glial cell numbers and density in C57 *rsh* were significantly increased over its C3H counterpart at P20 and P25. A similar pattern of increased glial cell density was reported in *jimpy* (Thomson *et al.*, 1999). Moreover, quantification of EM images of *shaking* pup cervical spinal cord and optic nerve indicated an increase in glial numbers (Duncan *et al.*, 1983). It contrasts with the results obtained from EM thymidine autoradiographic study of *md*-rat optic nerve which showed no increase in glial cell numbers (Jackson and Duncan, 1988).

The total glial cells include oligodendrocytes, astrocytes, microglia and various immature and unidentifiable glia. The main focus in this section is on the oligodendrocyte lineage. The microglial population is discussed later (see 4.3.5, page 90). The astrocyte response is described in (4.2.4 Discussion, page 54).

As indicated in the Introduction, loss of mature oligodendrocytes has been implicated as the main reason for the hypomyelination in many of the animal and human *Plp/PLP* gene mutations. *rumpshaker*, on the C3H background, was described as a *Plp* mutant with normal or probably increased numbers of oligodendrocytes (Griffiths *et al.*, 1990; Mitchell *et al.*, 1992; Fanarraga *et al.*, 1993); this finding was confirmed in the present study. The original quantification of cells was based largely on nuclear morphology in resin sections and comparative observations of electron micrographs. This approach has been criticised as not providing a definitive identification of cell type. It is worth mentioning that whatever method is used there are always problematic areas; for example using in situ hybridization for *Plp* or immunostaining for PLP it can be difficult to differentiate a weak positive from a negative cell. To provide an independent assessment of oligodendrocyte numbers we used the recently described APC antigen to mark these cells (Bhat *et al.*, 1996; Fernandez *et al.*, 2000). We obtained similar results showing that in the C3H *rumpshaker* the number of APC+ cells was increased at peak myelination, relative to wild type.

If oligodendrocyte loss is critical in determining the overall phenotype, it should be evident in the C57 *rsh*. However, analysis of oligodendrocytes using both morphological and immunostaining criteria showed that their numbers were not reduced compared with wild type. The assessments suggested that the numbers of oligodendrocytes in the C3H *rsh* was greater than the C57 mutant at P20, but the difference was not significant. The main reason for the difference in total glial cell numbers between the two mutants reflects changes in the microglial population (see 4.3.5, page 90). The data strongly support the argument that in *rumpshaker* a reduced number of oligodendrocytes is not the reason for the hypomyelination.

One problem in comparing oligodendrocyte numbers between different *Plp* mutants is that a variety of ages, locations and methods have been used, making it almost impossible to make meaningful comparisons. However, using in situ staining for galactcerebroside, it has been demonstrated that the oligodendrocyte number is not reduced in corpus callosum and cerebellum of P6, 10 and 15 *jimpy* mice (Ghandour and Skoff, 1988). Again in another species, the *paralytic tremor* rabbit, a combination of resin sections stained with toluidine blue and EM images from the dorsal funiculus of the cervical spinal cord, the intracranial portion of the optic nerve, and the middle portion of the anterior part of the corpus callosum at P8, 14 and 90 suggested the number of oligodendrocytes was maintained (Taraszewska and Zelman, 1987). However, in the cervical spinal cord and optic nerve of *shaking* pup at 4 and 8 weeks there appeared to be decreased numbers of oligodendrocytes (Duncan *et al.*, 1983).

Developmentally, oligodendrocytes develop from progenitor cells, which in turn arise from precursor cells in the neuroepithelium. Until recently, these earlier stages have been difficult to identify in situ, due to a lack of suitable markers; antibodies such as A2B5 and O4, which are used to surface stain cultured cells are difficult to use in tissue sections. The NG2 chondroitin sulphate proteoglycan has been found to label oligodendrocyte progenitors with a high degree of specificity (Stallcup and Beasley, 1987; Nishiyama *et al.*, 1996). This marker has been used to demonstrate a vast array of hitherto unrecognised cells in the parenchyma of animals and humans, including adults and the numbers of such cells increase in association with disease or injury (Reynolds and Hardy, 1997; Keirstead *et al.*, 1998; Nishiyama *et al.*, 1999; Chang *et al.*, 2000; McTigue *et al.*, 2001). It is known to label blood vessels but distinguishing these from the progenitors is relatively straightforward. A very recent report has suggested macrophages may, in certain circumstances, express NG2 (Jones *et al.*, 2002), although other reports indicate that reactive microglia are not NG2+ (Nishiyama *et al.*, 1997). Interestingly, in the murine cerebral cortex two sub-populations of NG2+ progenitors have been described on the basis of presence

or absence of expression of the *Plp* gene (Mallon *et al.*, 2002). Expression of NG2 overlaps with the earlier PDGF α-receptor marker. Other markers such as the transcription factors Olig1 and Olig2 and Nkx2.2 can be used to identify even earlier stages of the oligodendrocyte lineage. These were not used in the present study.

Although there are increased numbers of apoptotic glial cells, including oligodendrocytes, particularly in C57 *rsh* (see 4.3.3, page 78), the number of oligodendrocytes is not diminished. One possible reason is an increase number of progenitors that subsequently differentiate into oligodendrocytes. In keeping with this the NG2+ population was increased relative to wild type in the C57 *rumpshaker* between P15 and P30 whereas only at the latter age was it elevated in the C3H mutant. Studies of oligodendrocyte progenitors in other *Plp* mutants have produced varying opinions. In many of the early studies the more definitive markers were not available. In the *md*-rat the population of progenitors identified by PDGF α-receptor was reported as normal (Pringle *et al.*, 1997). In *jimpy*, progenitors (or presumed progenitors) are reported as being increased (Skoff, 1982; Wu *et al.*, 2000). The increased number of progenitors in both *jimpy* and *rumpshaker* is associated with increased proliferation (see 4.3.4 Glial cell proliferation, page 84).

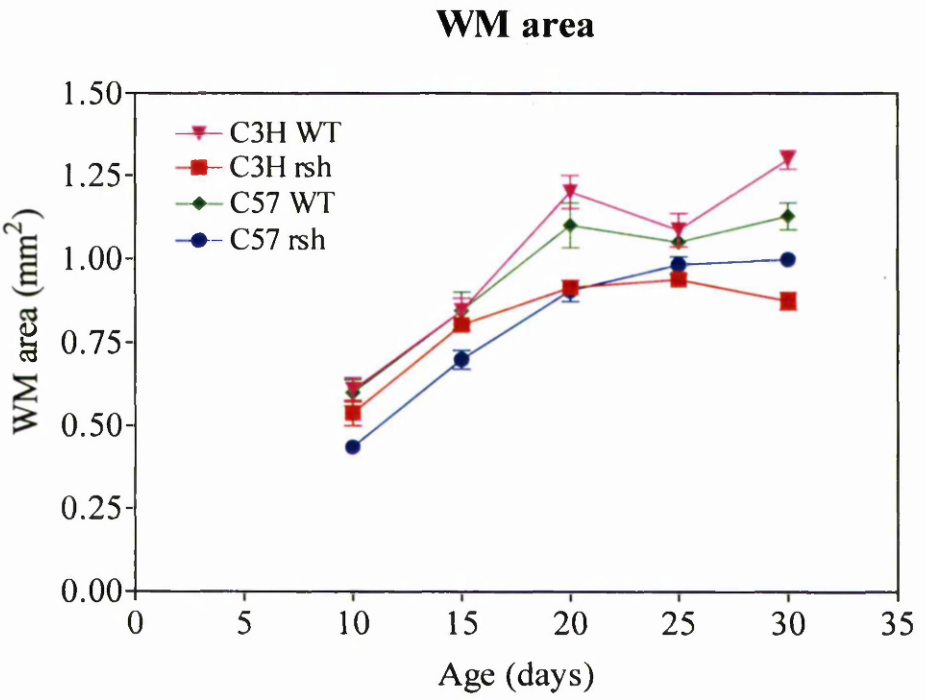

Fig. 19. Area of white matter of transverse section of the cervical spinal cord between P10 and P30. The area in the C3H mutant is less than the respective wild type after P15 whereas the C57 *rsh* is not different from its wild type except at P30. The two mutants differ only at P30.

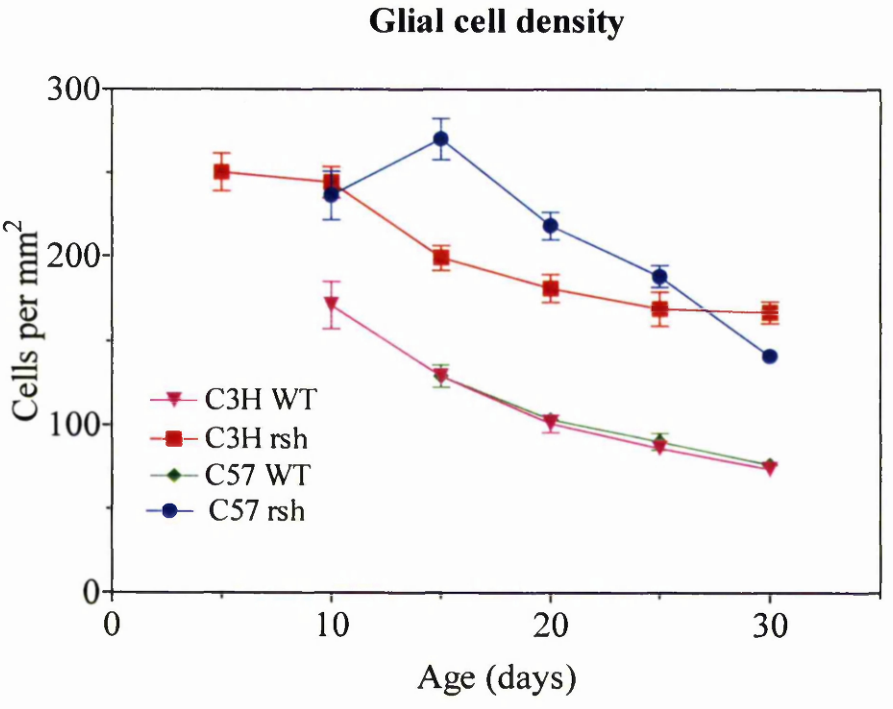

Fig. 20. Density of all glial cells in ventral white matter between P10 and P30. The two wild types are identical and differ from their respective mutants. The density in the C3H *rsh* is elevated relative to the C57 mutant at P15 and P20.

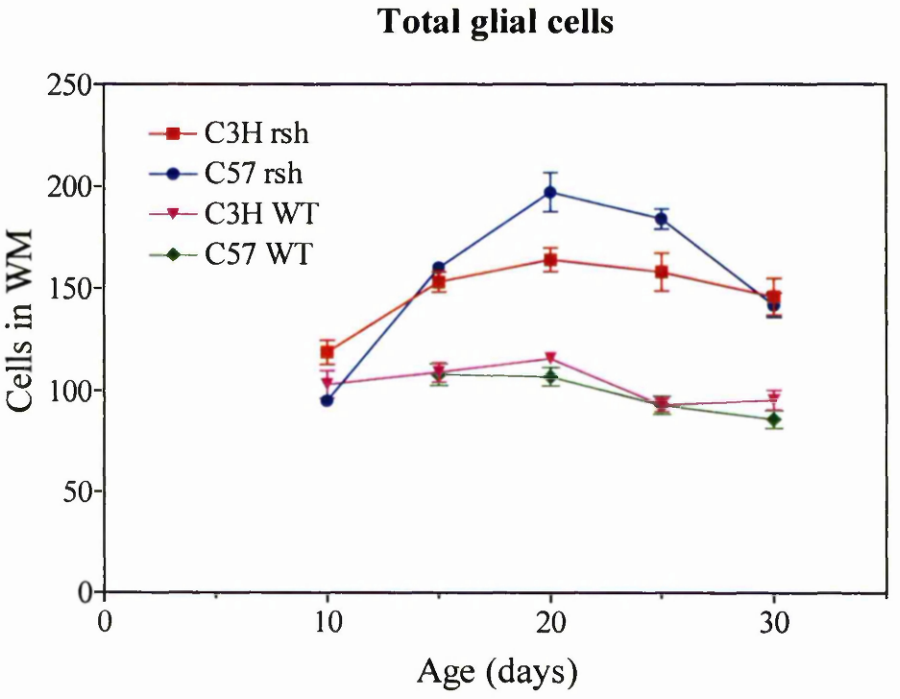

Fig. 21. Total number of glial cells in white matter of transverse section of cervical cord between P10 and P30. The two wild types are identical and different from the mutants except at P10. The two mutants differ from each other at P20 and P25.

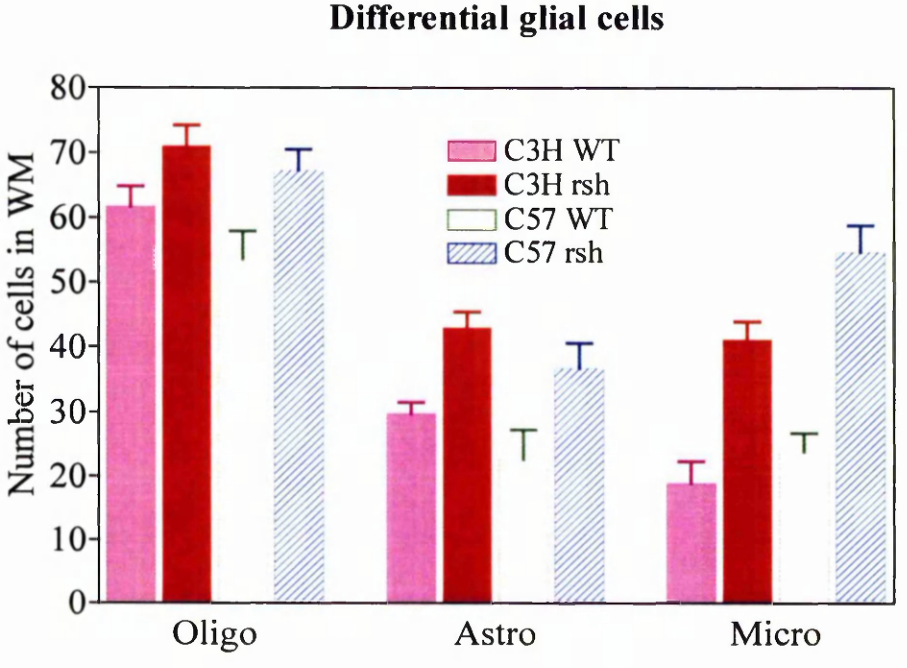

Fig. 22. Differential glial cell count at P20. There is no difference in the number of oligodendrocytes (Oligo) nor astrocytes (Astro). Both mutants have more microglia (Micro) than the respective wild types and the C57 *rsh* exceeds the C3H mutant.

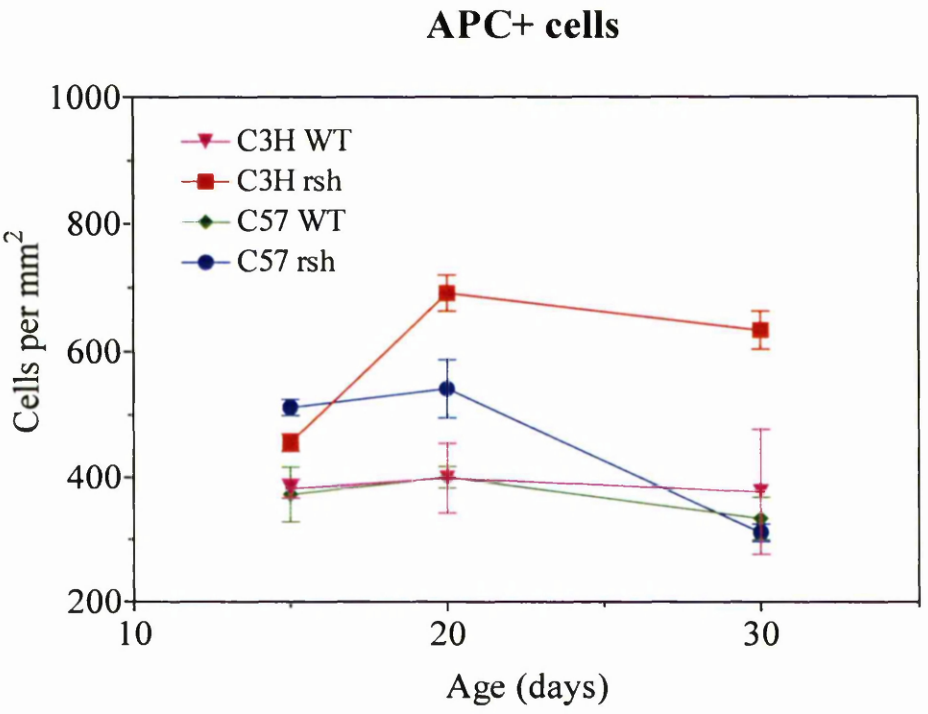

Fig. 23A. APC density. Both C3H and C57 wild types are similar at all ages but differ from their mutants at P15. The C3H *rsh* is also significantly different from this group of mice at P20-30.

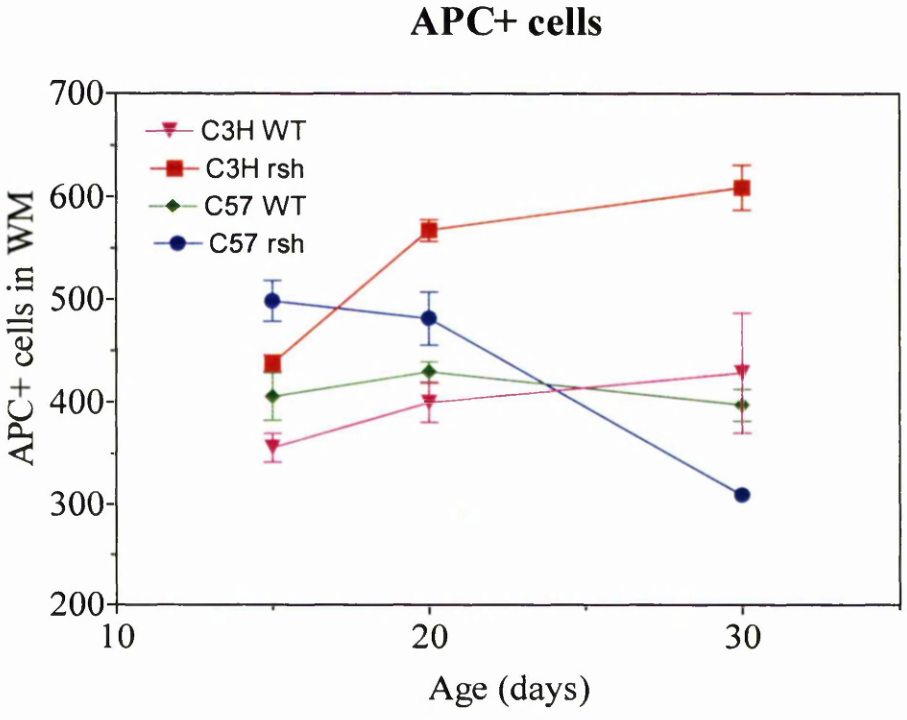

Fig. 23B. Total APC+ cells in the white matter of transverse section of cervical cord. There is no marked difference in the number of APC + cells between the four groups of mice at any age except at P30 where C3H mutant is different from its C57 counterpart.

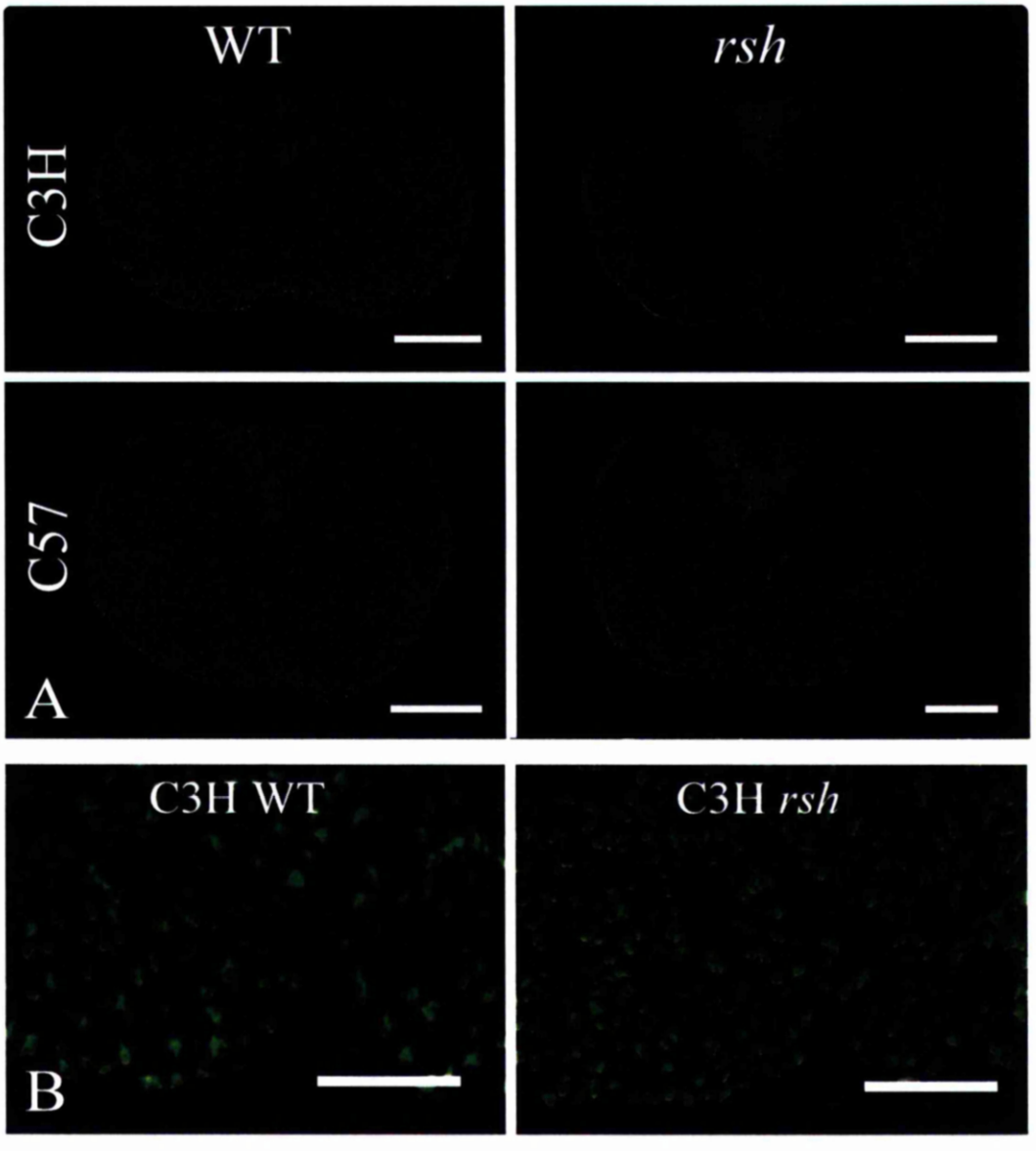

Fig24A. Immunostaining for APC. Spinal cords from mice of all genotypes, aged P20, immunostained for APC. Bars = 0.5mm

Fig. 24B. Ventral column of white matter from C3H wild type and mutant mice immunostained for APC. Bars = 100um.

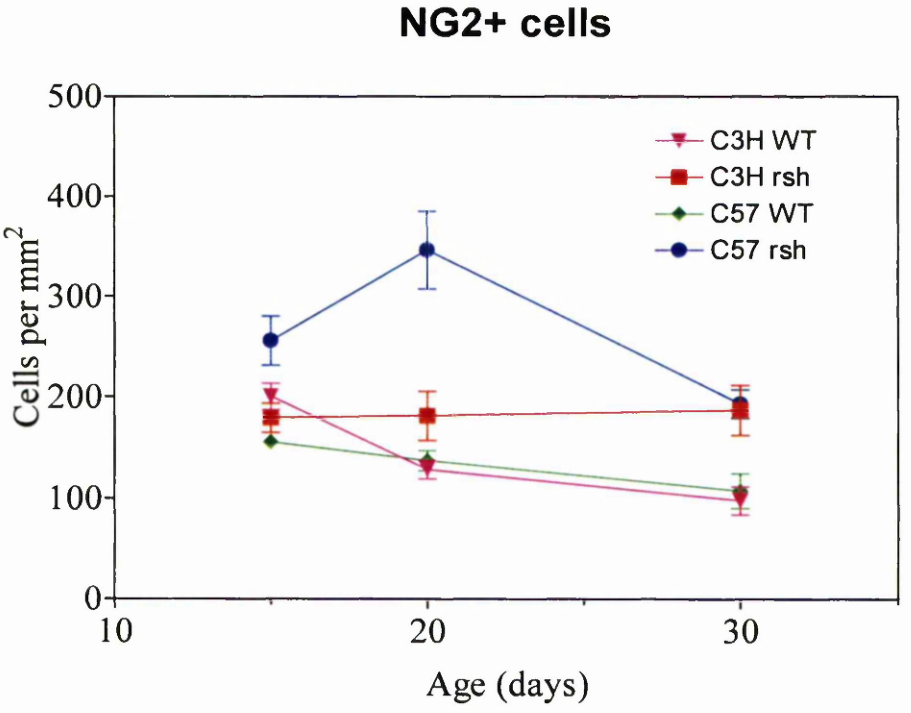

Fig. 25. NG2+ cell density. C3HWT and C57 WT have a similar NG2+cell density at all age and C3H *rsh* up to P20. C57 WT has less density than its mutant. The density of C57 *rsh* appears higher than C3H *rsh* at P15-20 but it is similar at P30.

4.3.3 Glial cell apoptosis

4.3.3.1 Introduction

Programmed cell death or apoptosis, a complex mechanism, is seen widely in diseases and normal development. Histopathologically, it is characterised by nuclear pyknosis, chromatin condensation, intact plasma membrane, cellular organelles and intracellular blebs (for review see Casaccia-Bonnefil, 2000). Mutations in the *Plp* gene result in a complex pathology including glial cell apoptosis (Skoff, 1995), presumably of oligodendrocyte lineages. Classical and immunostaining methods were applied to quantify apoptotic cells in the two mutants and their respective wild types. Attempts were also made to define the nature of the dead cells by double labelling of caspase-3-positive cells.

4.3.3.2 Material and methods

4.3.3.2.1 Quantification of pyknotic nuclei numbers

Quantification of Pyknotic nuclei numbers was performed as described in (3.7.3, page 34).

4.3.3.2.2 Quantification of Caspase-3-positive cells

Quantification of Caspase-3-positive apoptotic cells was performed as described in (3.9.5, page 43).

4.3.3.2.3 Identification of Caspase-3-positive glial cells

Double immunostaining of Caspase-3-positive glial cells for APC and CD45 was performed as described in (3.8.14, page 41).

4.3.3.3 Results

4.3.3.3.1 Pyknotic nuclei numbers

The numbers of dead cells between P10 and P30 was estimated by counting the number of pyknotic nuclei in all columns of the white matter in 1μm resin sections (Figure 26, page 82). Values in both strains of wild type were similar, being maximal at P10 and then declining to P30. The numbers of pyknotic nuclei in the both mutants were increased over their wild types at P15 and thereafter, by approximately two fold in C3H and seven fold in C57 *rumpshaker*. The difference between the two mutants was also significant between P15 and P30.

4.3.3.3.2 Caspase-3-positive apoptotic cells

In the resin sections the number of pyknotic nuclei had been counted throughout all columns of white matter. In order to provide an estimate of apoptotic cells in the ventral white matter we immunostained animals between P10 and P30 for caspase-3, an effector caspase, acting at a slightly earlier period of the pathway than the late-stage nuclear changes denoted by pyknosis. We calculated cell density and, from that value and the area, calculated the total numbers of cells in white matter; both parameters gave similar results. Surprisingly, the density of caspase-3+ cells in C3H wild type was significantly increased when compared with that of C57 wild type at P10 to P20 but similar at P30 (Figure 27, page 82). The values in the C3H *rsh* were increased over wild type between P15 and P30 whereas the C57 mutant was increased at all ages relative to its wild type and to the C3H *rsh*.

4.3.3.3.3 Identity of the caspase-3-positive cells

After quantifying the level of apoptosis using pyknotic nuclei and caspase-3-positive cells, the identity of the dying cells was examined. The caspase-3-positive cells were double labelled with other markers to define the nature of the cells undergoing apoptosis. Cervical cord sections from C57 *rsh* at P15 were selected, as this was an age and genotype of maximum involvement. Among the caspase-3-positive cells, 30.43% and 40.74% were APC-positive and CD45-positive cells, respectively (Figure 28, page 83).

4.3.3.4 Discussion

This study has shown that programmed cell death is a predominant feature in the *rumpshaker* phenotype and that this process is particularly prominent in the C57 mutant. In previous studies of C3H *rsh,* cell death was not included as a feature (Griffiths *et al.*, 1990; Schneider *et al.*, 1992), an aspect which the present study has shown to be incorrect although the basic tenet of the previous studies, that the number of oligodendrocytes is not reduced, has been confirmed. Increased numbers of dying cells is a feature of the *Plp* mutants such as *jimpy* (Privat *et al.*, 1982; Knapp *et al.*, 1986; Knapp *et al.*, 1990; Vermeesch *et al.*, 1990; Skoff and Knapp, 1990) and md-rat (Boison and Stoffel, 1989; Lipsitz *et al.*, 1998) and broadly correlates with the severity of hypomyelination (Skoff, 1995). Similarly, in the present study the number of apoptotic cells was greater in the more severe phenotype. The dying cells in *rumpshaker* and other *Plp* mutations show the classic morphological changes of programmed cell death and activation of the caspase cascade. The TUNEL technique, which end labels cleaved DNA has also shown increased numbers of labelled cells in *Plp* mutants (Skoff, 1995; Lipsitz *et al.*, 1998; Knapp *et al.*, 1999) although a close correlation between numbers of TUNEL+ cells

and pyknotic nuclei was lacking. These studies and others (Knapp *et al.*, 1986; Skoff, 1995; Gow *et al.*, 1998; Lipsitz *et al.*, 1998; Grinspan *et al.*, 1998; Beesley *et al.*, 2001) have indicated that the majority of dying cells were oligodendrocytes. As it is difficult to ascertain the nature of the apoptotic cells by classical preparations we used double labelling to define the cell lineage of caspase-3-positive apoptotic cells in the *rumpshaker*. It was found that approximately 30% were APC+ oligodendrocytes and 40% labelled with the CD45 antigen. It is possible that some of the CD45+/caspase-3+ cells have in fact phagocytosed apoptotic oligodendrocytes and thus, the proportion of dead oligodendrocytes is higher than estimated. An attempt to double stain for NG2 and caspase-3 was unsuccessful as both antibodies were from the same species. It is unlikely that many NG2+ cells would have been apoptotic as cells undergoing this process are usually immature to early mature oligodendrocytes rather than progenitors (Grinspan *et al.*, 1998).

Only the cervical spinal cord was assessed for apoptotic cells in the present study but it is probably that similar features would have been evident throughout the CNS. However, in general, the timing of the apoptosis correlates with the temporal sequence of myelination (Knapp *et al.*, 1986; Skoff, 1995; Lipsitz *et al.*, 1998; Grinspan *et al.*, 1998) and would be expected to be later in brain regions.

Increased numbers of apoptotic oligodendrocytes are also found in *Plp* transgenics with increased dosage of the *Plp* gene (Readhead *et al.*, 1994; Inoue *et al.*, 1996; Anderson *et al.*, 1999; Bauer *et al.*, 2002) but not in *Plp* null mice (Klugmann *et al.*, 1997; Yool *et al.*, 2001).

The mechanism of apoptosis in *Plp* mutations is not known. It may be linked to an "intrinsic toxicity" of the abnormal PLP product (Williams, II and Gard, 1997) or an accumulation of product in the RER (Gow *et al.*, 1994b; Gow and Lazzarini, 1996; Gow *et al.*, 1998), possibly evoking an unfolded protein response (Southwood and Gow, 2001). In this hypothesis, changes in the frequency of apoptosis between mutations is ascribed to differences in the toxicity of the encoded PLP. It is also possible that the effect may be indirect; for example, the mutant oligodendrocyte may fail to establish proper connections with an axon and thus be deprived of critical trophic factors (Thomson *et al.*, 1999). This study suggests that if the misfolded PLP is toxic to the cell it cannot be the only operating factor. If it was, then one would expect the same frequency of apoptosis between the two rumpshakers as the primary, secondary and possibly the tertiary structure of the *rumpshaker* PLP should be identical.

Although increased death of oligodendrocytes is a feature of *rumpshaker* the oligodendrocyte numbers are maintained. This would argue that the apoptosis is not

the primary direct cause of the dysmyelination, which must be related to a inability of the mutant oligodendrocyte to synthesise appropriate amounts of myelin. Nevertheless, the frequency of apoptosis in the more severe mutants is likely to compound the problem and may well contribute to the degree of dysmyelination, particularly as the condition advances.

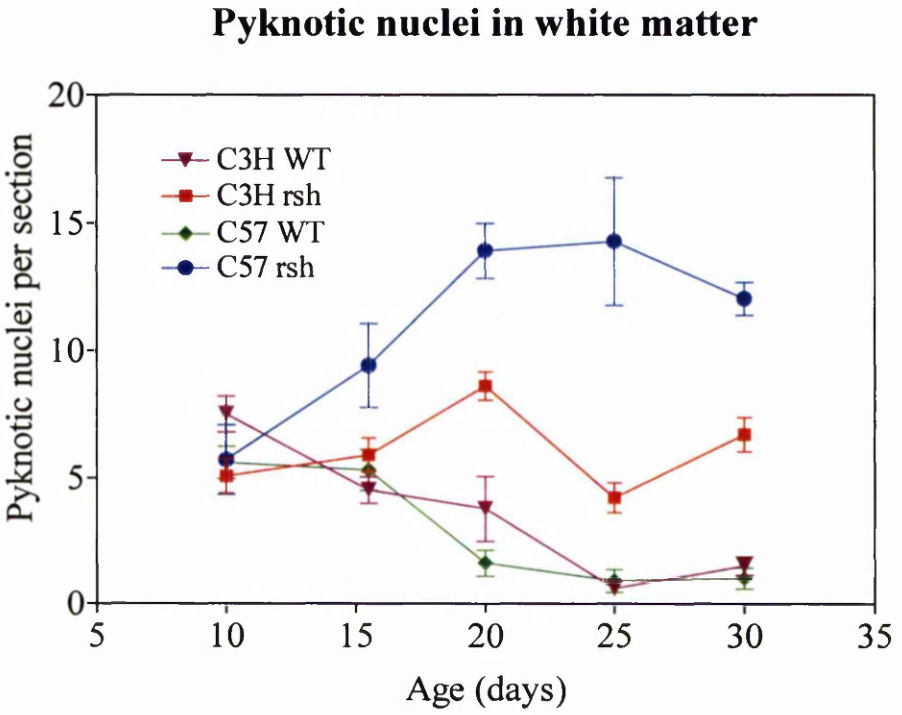

Fig. 26. Pyknotic nuclei in the white matter of transverse sections of cervical cord. All group of mice appear similar at P10 and the two wild types are identical at all ages. The difference in dead cells is more obvious between the two wild types and their mutants and between the two mutants themselves from P15-30.

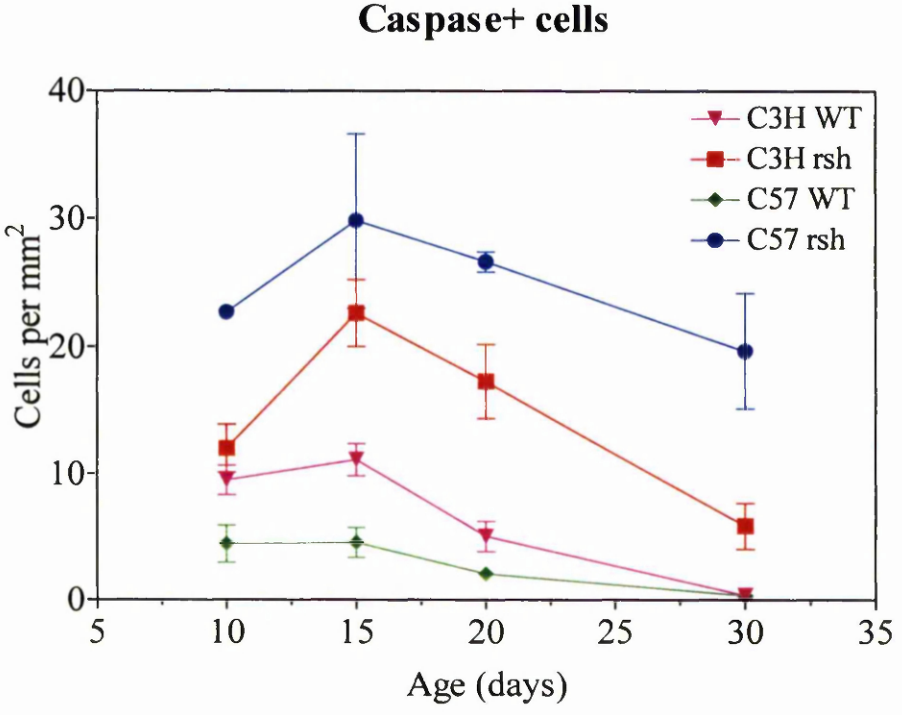

Fig. 27. Total caspase-3 +cells. C3H and C57 wild types are both showing great similarity in caspase-3 + cells at all age. C3H WT and its mutant are also similar at P10-20 but different at P30. Substantial difference is noted between C57 WT and its mutant and the two mutants at all age except P20.

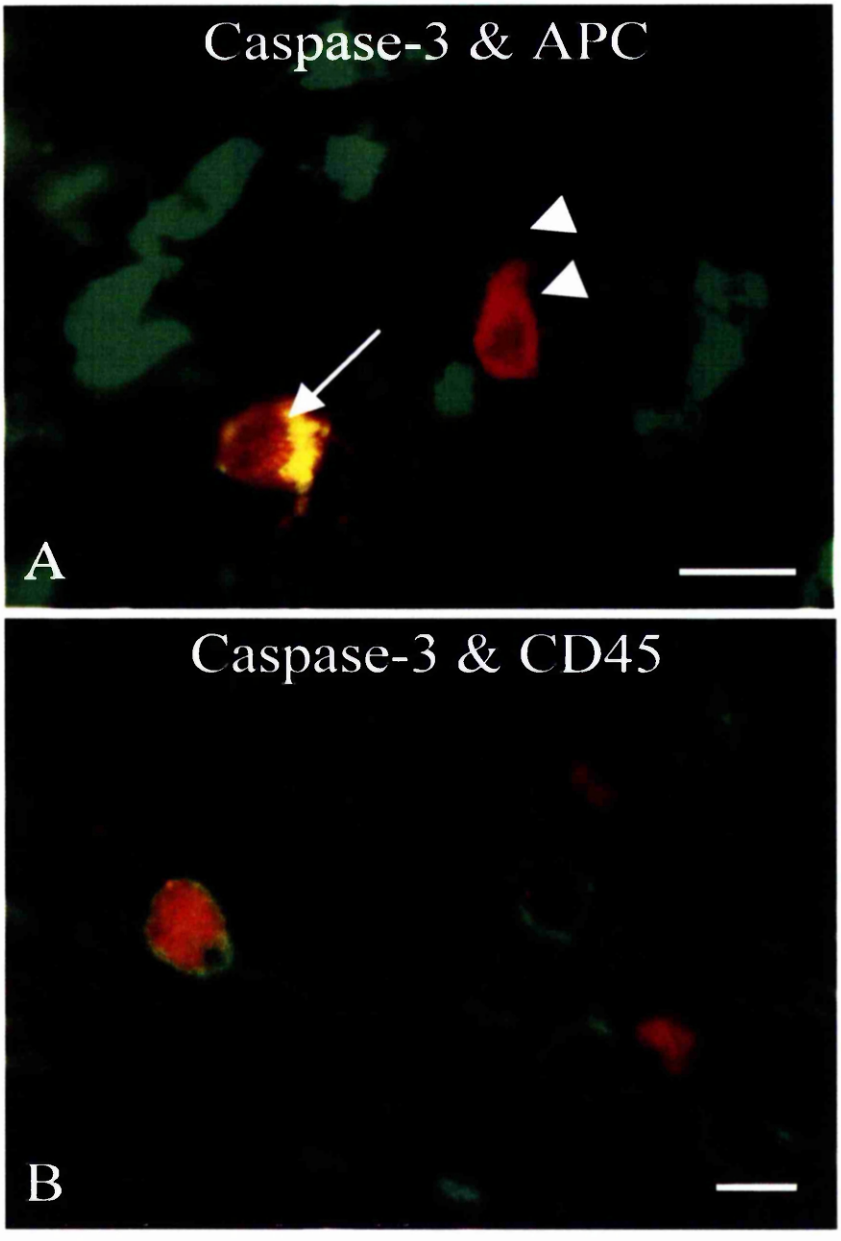

Fig. 28. Identification of caspase-3+ cells. **A**. Ventral white matter from C57 *rsh* at P20, double stained with APC to show one oligodendrocyte (arrow) undergoing apoptosis together with an unidentified cell (arrowhead). **B**. Labelling of ventral white matter from C3H *rsh* at P15 for CD45 shows a caspase-3+ microglia/macrophage. Bars = 10um.

4.3.4 Glial cell proliferation

4.3.4.1 Introduction

Neuroglia form a substantial part of the cellular mass of the CNS. In normal development, proliferation of glial cell types, which is pronounced during the later stages of embryogenesis, declines after birth. The exact timing depends on both the CNS region and the cell type. In general terms astrocytes are generated prior to oligodendrocytes and the ventral spinal cord represents a region in which glial cell proliferation almost ceases within about 2 weeks of birth (Noll and Miller, 1993; Miller *et al.*, 1997; Calver *et al.*, 1998). However, occasional dividing glial cells are seen throughout the life of animals (Horner *et al.*, 2000). Diseases of the CNS are often associated with proliferation of neuroglial cells, in particular microglia, astrocytes and, on limited occasions, cells of the oligodendrocyte lineage. Glial cell proliferation is common in dysmyelinating diseases. Using BrdU *in vivo*, neuroglial cell proliferation was investigated in *rumpshaker* and normal animals. Double labelling of BrdU-positive cells was also performed to define the nature of mitotic cells.

4.3.4.2 Material and methods

4.3.4.2.1 Injection of mice with BrdU

Mice were injected intraperitoneally with BrdU as described in (3.1.4, page 28).

4.3.4.2.2 Quantification BrdU labelled nuclei

Quantification of BrdU labelled nuclei was performed as described in (3.9.2, page 42).

4.3.4.2.3 Identification of double labelled BrdU-positive glial cells

Double immunolabelling of BrdU-positive cells was performed as described in (3.8.13, page 41).

4.3.4.3 Results

4.3.4.3.1 BrdU labelled nuclei

In order to investigate the proliferation of cells in the white matter of the ventral cervical cord animals were pulse labelled with BrdU at ages between P5 and P30. All labelled cells were counted with no attempt to differentiate cell types; it was

noted that very occasional endothelial cells were labelled but the vast majority of labelled cells were glial. In both strains of wild type the profile was identical with maximum labelling between P5 and P10 followed by a sharp decrease to negligible levels at P30. The density of labelled nuclei and the labelling index (LI) were unchanged at P5 and P10 in C3H *rsh* but thereafter moderately elevated compared with the appropriate wild type. The values in the C57 mutant were raised at P10 and subsequently, compared with its wild type, and also increased in comparison with the C3H *rsh* (Figure 29, page 87 and Figure 30, page 88).

4.3.4.3.2 BrdU-positive glial cells

The BrdU-positive cells were abundant in the cervical cord white matter of the mutants, in particular at P15 and this age was selected to define the nature of the proliferating cells. Double immunolabelling for BrdU and APC, NG2 and CD45 was performed at P15 in both mutants (Figure 31, page 89). As expected, few BrdU+ nuclei (<1%) were associated with APC+ oligodendrocytes. The proportions of BrdU+/NG2+ cells were 61.5 ± 2.4% and 43.0 ± 2.9% in C3H and C57 mutants, respectively. Taking into account the far greater number of BrdU-labelled nuclei in the C57 *rsh*, the actual number of proliferating NG2+ cells was ~ 1.5 fold greater than in the C3H *rsh*. The proportions of BrdU+/CD45+ cells were 7.3 ± 1.9% and 22.8 ± 1.4%, respectively. As indicated above, occasional labelled endothelial cells were also seen. No attempt was made to identify other BrdU-labelled cells, such as astrocytes.

4.3.4.4 Discussion

BrdU, an analogue of thymidine, is incorporated specifically into newly synthesised deoxyribonucleic acid (DNA). The incorporation of BrdU by proliferating cells and its detection using monoclonal antibodies has gained popularity as a reliable technique for identifying cells in the S (synthetic) phase of the cell cycle (Magaud *et al.*, 1989). The BrdU LI and density are, in general, both increased in the mutant animals. Furthermore, the increase in these two variables is more marked in the C57 *rsh* compared with the C3H *rsh*. This result is consistent with the increase in total glial cells in and between the two mutant strains identified by examining resin sections (see 4.3.2 Evaluation of total glial cell and oligodendrocyte numbers, page 68) and is also in agreement with the previous finding (Fanarraga *et al.*, 1992). In the present study the cells were labelled for one hour with BrdU which is sufficient to label cells that have been within the S phase within that period; however, as the S phase represents about 1/3 of the cell cycle (depending on cell type) the actual number of proliferating cells will be considerably greater. Despite this caveat, the data do allow valid comparisons between the various genotypes. In general terms,

the profile of BrdU-labelled cells followed that for wild type but persisted for much longer. Even at P30 there were significant numbers of such cells in the C57 mutant. We have not followed the C3H *rsh* to older ages nor increased the duration of BrdU administration. It is quite possible that a heightened level of proliferation might persist into the adult mutant mouse. Recent studies in spinal cord and brain of normal rodents have identified slowly proliferating glial populations (Horner *et al.*, 2000; Levine *et al.*, 2001).

Some other *Plp gene* mutants (for example *jimpy* and *shaking* pup) also display an increase in glial cell proliferation (Knapp *et al.*, 1986; Jackson and Duncan, 1988; Gencic and Hudson, 1990; Macklin *et al.*, 1991) whereas the *md* rat does not show an increase in total glial cell population (Jackson and Duncan, 1988; Boison and Stoffel, 1989).

The present study clearly identifies the NG2+ oligodendrocyte progenitor as one source of the BrdU-labelled nuclei. This is not unsurprising, as this cell type is known to respond in myelin disorders (Keirstead *et al.*, 1998; Grinspan *et al.*, 1998; Di Bello *et al.*, 1999; Chang *et al.*, 2000). Increased proliferation is a means of maintaining (or restoring) the oligodendrocyte population in the presence of increased frequency of apoptosis.

The other labelled cell type was the CD45+ cell. In the *rumpshaker* it is probable that this marker identified predominantly microglia/macrophages rather than lymphocytes, as the labelling pattern correlated with F4/80 and few if any lymphocytes were seen in resin sections.

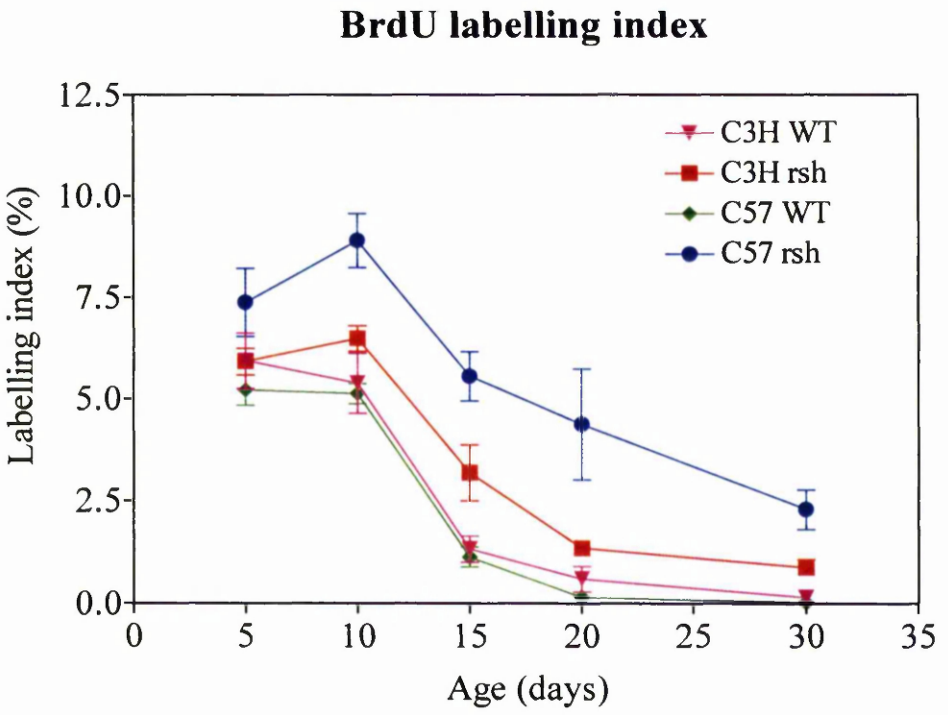

Fig. 29A. BrdU labelling index. At P5, there is no significant difference between the wild types and the mutants. At P15 and thereafter, there is an increase in the labelling index in C57 *rsh* over the two wild types and only at P30 a considerable difference is noted between C57 *rsh* and C3H *rsh*.

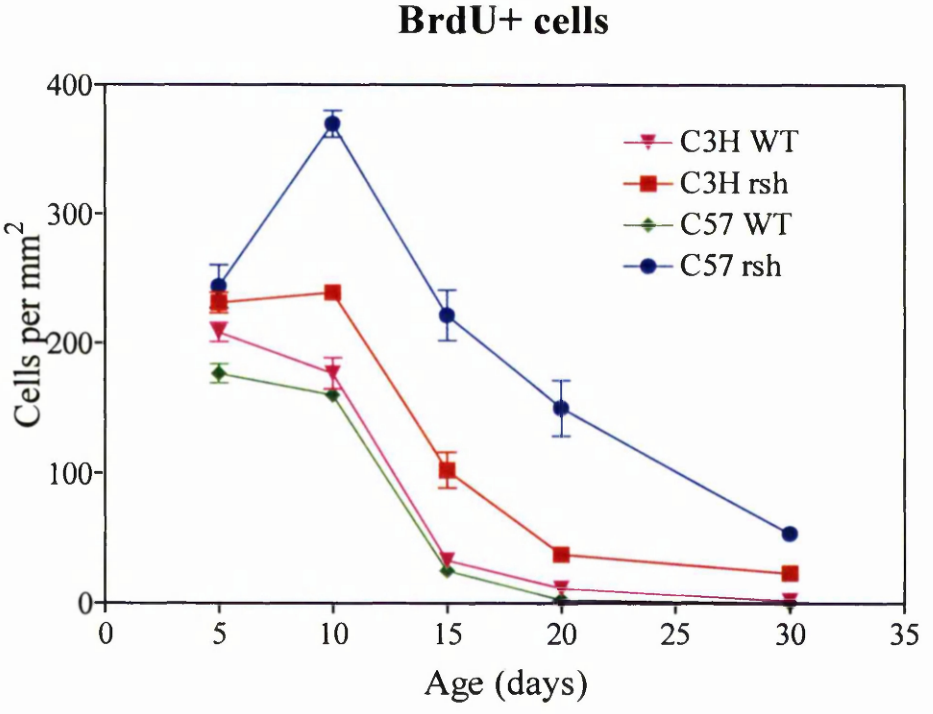

Fig. 29B. BrdU+ Cell density. BrdU density and Labelling index are similar at P5. There is no difference between the wild types and C3H mutant. Of the group of mice, C57 mutant has significant increase in the density at P10-30 but at P20 there no difference between the mutants.

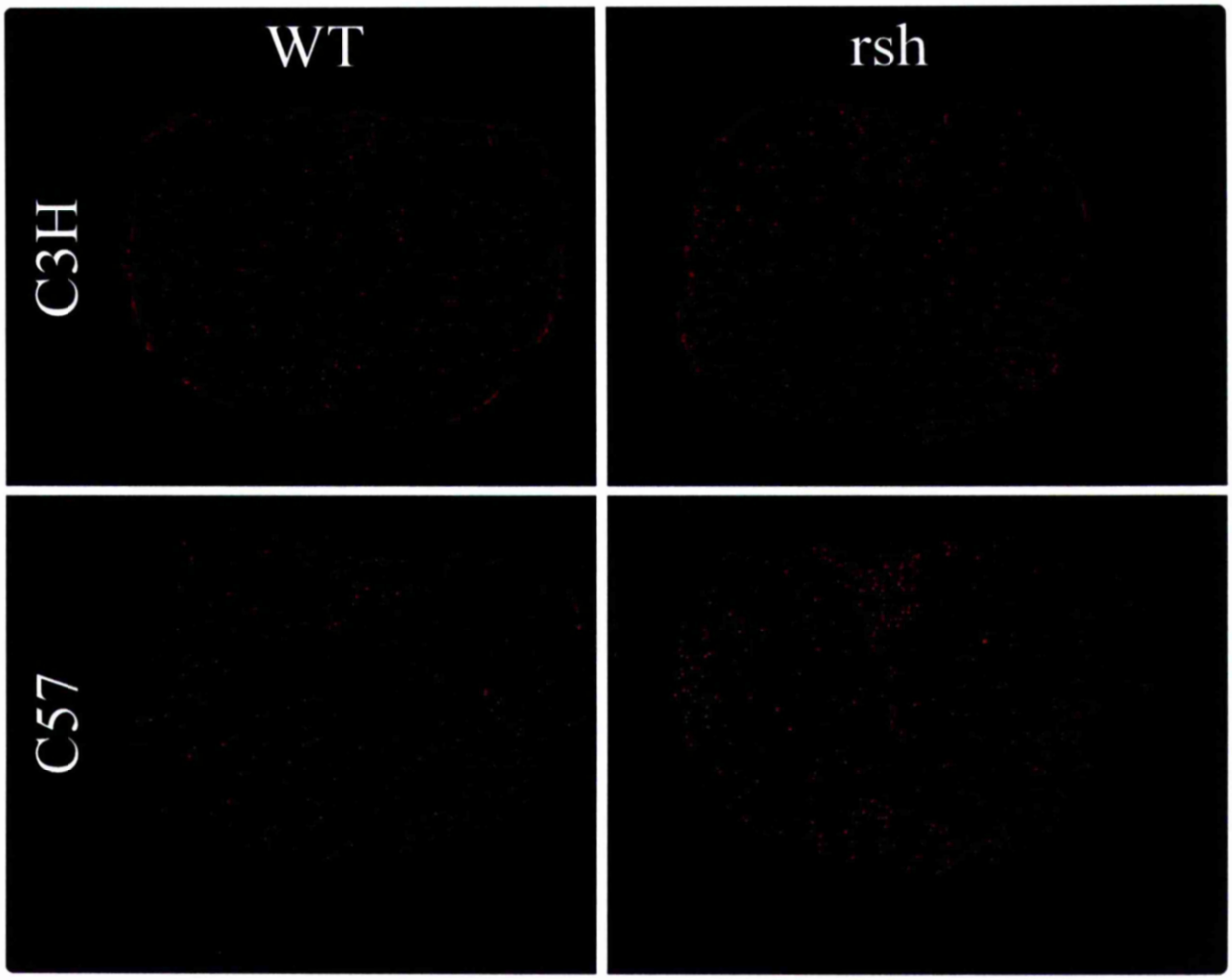

Fig. 30. Montage of BrdU-labelled spinal cords at P10. The difference in the number of labelled nuclei between mutants and wild type and between mutants is shown.

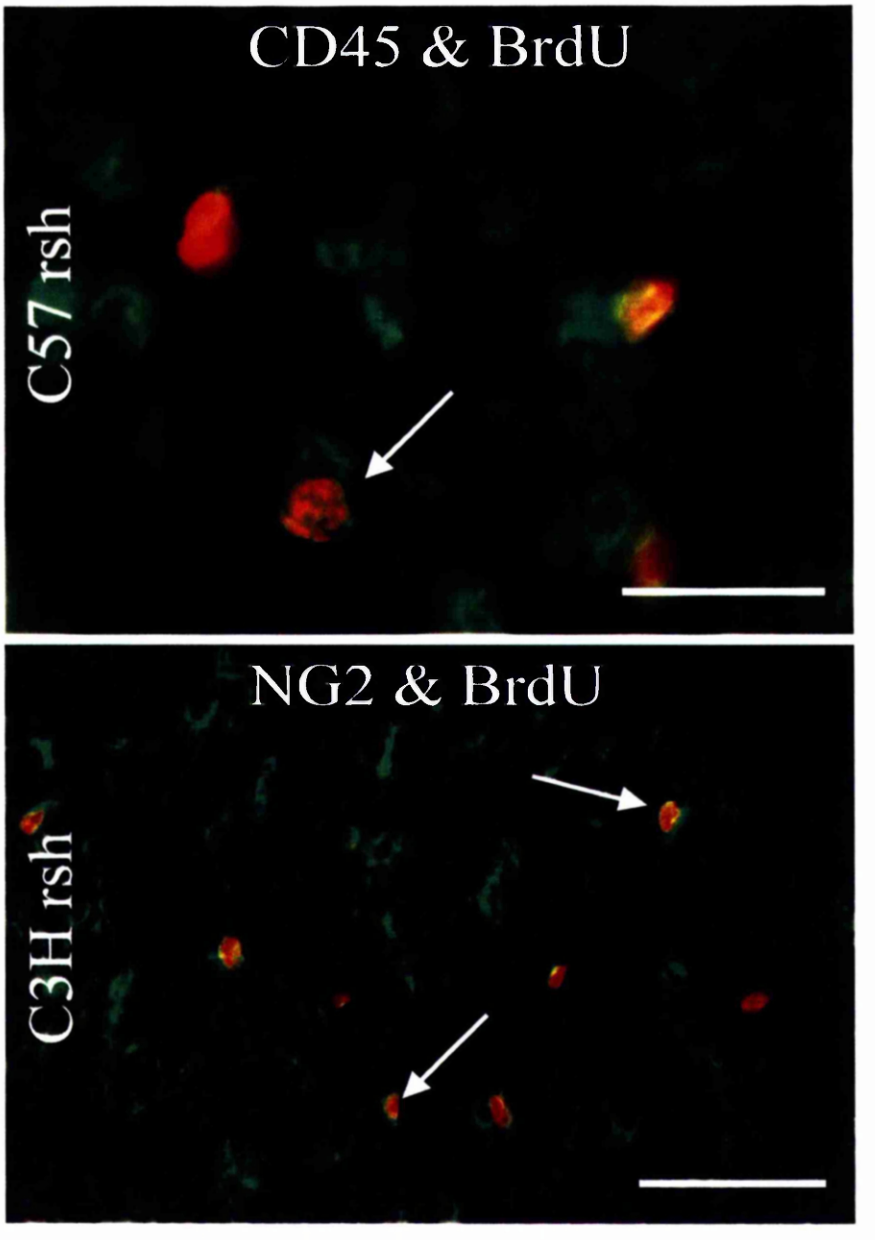

Fig. 31A. Immunofluorescence for CD45 and BrdU. A double-labelled cell is indicated (arrow). Bar = 20um.
Fig. 31B. Immunofluorescence for NG2 and BrdU. Several double-labelled cells are shown (arrows). Bar = 50um.

4.3.5 Macrophage/microglial cell response

4.3.5.1 Introduction

Macrophage/microglial cells represent the least common glial cell type in normal CNS and also have a different origin from the macroglia. However, in many diseases this cell population proliferates and/or activates depending on the cause(s) of the lesions. This population is potentially functional in some dysmyelinating diseases. In *rumpshaker*, macrophage/microglial cells are heavily dispersed in the white matter and less in the grey matter, especially in C57 strain. Using anti-CD45 antibody, this population of cells was estimated. Additionally, the staining pattern of CD45 was compared with that of F4/80.

4.3.5.2 Material and methods

4.3.5.2.1 Quantification of CD45-positive microglia

Quantification of CD45-positive microglia was performed as described in (3.9.4, page 43).

4.3.5.2.2 Qualitative study of F4/80 and CD45-positive microglia

Immunostaining for F4/80-positive and CD45-positive microglial cells were performed as described in (3.8.5, page 39) and the sections were qualitatively investigated.

4.3.5.3 Results

4.3.5.3.1 CD45-positive microglia

Activated microphage/microglial cells were seen frequently in the resin sections of *rumpshaker* particularly in the C57 mutants at P15-30 (Figure 32, page 93 and Figure 33, page 94). To confirm this; CD45 antibody, a pan-leukocytic surface marker, was used to detect this particular type of cell population. The two groups of wild type appeared to have similar CD45+ cell density. The mutant mice had a significantly higher density than their respective wild types with C57 *rsh* being the highest. This value was higher in the C57 mutant than its C3H counterpart (Figure 34, page 95).

4.3.5.3.2 F4/80-positive and CD45-positive microglia

Of the surface markers found on the macrophages/microglial cells, F4/80 and CD45 were used independently to detect this cell population. Brain and cervical cord sections from both mutants at P20 were immunostained with either marker using the ABC method. Interestingly, the intensity of F4/80 staining followed the same pattern as CD45 in both regions of the CNS (data not shown).

4.3.5.4 Discussion

F4/80 represents a marker specific for microglia/macrophages (Perry *et al.*, 1985; Perry and Gordon, 1988) whereas CD45 additionally recognises lymphocytes. On resin sections and electron microscopy very few, if any lymphocytes were detected suggesting that the majority of CD45+ cells were microglia/macrophages and, indeed, the staining pattern of the two markers was similar. As the staining intensity for CD45 was greater than F4/80, the former was used to simplify identification and quantification of cells.

Microglia form an important part of the cellular response to CNS dysmyelination. They are recruited in significant numbers to the site of lesions (Frank and Wolburg, 1996). However, their responses not only includes an increase in actual numbers but also hypertrophy, change of gene expression with or without cellular proliferation and release of inflammatory cytokines. Macrophage/microglial cells in *rumpshaker* spinal cord showed considerable increases in their number. This result agreed with that result of examining the resin sections (see 4.3.2.3.1 Glial cell population (resin sections), page 69). In this context, the *jimpy* mutant mouse also has a marked increase in macrophage/microglial cell population (Vela *et al.*, 1995). The early formation of a reserve of glial cells including microglia in mutant CNS may suggest a reciprocal temporal dialogue between these cells and, therefore, the microglial cells are in place to prepare for potential phagocytosis which may occur later when dysmyelination develops and the extent of the lesion increases, that is to say the dead cells. In *rumpshaker*, these cells not only increase in number, but also upregulate cell surface markers, such as CD45 and F4/80, during the course of the dysmyelination. The scattering of reactive microglia predominantly in the white matter tracts suggests that the signal for microglial reaction during this period may come locally from abnormally ensheathed or unsheathed axons. The unsheathed or abnormally wrapped axons of *rumpshaker* appear physically intact but are likely to be functionally abnormal as is the case in other dysmyelinating mutants, such as the *shiverer* mouse and *md*-rat (Kaplan *et al.*, 1997; Brady *et al.*, 1999). The cross talk between abnormally functioning axons and microglia may initiate a microglial response. Additionally, the mutant oligodendrocytes may also contribute to

triggering the microglial response. Another possible explanation for microglial response is the presence of the myelin debris and dead cells, which demanded fast removal. Morphologically, apoptotic cells are often seen within other cells at the light and electron microscopic levels. This observation is supported by double labelling of caspase-3-positive cells (see 4.3.3.4 Discussion, page 79) in which caspase-3-positive immunostaining was seen within CD45 positive cells. Although this might be explained by stimulation of microglial phagocytosis by dead cells and degenerated myelin, the numerous undigested debris in activated microglia suggest an active phagocytosis. However, the signals that lead to microglial activation and the functional consequences of microglial reaction remain to be understood. Finally, the high cellularity noted in the *rumpshaker* mutant animals is attributed largely to proliferation of macrophage/microglia cell series.

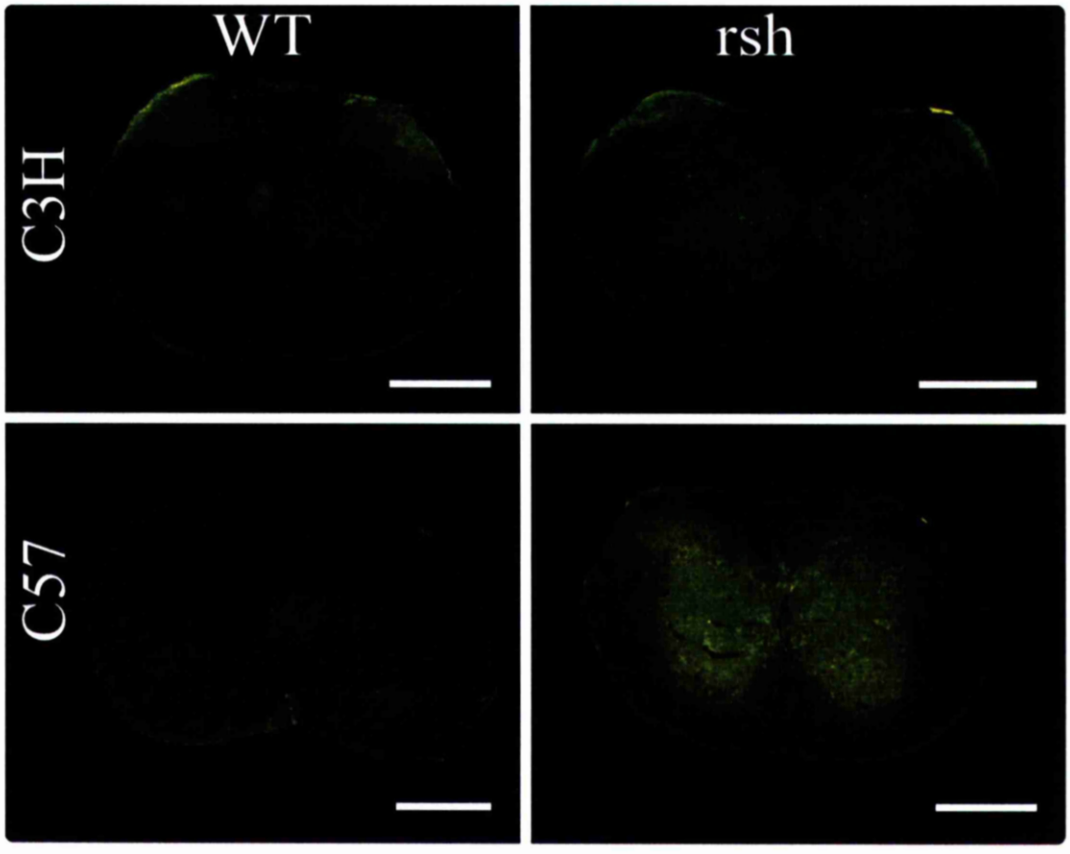

Fig. 32. Montage of CD45+ cells in spinal cord. Spinal cords from P20 C3H and C57 wild type and *rumpshaker* immunostained for CD45. Bars = 0.5 mm.

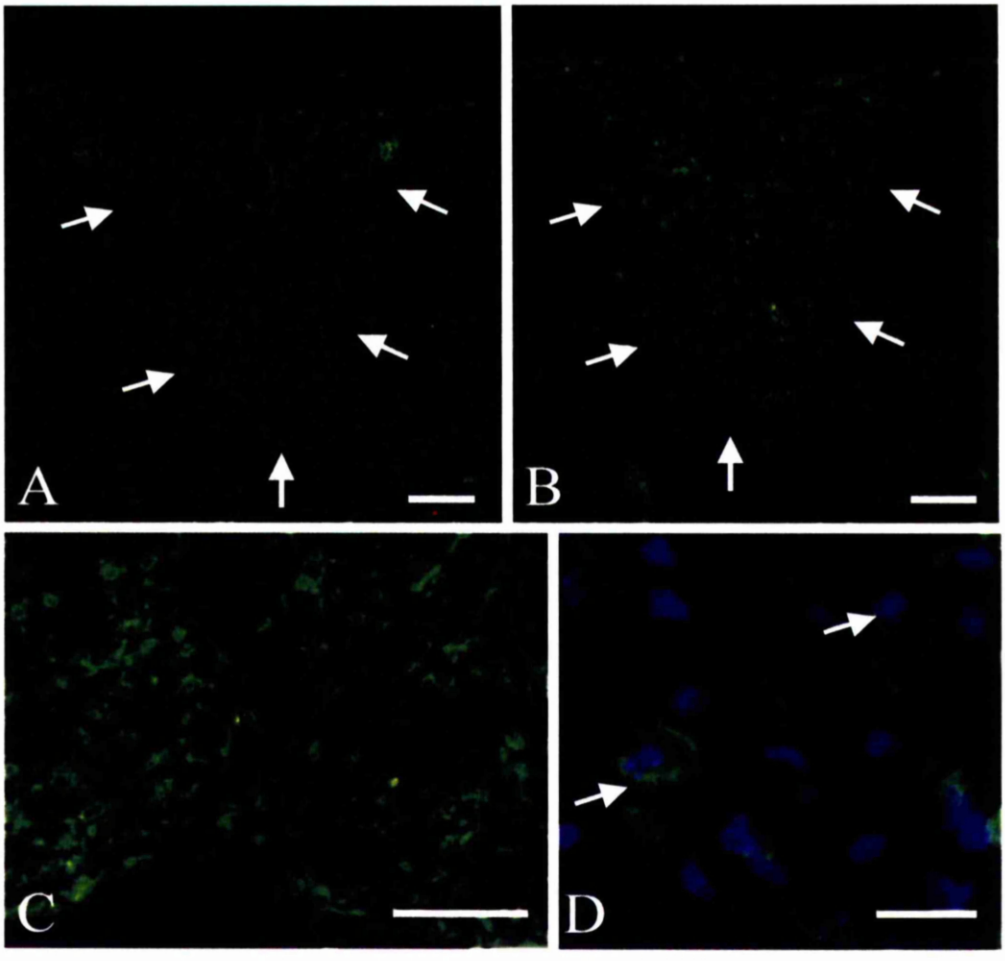

Fig. 33A, B. Immunostaining for CD45 in dorsal columns of C57 wild type (A) and rsh (B) at P20. The dorsal columns are outlined (arrows). Bars = 100um.

Fig. 33C. Immunostaining for CD45 in ventral columns of C57 rsh at P20. There is marked increase in the number and size of the positive cells. Bar = 100um.

Fig. 33D. Immunostaining for CD45 and DAPI in ventral columns of C57 rsh at P20. Two typical cells are indicated (arrows). Bar = 20um.

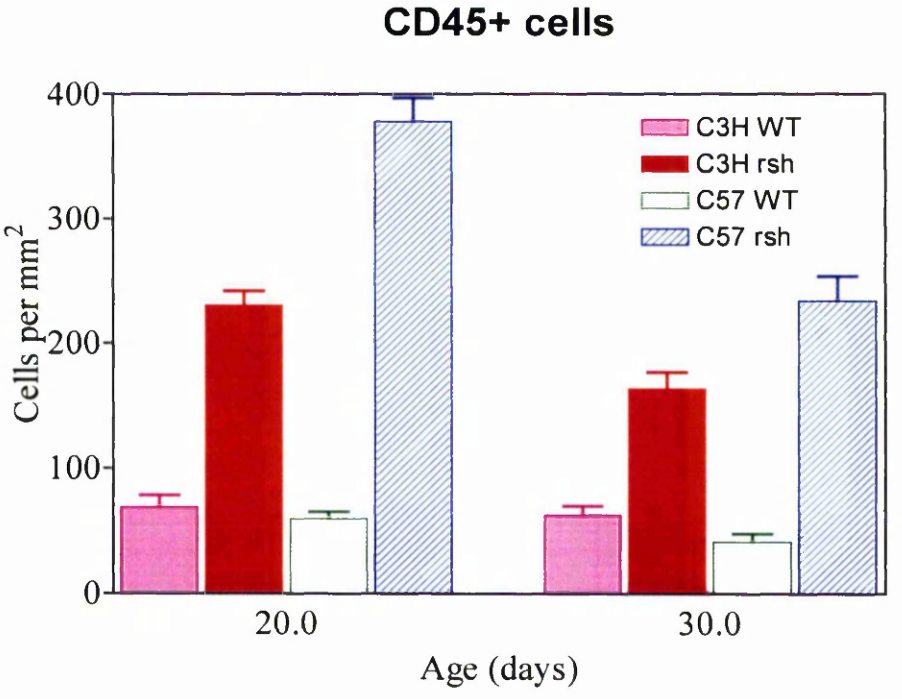

Fig. 34. CD45+ microglial cell density. C3H and C57 wild types are both identical in their CD45+cell density at P20-30. The mutants are significantly greater than the wild type groups. C57 *rsh* is obviously greater in its CD45+ cell density than C3H *rsh* especially at P20.

4.4 Protein analysis

4.4.1 Introduction

The major myelin proteins in the CNS are PLP (see 1.12.5, page 11) and MBP (see 1.12.3, Page 11). Several minor proteins are also found in myelin (see 1.12.1, page 10; 1.12.2, page 10 and 1.12.4 page 11). Many diseases of the CNS have been shown to involve these myelin proteins in man and animals. Abnormalities of myelin proteins were reported in various mutant mice such as *jimpy* and *shiverer*. It was known from the previous investigations and the current study that *rumpshaker* has defective myelination in the CNS. In this study, immunoblotting analysis was used as another independent method to compare the abnormality in the expression of myelin proteins and GFAP in the mutants and their respective normal littermate animals. Thus, analysis of myelin proteins and non-myelin proteins are important for understanding the pathology of myelin-related diseases.

4.4.2 Material and methods

4.4.2.1 Protein analysis

Samples of the whole brain and spinal cord were homogenised, myelin extracted and the proteins were semi-quantified with Western blot using the anti-PLP C-terminal antibody, anti-MBP antibody, anti-MAG, anti-CNP and anti-GFAP antibody (see 3.11, page 44).

4.4.3 Results

4.4.3.1 Myelin proteins

The yield of purified myelin appeared similar in both wild types but was reduced in both mutants, particularly in C57 *rsh*. Semi-quantitative western blotting of myelin proteins revealed that the levels PLP/DM20 were markedly reduced in both mutants (<20%), with C57 *rsh* being lower than C3H *rsh*. However, in C3H *rsh* the levels of MBP, MAG and CNP were only minimally reduced. In contrast, all values were less than 40% of wild type in C57 *rsh*. (Figure 35, page 99; Figure 37, page 101). However, both wild types had the similar levels of PLP/DM20, MBP, CNP and MAG.

4.4.3.2 GFAP

GFAP is the widely applicable marker of astrocytes in normal and diseased conditions. It was used in this study to evaluate the astrocytic response in the *rumpshaker*. There was a slight increase in GFAP bands of the mutant animals compared with wild types although the intensity appeared identical in both mutants. However, a minor, low molecular weight GFAP isoform was markedly increased in rumpshaker (Figure 36, page 100 and Figure 37, page 101).

4.4.4 Discussion

Biochemical analysis of dysmyelinating mutant animals gives an insight into the molecular mechanisms of gene expression, the structure-function relationship of myelin proteins and their interaction during normal myelin formation. *rumpshaker* shows dysmyelination in the CNS (see the results, 4.2.3.1 Morphology, page 54 and 4.2.3.2 Immunostaining, page 54) and this feature correlates the reduced amounts of myelin extracted from these mutants with the C57 *rsh* being the more sevely affected. On the basis of the morphological parameters examined (see 4.3.1.3.1 Myelin areas, page 64; 4.3.1.3.2 Myelin volume, page 64; and 4.3.1.3.3 Percentage of myelinated axons, page 65), the reduction in the yield of purified isolated myelin from these mutants appeared to be mostly a consequence of reduction in both myelin sheath thickness and myelinated fibre number, particularly in C57 *rsh*.

Analysis of protein levels in myelin show marked reduction in PLP with the C57 *rsh* being more sevely affected. In contrast, MBP was minimally reduced in C3H *rsh* but in C57 *rsh* was less than 40% of its wild type. CNP and MAG were minimally reduced in C3H *rsh* whereas both proteins were substantially reduced in C57 *rsh*, compared with its normal littermates and CNP was lower than MAG. A previous study (Mitchell *et al.*, 1992) of the C3H *rsh* also found markedly reduced levels of PLP/DM20 but, in contrast to the present study, found lower levels of MBP (58%). Message levels of the two major proteins were not reduced to the same extent as the corresponding protein (Mitchell *et al.*, 1992). It is, therefore, clear that the *rumpshaker* mutation differentially influences the incorporation of myelin proteins into the sheath and does not solely reflect the overall dysmyelination. In the *jimpy* mutants of the *Plp* gene the amount of PLP was less than 1% and MBP was 2% although CNP and MAG were 10% and 5%, respectively (Yanagisawa and Quarles, 1986). The *jimpy* mutation therefore has a very similar effect on the incorporation of all myelin proteins into the sheath.

Another possible explanation for the low levels of these proteins in *rumpshaker* and some *Plp* gene mutants might be due to failure of oligodendroblasts to differentiate into mature oligodendrocytes (Meier and Bischoff, 1975; Skoff, 1982). Since

maximal synthesis of PLP lags behind MBP synthesis during normal development (Campagnoni and Hunkeler, 1980), it is possible that extremely low levels of PLP synthesis might be expected in oligodendroglial cells that do not fully differentiate.

The morphological studies revealed little information regarding the astrocyte population and the immunohistochemistry suggested a moderate increase in GFAP but little difference between the mutants. GFAP immunoblotting was considered to extend these observations. The slight increase in GFAP coupled with no change in the number of astrocyte nuclei suggests that the astrocytes in *rumpshaker* increase expression of the *Gfap* gene, rather than proliferate. Since the response of GFAP is moderate and the fact that the astrocyte number is unchanged in both mutants, the astrocyte population may not be important in influencing the difference in phenotype.

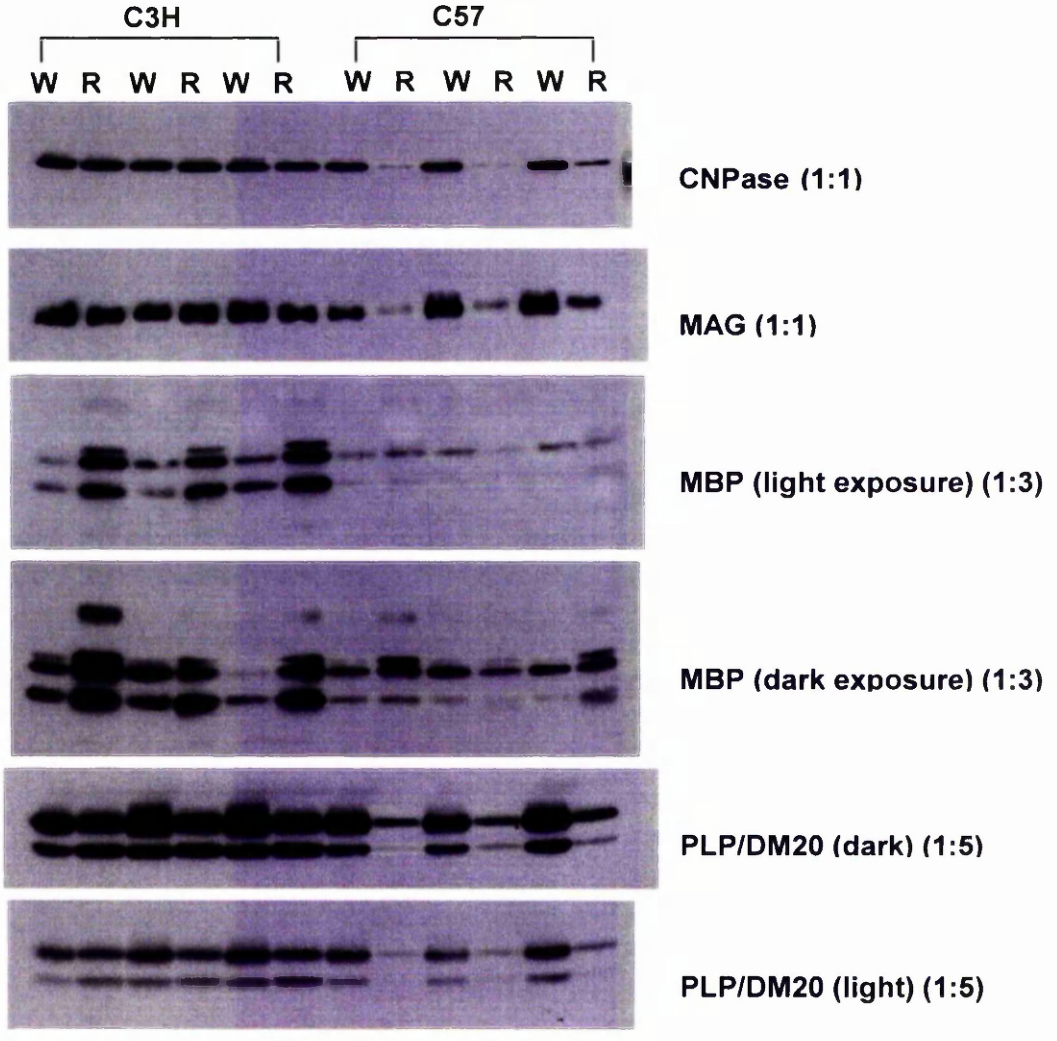

Fig. 35. Western blots of myelin proteins in myelin fractions from the spinal cords of P20 mice. Selected myelin proteins were compared between the two mutants and their normal littermates. Data from 3 separate animals in each group is shown. The intensity of the mutant bands is reduced compared to normal animals. Nonetheless the levels of myelin proteins are more markedly reduced in C57 *rsh*. (W: wild type; R: *rsh*).

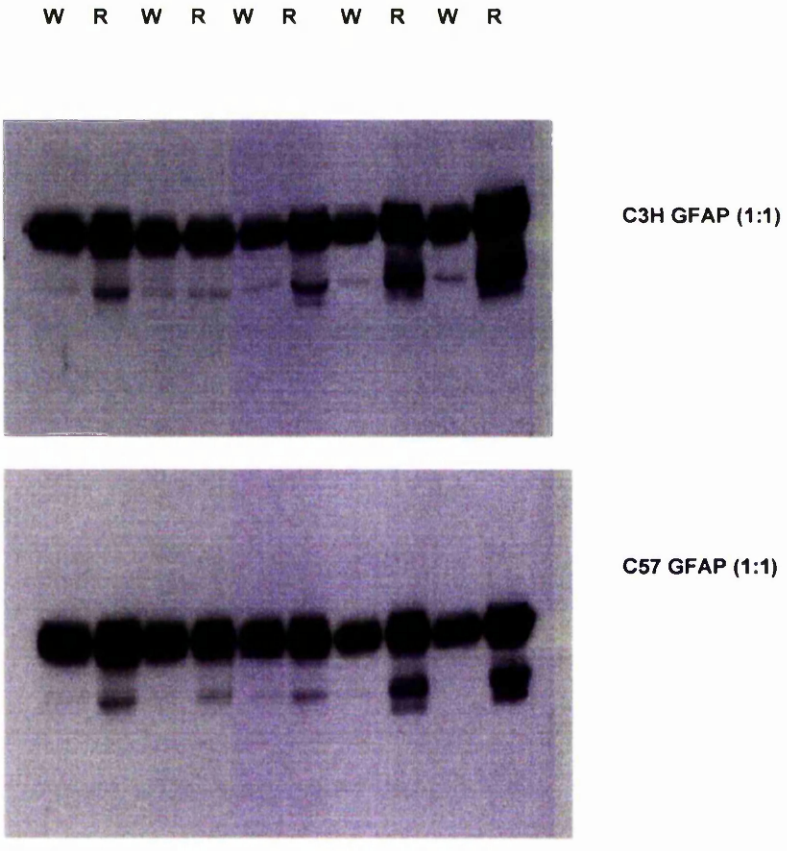

Fig. 36. Western blots of GFAP from homogenates of P20 mouse spinal cords. Data from 3 separate animals in each group is shown. There is a slight increase in the intensity of bands from the mutants, suggesting gliosis, but no obvious difference between the two mutants. (W: wild type; R: *rsh*).

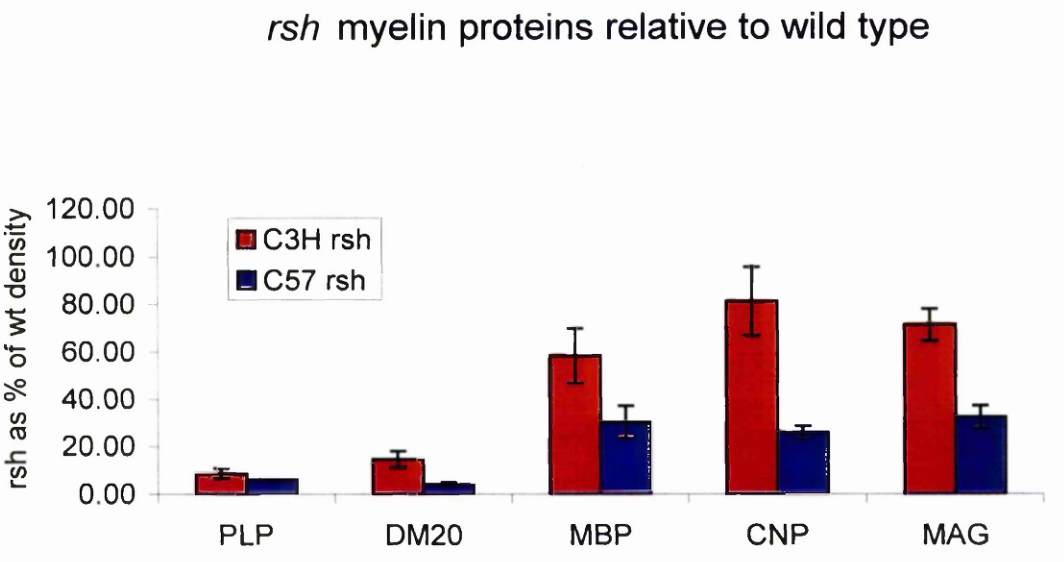

Fig. 37A. Semi-quantification of myelin protein Western blots from P20 mouse spinal cords. The levels of myelin proteins were reduced in the mutants. The obvious reduction in all protein is noted in C57 *rsh* particularly in PLP/DM20.

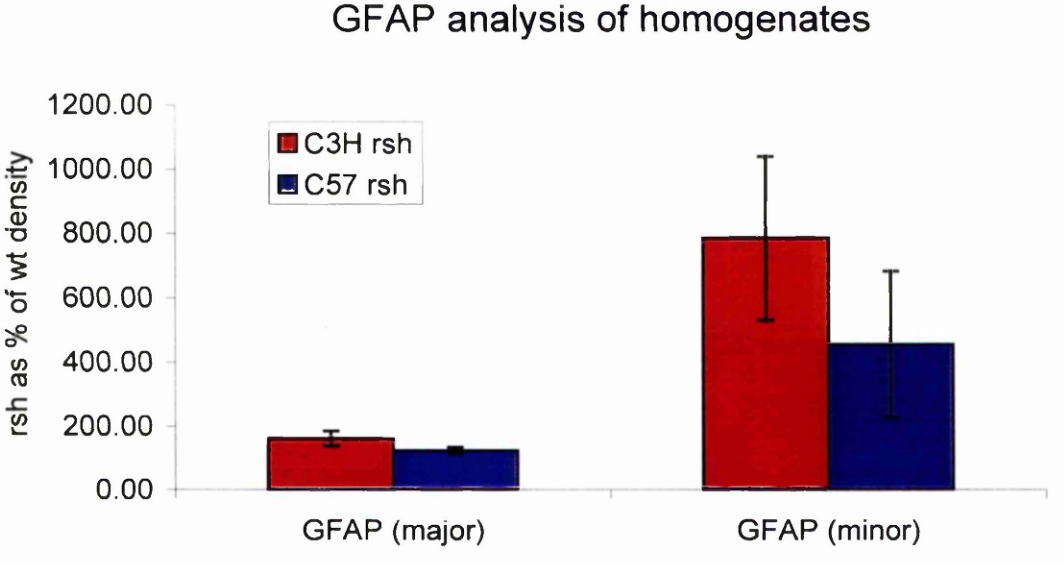

Fig. 37B. Semi-quantification of GFAP Western blots from P20 mouse spinal cords. Despite the minimal increase in GFAP, the two mutants appeared similar.

5. Final discussion and future work

The accumulated data presented in this study, which is derived from the comparison of the phenotypes of *rumpshaker* mutation on two different genetic backgrounds, indicated that the same single mutation had more pronounced effects in the C57 strain than the original C3H strain. Thus, the C57 *rumpshaker* is considered the severe phenotype of the mutation while the C3H *rumpshaker* is the mild form in terms of clinical manifestation and pathological findings. However, although there were quantitative and qualitative differences according to the present study, the similarities in response were more striking. Furthermore, this study adds weight to the contention that oligodendrocyte death and hypomyelination are two independent mechanisms with no direct relation between them. This study provided strong evidence that the oligodendrocyte population is maintained in the mutant *rumpshaker*. This study also emphasised that the severity of the pathology correlates with the severity of the phenotype, regardless of its nature. This section aims to amalgamate the information accumulated from the phenotypic studies of *rumpshaker* mutation and to direct the prospective work.

The *rumpshaker* mutant animal is distinguishable from normal littermates at about P10-13, by obvious tremors. The C57 *rsh* is also susceptible to seizures at about P25 with death by about a month of age. Despite the obvious clinical signs and pathology, it has proved difficult to correlate the two. It was not possible, because of time constraints to quantify changes or perform detailed neuropathology throughout all the CNS; therefore, the sampling of the CNS may be inadequate or the methods applied are not sensitive enough to detect the cause for all the clinical signs. For example, the techniques used with paraffin sections of the brain would not detect minute lesions or changes in soluble factors in certain tracts that might cause tremor and later severe seizures. Clearly, a more detailed study of other CNS regions would be useful.

The tremor is most probably related to the myelin deficit possibly leading to cross talk between axons. Detailed analysis of the ion channel distribution has not been performed in either strain of *rumpshaker* and, based on similar analyses in other myelin mutants (Wang *et al.*, 1995; Baba *et al.*, 1999; Rasband *et al.*, 1999b; Tait *et al.*, 2000; Rasband and Trimmer, 2001; Jenkins and Bennett, 2002), is likely to be abnormal. This may also be involved in the generation of the tremor, and possibly seizures, and is an area for future study. The changes which might be responsible

for the tremors and/or seizures are very difficult to dissect with the methods used in this thesis. Other future studies might involve electrophysiological techniques or metabolic mapping to determine the site of origin of the seizures.

The underlying mechanism responsible for dysmyelination in the *Plp* mutant animals, including *rumpshaker,* is poorly understood. It has been demonstrated that oligodendrocytes differentiate and begin to synthesised myelin membrane components; unfortunately, they fail to complete this process (Koeppen *et al.*, 1992). In this regard the expectation is that numerous oligodendrocyte progenitors arrive at their final destination and await a putative signal from either axons or generated in a cell-autonomous manner. At this point the scheduling of cell differentiation and maturation takes priority over cell division. The first cells that arrive manage to have that signal communication and to some extent are able to differentiate and mature to a level that produces the myelin sheaths seen in the mutant animals. The later arriving or dividing cells remain in continued proliferation due to the lack of the signal. Another potential explanation for dysmyelination is that astrocytic hypertrophy may interfere with oligodendrocyte contact with axons. Such a lesion has been recognised in *jimpy* mice (Skoff, 1976).

In vivo and *in vitro* studies provide evidence that PLP/DM20 protein trafficking is arrested in the RER preventing the elaboration of myelin membranes in some of these mutants (Nussbaum and Roussel, 1983; Roussel *et al.*, 1987; Gow and Lazzarini, 1996; Gow *et al.*, 1998). However, it is not clear from these static images what happens to the PLP/DM20. This and previous studies have shown that the steady state levels of PLP and other myelin proteins are reduced in total CNS and myelin fractions of *rumpshaker* mice (Mitchell *et al.*, 1992). The reduction in protein is disproportionate to the change in message levels and similar findings have been reported in the *jimpy* mouse (Sorg *et al.*, 1986; Sorg *et al.*, 1987). Ongoing studies in this unit using radioisotope incorporation have shown that the rate of PLP synthesis is not decreased in *rumpshaker*; the same work has shown that the abnormal PLP appears to decay more rapidly than wild type PLP (Dr. Mark McLauchlin, unpublished data). An explanation for this view is that the synthesised PLP is rapidly degraded before reaching the membrane where it could incorporate into myelin sheath. An alternative explanation is that the PLP protein reaches the membrane, however, it fails to incorporate correctly into the myelin sheath in a stable manner, presumably due to abnormal conformational structure of the protein. Studies are ongoing to determine the intracellular dynamics of *rumpshaker* PLP/DM20 and what mechanism accounts for its rapid degradation. Immunostaining studies using the O10 antibody (Jung *et al.*, 1996) applied to live cells has shown that approximately 60% to 70% of both C3H and C57 *rumpshaker*

oligodendrocytes are surface labelled (Ian Griffiths, unpublished data). While the amount of PLP reaching the membrane or the time taken was not determined, the study demonstrated that at least some PLP/DM20 was capable of inserting into myelin. Even at a simple level, the immunostaining of tissue sections performed in the current study showed that myelin sheaths were positive for PLP/DM20. It is possible that different "pools" of PLP/DM20 are present so that a fraction is degraded prior to reaching the membrane while another portion is turned over more rapidly from the myelin membrane. The isotope labelling studies previously mentioned should help determine the fate(s) of PLP/DM20. In normal myelin, it is believed that the PLP is important in maintaining the close apposition of the extracellular face of the lipid bilayer to form the double intraperiod line (Duncan *et al.*, 1987; Duncan *et al.*, 1989; Boison and Stoffel, 1994; Boison *et al.*, 1995; Klugmann *et al.*, 1997). *rumpshaker* myelin has an abnormal intraperiod line (Griffiths *et al.*, 1990) and this presumably reflects the decreased or disproportionate levels of PLP and DM20.

The role of *Plp* gene mutations in programmed cell death (apoptosis) and survival of oligodendrocyte population is uncertain. However, it is clear that the frequency of apoptosis in APC+ oligodendrocytes is greater in the C57 compared with the C3H *rumpshaker*. Although the primary structure and presumably the secondary structure of PLP/DM20 will be identical in both strains of *rumpshaker* it is possible that tertiary structure and also protein processing could be different between the two mutants. In *Plp* mutant animals oligodendrocyte death correlates with the expression of PLP (Knapp *et al.*, 1986; Bongarzone *et al.*, 1997; Williams, II and Gard, 1997). However, evidence from gene targeted mice support the contention that oligodendrocytes survive in the absence of PLP protein (Klugmann *et al.*, 1997; Yool *et al.*, 2001). Cell death in the *Plp* mutant animals, therefore, is due to causes other than insufficient functional PLP. Death in the oligodendrocyte lineage, perhaps due to misfolding of PLP protein, raises at least two possibilities. One hypothesis suggests that oligodendrocyte death correlates with the PLP accumulation in the endoplasmic reticulum (Gow *et al.*, 1998) due to misfolding (Jung *et al.*, 1996) The second possibility arises from the signalling components linking altered PLP synthesis to cell death. Misfolding of PLP and altered trafficking can be interpreted by the cell as stress signals originating from the endoplasmic reticulum and therefore activate two protein kinases called PERK and PKR, as part of the unfolded protein response (UPR), as shown in other systems. These kinases will then be responsible for the phosphorylation of the eIF-2 translation factor, with direct consequential reduction of the translation rate as a way to protect the cell from additional accumulation of misfolded protein. In the case of severe endoplasmic reticulum stress, however, the cell may not be able to

overcome the level of damage thus resulting in apoptosis, probably mediated by phosphorylation of eIF-2 itself and potential involvement of the transcriptional activator CHOP (Kaufman, 1999). The UPR can also activate caspase-12 (Rao *et al.*, 2001) and initiate the subsequent caspase cascade culminating in apoptosis. However, these scenarios are still theories in respect to the oligodendrocyte lineage and further study is required to evaluate their relevance. A further line of evidence speculates that the death of oligodendrocytes may involve a perturbed axo-glial relationship, an association that is necessary to ensure oligodendrocyte survival during normal myelinogenesis (Barres *et al.*, 1992; Barres and Raff, 1994; Barres and Raff, 1999). In contrast, mature oligodendrocytes seem more independent of axonal contact (McPhilemy *et al.*, 1990; Ludwin, 1990). The inference from this data is that the oligodendrocytes die in the mutant animals from the lack of proper axonal contact, consequently no survival factors are delivered from axons, which are essential for the cells. This may explain the increase in number of apoptotic nuclei in C57 *rsh* compared to C3H *rsh* as the surface of contact with axons is much reduced due to abnormal contact of axons with astrocytes and crowding of the white matter with proliferative glial cells, abnormal myelin debris and pyknotic nuclei. Again, in C57 *rsh*, the increased numbers of pyknotic nuclei may need not be due to exclusively to increased death of cells but could be due to in part to a reduced rate of removal of chromatin debris compared with C3H *rsh*. It is worth noting that these mutants at least share one common feature; namely, oligodendrocyte death, irrespective of at what stages of development and differentiation the particular cells undergo apoptosis. *rumpshaker* may provide a suitable model to test the hypothesis that intrinsic factors other than PLP may modify the cell fate from following the death pathways; instead of undergoing apoptosis the cell may continue to proliferate. Tissue culture could be used to investigate the role of these postulated "other factors".

Another interesting finding in the *Plp* mutant animals is the abundance of activated macrophage/microglial cells in the affected areas of the CNS. The origin of microglia CNS remains a controversial issue. These cells have the capacity to proliferate in the diseased CNS tissue and blood monocytes migrate to transform into macrophages in the injured CNS tissue (Perry and Gordon, 1988; Giulian, 1995; Perry, 1996; González-Scarano and Baltuch, 1999; Kaur *et al.*, 2001). To-date, there are no available markers to discriminate the endogenous (proliferation of resident microglia) or exogenous (infiltration of monocytes) origin of a given reactive cell within the CNS, the specific contribution of these two mechanisms seems to be closely related to the type of the lesion (González-Scarano and Baltuch, 1999; Stoll and Jander, 1999; Aldskogius, 2001). In dysmyelinating mutant animals, for instance *rumpshaker*, the blood brain barrier in the white matter areas remains

relatively undisturbed as judged by morphological criteria, such as absence of oedema, although no definitive studies of its integrity have been conducted. The precise origin of additional microglial/macrophage cells in this mutant remains to be elucidated. However, there are clues, such as the absence of inflammation (inflammatory reaction) elsewhere in the CNS, suggesting that the main source of reactive microglial/macrophages in *rumpshaker* is the proliferation of endogenous microglial cells. Additionally, the presence of BrdU+/CD45+ cells within one hour of BrdU administration is probably too short a time for these cells to have originated from the blood. Further definitive studies to determine the origin of the CD45+ cells could involve labelling haematogenous cells or constructing chimeras with haemopoietic tissue of a different origin; although, until the importance of the response is established these studies are probably premature. The proliferation of microglial cells probably results from release of chemical mediators (cytokines). Moreover, activated microglia, and to some extent astrocytes, are a source of cytokines (Cross and Woodroofe, 2001; Gebicke-Haerter, 2001) that may adversely affect the pathogenesis of the dysmyelination. These cytokines may worsen the lesion through damaging myelin and possibly participating in inducing signals that stimulate apoptosis. The variability in degree of microglial response seems, however, to depend upon many complex factors including, age, type of lesion, CNS regions, species and the genetic background within species. Evidence for the influence of genetic background on the microglial response is obviously relevant in *rumpshaker* in which the C57 *rsh* shows more microglial cells in the white matter than C3H *rsh*. Overall, as with the deficit in myelin and glial death, the microglial response is parallel in the two mutants but considerably greater in C57 *rsh*. The importance of the microglial/macrophage activity in *rumpshaker* is worthy of further study and different strategies could be used to attenuate the microglial activity. For example, the anti-inflammatory antibiotic minocycline has been shown to reduce microglial-mediated damage in other CNS pathologies (Yrjänheikki *et al.*, 1999; Tikka *et al.*, 2001; He *et al.*, 2001; Tikka and Koistinaho, 2001). Various mutant mice deficient in key components of the leukocyte repertoire are available and could be crossed with the *rumpshaker* mice to determine if this reduced the lesions.

This study also supports the glial proliferation compensation mechanism. In some dysmyelinating animals there is an increment in glial cell population, which is coupled with an increase in dead cells. This implies underlying mechanisms, which control the numbers of the cells. There are several explanations for continued proliferation of glial cells. One possibility is that the competition for the inadequate available extracellular growth factors such as FGF and PDGF results in abnormal continued proliferation and death of glial cells. Lines of evidence support this view;

for instance, vulnerability of oligodendrocytes to apoptosis is prevented in an environment conditioned with basic FGF (Yasuda *et al.*, 1995). Additionally, providing *jimpy* oligodendrocytes with alternative environmental factors *in vivo* (Lachapelle *et al.*, 1991) or medium conditioned by cell lines which express normal products of the *Plp* gene *in vitro* (Knapp *et al.*, 1999), increases their survival. An abnormal microenvironment where the mutant oligodendrocytes develop could contain factors or signals responsible for glial cell proliferation and/or apoptosis. The GRO-1 chemokine which stimulates proliferation of oligodendrocyte progenitors is increased in *jimpy* spinal cords (Wu *et al.*, 2000). The microenvironmental factors and/or feedback signal pathways from the degenerative neural tissue seem to be particularly important for glial proliferation and/or death. The more realistic conclusion for the glial proliferation and/or death is that there is a cross talk between the survival and death factors or signals, which might be mediated by any of the normal *Plp* gene products in some stages. Interestingly, a soluble product of the *Plp* gene representing a C-terminal fragment, has been stated to have mitotic activity (Yamada *et al.*, 1999) although this function was not retained by mutant proteins, including *rumpshaker* (Yamada *et al.*, 2001).

Additionally, differentiation and maturation of glial cell lineages in dysmyelinating mutant animals have received little attention over the last period. The scientists involved have been more interested in studying the most advanced stages of the pathology in these mutants (for instances the abnormalities of myelin, proliferation or apoptosis of glial cell lineages, etc.) trying to explore the possible function of PLP/DM20. DM20 is an alternative transcript of the PLP; the significance of its appearance at mid-gestation (Timsit *et al.*, 1992; Timsit *et al.*, 1995; Dickinson *et al.*, 1996; Spassky *et al.*, 1998) prior to the onset of normal myelination in mice, is unknown. One possible opinion is that DM20 may have a role in the differentiation, maturation and specification of various systems in the embryos. As this protein or message is expressed specifically in the oligodendrocyte lineage within the CNS one might expect its influence to be on differentiation and maturation of these cells and on myelination. In the case of *Plp* gene mutant animals, oligodendrocyte progenitors may continue to proliferate rather than differentiate and mature, due to the abnormal *DM20* message or protein. Thus, a population of cells which is dividing without differentiation can obviously produce more cells over a period of time than one in which cells differentiate and exit the cell cycle, as in normal development. Another interesting possibility is that abnormal DM20 may delay the differentiation and maturation by some modification or suppression events.

Although severity of the phenotypes still considers an open question. Example of the mild form or severe form of the disease is well demonstrated in *rumpshaker* in

which C3H *rsh* (mild) and C57 *rsh* (severe). Similarly, in humans the mild form is SPG2 while the more severe form is PMD. To address such a question, it would be useful to understand the correlation between the accumulation of mutant DM20 and the severe phenotype as many studies provide some evidences that stressed its effect on the resultant phenotypes of the mutation. A strong correlation between the accumulation of mutant forms of DM20 in the RER and severe disease in humans has been proposed (Tosic *et al.*, 1996; Gow and Lazzarini, 1996; Tosic *et al.*, 1997). Using the COS-7 cells, the non-oligodendrocyte related system, it has been domenstrated that only mutations associated with severe disease in patients interrupt DM20 trafficking and cause the protein to accumulate in the RER (Gow and Lazzarini, 1996; Southwood and Gow, 2001); mutations that do not perturb DM20 trafficking cause mild forms of the disease. This suggests that either the accumulation of DM20 may be extremely toxic to cells and further increases the vulnerability of oligodendrocytes to apoptosis or that failure to transport DM20 to the cell membrane is necessary for normal function. In other words, mutations that interrupt the trafficking of both PLP and DM20 can be viewed simply as causing more pronounced manifestations of the phenotypes than those that are observed in mildly affected human patients. In this perspective, the disease process can be largely accounted for by an accumulation of mutant PLP in the perinuclear region of oligodendrocytes and additional accumulation of mutant DM20 simply increases severity (Southwood and Gow, 2001). In relation to the above view, immunoblotting suggests that the amount of PLP in C57 *rsh* is 50% of that of C3H *rsh*. The amount of DM20 is 2/3 reduced in C57 *rsh* compared with its C3H counterpart. This data, if interpreted in favour of the previously mentioned explanation, should be treated with care as one expected that the compartmental arrest of DM20 mirrors the severity of the phenotype in C57 strain. In contrast, C3H *rsh* has minor alteration in the level of DM20, thus, the phenotype is mild. Thus, tracing the *Plp* gene products in the different strains of *rumpshaker* would clarify this theory.

The results from the current study provide further evidence that *rumpshaker* mutants are an appropriate model for SPG2 and PMD and are available for testing any hypothesis that could not easily be addressed in human materials. This mutation on both different genetic backgrounds embodies the broad spectrum of PMD/SPG2 phenotypes in some, but not all, aspects. These two mutants provides advantages over each other in which C57 *rsh* could be used for studying some mechanisms such as apoptosis, macrophage/microglial response, proliferation or protein pathways, for example. Whereas the C3H *rsh* could be a useful model for testing some features, for instance, the differentiation and maturation of glial lineages in oligodendrocytes and the mechanisms or factors controlling these developmental

processes under the influence of the mutation. Studying the genetic aspect in relation to the *rumpshaker* mutation on the two different genetic backgrounds could give us a clue to the genetic interactions that give rise to the divergent phenotypes.

Clearly, the time is now appropriate to initiate further studies into several aspects of the *rumpshaker* mutation, related to the phenotypic differences induced by the two genetic backgrounds. A mapping study to identify regions harbouring putative modifying loci, with the eventual aim of cloning the genes, is an immediate priority. The use of new molecular tools of microarray and proteomics would seem appropriate to determine patterns of gene expression that differ between the two strains. It is quite probable that some of these genes showing differences in expression will also correlate with those identified in the mapping study. The recent developments in mouse genomics make all these approaches viable options.

6. Appendix 1

6.1.1 APES-coated slides

APES-coated slides were generally used for Immunohistochemistry because they keep the sections adhered. For cleaning grease, slides were soaked overnight in 5% Decon 90 (Decon Lab Ltd) and washed in distilled water and oven dried. The dried slides were then soaked in 0.25% APES (Sigma) in methylated spirit in a fume hood for 2 minutes. Finally, the slides were rinsed in DEPC-treated water for 2 minutes and oven dried wrapped in foil. APES-coated slides were stored at room temperature.

6.1.2 DEPC-treated water

0.1% solution of DEPC was made in distilled water and left for at least 12 hours to inactivate contaminating RNases. The water was autoclaved at 15lb.in^{-2} for 20 minutes to destroy the DEPC before use and stored sealed at room temperature until require.

6.1.3 Fixatives

6.1.3.1 Karnovsky's modified fixative (paraformaldehyde/glutaraldehyde 4%/5%)

Preperation of 500 ml of the fixative:

8% Paraformaldehyde: 20 g of paraformaldehyde was added to 250 ml of dH_2O and heat to 65°C. Few drops of 1M NaOH was added to clear and solution was allowed to cool .

0.08M Cacodylate buffer: 17.1224 sodium cacodylate was dissolved in a 1 litre of dH_2O and adjusted to pH 7.2.

250 ml	8% paraformaldehyde
100 ml	25% glutaraldehyde
150 ml	0.08M cacodylate buffer
250 mg	Calcium chloride

Add volumes, dissolve calcium choride, adjust to pH 7.2, filter, and store at 4%.

6.1.3.2 4% paraformaldehyde

Preperation of 500 of the fixative:

20g paraformaldehyde was added to 500ml PBS and heat to 65°C. Few drops of 1M NaOH were added to clear the solution, filtered, cooled, and adjusted to pH 7.2.

6.1.3.3 Periodate-lysine-paraformaldehyde (P-L-P) fixative

Preperation of 1litre of the fixative:

Buffered lysine solution: 13.7g lysine monohydrate dissolved in 375ml dH_2O. 1.8g sodium hydrogen phosphate dissolved in 100ml dH_2O. The two solutions were mixed to give 475ml and pH 7.4

10% Paraformaldehyde: 20g paraformaldehyde dissolved in 200 ml dH_2O and heated to 65°C. Few drops of 1M NaOH were added to clear and allowed to cool.

The two solutions were separately stored at 4°C overnight. Immediately before use the two solutions were mixed and the final volume is made up to 1litre using 0.1M phosphate buffer. 2.14g sodium periodate was also dissolved .

6.1.3.4 Buffered neutral formaldehyde

Preperation of 1 litre of the fixative:

100 ml	40% formaldeyde (Merck)
900 ml	tap water
4 g	sodium dihydrogen phosphate
8 g	di-potasium hydrogen phosphate

6.1.4 Tissue processing protocols

6.1.4.1 Paraffin wax processing

BNP fixed materials were passed through below various solutions and finally blocked in paraffin wax.

NB: Necoloidine (Merck) solution for microscopy was considered to be a 100% celloidin, therefore, 1ml was added per 100ml methyl benzoate.

1-	70% methylated spirit/5% phenol	2 hr	room temperature
2-	90% methylated spirit/5% phenol	2hr	room temperature
3-	methylated spirit	2hr	room temperature
4-	ethanol/5% phenol	2hr	room temperature
5-	ethanol/5% phenol	1hr	room temperature
6-	ethanol/5% phenol	1hr	room temperature
7-	1% celloidin in methyl benzoate	4hr	room temperature
8-	xyelene	1hr	room temperature
9-	xyelene	1hr	room temperature
10-	xyelene	1hr	room temperature
11-	paraffin wax	6hr	60°C
12-	paraffin wax	6hr	60°C

6.1.4.2 Resin processing

CNS tissues were passed through below various solutions and finally blocked in resin:

1-	isotonic cacodylate buffer	50 min	4°C
2-	1% OsO4 in cacodylate buffer	2hr	room temperature
3-	isotonic cacodylate buffer	30 min	room temperature
4-	50% ethanol	5 min	4°C
5-	50% ethanol	10 min	4°C
6-	70% ethanol	5 min	4°C
7-	70% ethanol	10 min	4°C
8-	80% ethanol	5 min	4°C
9-	80% ethanol	10 min	4°C
10-	90% ethanol	5 min	4°C
11-	90% ethanol	10 min	4°C
12	ethanol	20 min	4°C
13	ethanol	20 min	4°C
14-	propylene oxide	15 min	room temperature
15-	propylene oxide	15 min	room temperature
16-	1:2 resin: propylene oxide	13 hr	room temperature
17-	1:1 resin: propylene oxide	6 hr	room temperature
18-	2:1 resin: propylene oxide	18 hr	room temperature
19-	resin	4 hr	30°C

Isotonic cacodylate buffer:

16.05 g	sodium cacodylate
3.8 g	sodium chloride
0.055 g	calcium chloride
0.102 g	magnesium chloride

Dissolved in 1litre dH_2O and adjusted to pH 7.2

Araldite resin:

1-	30 g	araldite CY212 (resin)
2-	25.2 g	dodecanyl succinic anhydride
3-	1.2 ml	2,4,6-tri-dimethylaminomethyl-phenol
4-	0.75 ml	di-butylphthalate

Add 1and 2, place in an oven at 65°C for 10-15 min and mix. Add 3 and 4, and Stear until mixure well homogenised and stored at -20°C.

6.1.5 Staining protocols

6.1.5.1 Dewaxing and rehydration of paraffin sections

1-	xylene	2 mins
2-	absolute alcohol	2 mins
3-	methylated spirits	2 mins
4-	water	2 mins
5-	Lugols iodine	1 min
6-	water	1 min
7-	5% sodium thiosulphate	1 min
8-	water	2 mins

6.1.5.2 Dehydration and cleaning of sections

1-	methylated spirits	2 mins
2-	absolute alcohol	2 mins
3-	absolute alcohol	2 mins
4-	histoclear	2 mins
5-	xylene	2 mins

6.1.5.3 Haematoxylin and eosin

1-	xylene	2 mins
2-	absolute alcohol	2 mins
3-	methylated spirits	2 mins
4-	water	2 mins
5-	Lugols iodine	1 min
6-	water	1 min
7-	5% sodium thiosulphate	1 min
8-	water	2 mins
9-	Mayers haematoxylin	10 mins
10	1% acid alcohol	3 dips
11-	water	2 mins
12-	Scots tap water substitute	1 min
13-	water	2 mins
14-	methylated spirits	10 secs
15-	saturated alcoholic eosin	2 mins
16-	methylated spirits	10 secs
17-	absolute alcohol	2 mins
18-	histoclear	2 mins
19-	xylene	5 mins

6.1.5.4 Haematoxylin

1-	Running water	2 mins
2-	Mayers haematoxylin	50 secs
3-	water	wash off excess haematoxylin
4-	Scots tap water substitute	30 secs

6.1.5.5 Staining for electron microscopy

1-	saturated uranyl acetate in 50% ethanol	15 min
2-	50% ethanol	rinse
3-	50% ethanol	rinse
4-	dH_2O	rinse
5-	dH_2O	rinse
6-	air dry	
7-	Reynold's lead citrate (Sodium Hydroxide moistened chamber)	10 mins
8-	1M sodium hydroxide	rinse
9-	1M sodium hydroxide	rinse
10-	1M sodium hydroxide	rinse
11	dH_2O	Several rinses

Reynold's lead citrate (1.2mM lead citrate, 1.8mM sodium citrate, pH 12.0)

1-	1.33 g lead nitrate dissolved in 15 ml dH_2O	1 min vigorous shaking
2-	1.76 g sodium citrate dissolved in 15 ml dH_2O	1 min vigorous shaking

Add 1 to 2 and equilibrate over 30 minutes with occasional shaking. Clear with 1M NaOH and make up to the final volume of 50 ml with dH_2O.

6.1.6 Staining solutions

6.1.6.1 Methylene blue/ azure II

1%	methylene blue
1%	azure II
1%	borax

diluted dH_2O and filtered before use

6.1.6.2 Mayers haematoxylin

1 g	haematoxylin
10 g	potassium alum
0.2 g	sodium iodate

in 1 litre of dH_2O, bring to boiling point, allow to cool overnight, and then add:

1 g	citric acid
50 g	chloral hydrate

6.1.6.3 Scots tap water substitute

3.5 g	sodium bicarbonate
20 g	magnesium sulphate

in 1 litre of dH_2O

6.1.7 General Buffers

6.1.7.1 Phosphate buffer saline (PBS)

8 g	sodium chloride
1.44 g	disodium hydrogeg phosphate
0.24 g	potassium dihydrogeg phosphate
0.2 g	potassium chloride

Dissolved in 800 ml of dH_2O, adjusted to pH 7.4 with 1M HCl and the volume made up to 1 litre with dH_2O

6.1.7.2 0.1 M phosphate buffer

77.4 ml	1M disodium hydrogeg phosphate
22.6 ml	1M potassium dihydrogeg phosphate

combined two volumes and adjusted to pH 7.4 with 1MHCl

6.1.7.3 Tris buffer saline

3 g	tris base pH 7.5
8 g	sodium chloride
0.2 g	potassium chloride

dissolved in 800 ml of dH_2O, adjusted to pH 7.4 with 1M HCl and the volume made up to 1 litre with dH_2O.

6.1.7.4 Tris-EDTA buffer (TE buffer)

500 µl	1M tris pH 8.0
100 µl	0.5M EDTA

Volume made up to 50 ml with dH_2O

6.1.7.5 Tris acetate EDTA buffer x10 (TAE buffer)

48.4	tris base
11.4 ml	glacial acetic acid
20 ml	0.5M EDTA

Volume made up to 1 litre with dH_2O

7. Appendix 2. Details of statistical analyses

Parameter	C3H WT			C3H *rsh*			C57 WT			C57 *rsh*			P 1	P 2	P 3
	M	SEM	N	M	SEM	N	M	SEM	N	M	SEM	N			
Glial density P10	172	14	6	245	9	9				236	15	2			
Glial density P15	129	4	5	199	7	9	130	7	5	271	13	6	***	***	***
Glial density P20	101	5	5	182	8	11	103	2	5	218	8	12	***	***	**
Glial density P25	87	3	5	169	10	5	91	5	4	188	6	7	***	***	NS
Glial density P30	74	3	6	167	6	10	78	3	5	141	4	11	***	***	**
Total glia P10	104	7	6	119	6	9				95	0	2			
Total glia P15	109	5	5	153	5	9	108	5	5	160	29	6	NS	NS	NS
Total glia P20	116	2	5	165	6	11	107	4	5	197	10	12	*	***	*
Total glia P25	94	3	5	158	9	5	94	5	4	184	4	7	***	NS	***
Total glia P30	96	5	6	147	9	10	86	4	5	142	6	11	***	***	NS

Significance: P1 = C3H WT v C3H *rsh*. P2 =C57 WT v C57 *rsh*. P3 = C3H *rsh* v C57 *rsh*

* <0.05. ** <0.01 *** <0.001

Parameter	C3H WT			C3H *rsh*			C57 WT			C57 *rsh*			P 1	P 2	P 3
	M	SEM	N	M	SEM	N	M	SEM	N	M	SEM	N			
WM area P10	0.61	0.04	6	0.49	0.02	9				0.4	0.02	2			
WM area P15	0.84	0.03	5	0.77	0.02	9	0.84	0.06	5	0.69	0.03	6	NS	NS	NS
WM area P20	1.16	0.05	5	0.92	0.02	11	1.03	0.02	5	0.9	0.03	12	***	NS	NS
WM area P25	1.09	0.05	5	0.94	0.02	5	1.03	0	4	0.98	0.03	7	NS	NS	NS
WM area P30	1.3	0.03	6	0.87	0.03	10	1.12	0.04	5	1	0.01	11	***	*	**
Total Ols P20	62	3	5	71	3	11	54	4	5	67	3	12	NS	NS	NS
Total Astro P20	30	2	5	43	2	11	23	5	5	37	4	12	NS	NS	NS
Total Microgl P20	19	3	5	41	3	11	24	3	5	55	4	12	***	***	*

Significance: P1 = C3H WT v C3H *rsh*. P2 =C57 WT v C57 *rsh*. P3 = C3H *rsh* v C57 *rsh*

* <0.05. ** <0.01 *** <0.001 Ols = Oligodendrocyte Astro = Astrocyte Microgl = Microglia

Parameter	C3H WT			C3H *rsh*			C57 WT			C57 *rsh*			P 1	P 2	P 3
	M	SEM	N	M	SEM	N	M	SEM	N	M	SEM	N			
Pyknotic nuclei P10	7.5	0.7	7	5.1	0.7	10	5.6	0.6	5	5.8	0.9	7	NS	NS	NS
Pyknotic nuclei P15	8.9	1	5	3.7	0.2	5	5.3	0.8	5	9.4	1.7	6	*	NS	*
Pyknotic nuclei P20	3.8	1.3	5	8.6	0.6	11	1.7	0.5	6	13.9	1.1	12	**	***	***
Pyknotic nuclei P25	1.3	0.7	5	4.3	0.8	5	0.9	0.5	5	14.3	2.5	7	NS	***	**
Pyknotic nuclei P30	2.3	0.4	6	8.4	0.8	10	1	0.4	5	12.1	0.6	12	***	***	**
MBP myelin P10	474	11	4	394	3	4	528	9	4	321	16	4	**	***	**
MBP myelin P15	519	4	4	415	7	4	511	9	4	319	16	4	***	***	***
MBP myelin P20	553	15	4	413	8	4	552	3	4	328	14	4	***	***	**
MBP myelin P30	542	9	7	398	7	23	556	13	4	352	18	4	***	***	*

Significance: P1 = C3H WT v C3H *rsh*. P2 =C57 WT v C57 *rsh*. P3 = C3H *rsh* v C57 *rsh*

* <0.05. ** <0.01 *** <0.001

Parameter	C3H WT			C3H *rsh*			C57 WT			C57 *rsh*			P 1	P 2	P 3
	M	SEM	N	M	SEM	N	M	SEM	N	M	SEM	N			
Myelin vol P20				0.118	0.01	9				0.070	0.003	4			*
Myelin vol P30				0.137	0.005	5				0.11	0.004	6			
APC density P15	381	15	4	455	14	4	372	45	4	511	13	4	NS	*	NS
APC density P20	398	57	5	691	28	4	400	17	4	541	46	4	**	NS	NS
APC density P30	376	100	4	633	30	4	334	34	4	310	12	6	*	NS	**
Total APC+ P20	399	43	4	567	21	4	429	20	4	497	54	6	NS	NS	NS
Caspase-3+ P10	9.5	1.2	4	12	1.9	4	4.4	1.5	5	22.7	0.3	5	NS	***	***
Caspase-3+ P15	11.1	1.3	4	22.2	1.8	6	4.5	1.2	4	29.8	6.8	6	NS	*	NS
Caspase-3+ P20	5	1.2	5	17.3	2.9	6	2	0.5	4	26.6	0.8	4	**	***	*
Caspase-3+ P30	0.3	0.3	4	5.9	1.8	4	0.3	0.3	4	19.7	4.5	6	NS	**	*

Significance: P1 = C3H WT v C3H *rsh*. P2 =C57 WT v C57 *rsh*. P3 = C3H *rsh* v C57 *rsh*

* <0.05. ** <0.01 *** <0.001

Parameter	C3H WT			C3H *rsh*			C57 WT			C57 *rsh*			P 1	P 2	P 3
	M	SEM	N	M	SEM	N	M	SEM	N	M	SEM	N			
BrdU LI P5	5.92	0.7	4	5.9	0.3	4	5.2	0.4	5	7.4	0.8	3	NS	NS	NS
BrdU LI P10	5.4	0.7	3	6.5	0.3	5	5.1	0.2	5	8.9	0.7	5	NS	***	*
BrdU LI P15	1.3	0.3	5	3.1	0.7	5	1.2	0.2	3	5.5	0.6	3	NS	**	NS
BrdU LI P20	0.6	0.3	4	1.3	0.07	4	0.2	0.07	4	4.4	1.4	5	NS	*	NS
BrdU LI P30	0.1	0.03	3	0.9	0.2	5	0.02	0.02	3	2.3	0.5	4	NS	***	*
BrdU density P5	208	15	4	231	16	4	176	15	5	244	29	3	NS	NS	NS
BrdU density P10	176	22	3	239	13	5	160	5	4	378	25	4	NS	***	***
BrdU density P15	33	8	5	103	21	5	25	7	3	222	34	5	NS	***	**
BrdU density P20	11	5	4	37	2	4	3	1	4	149	48	5	NS	*	NS
BrdU density P30	2	0.4	3	23	5	5	0.3	0.3	4	54	11	4	NS	***	*

Significance: P1 = C3H WT v C3H *rsh*. P2 =C57 WT v C57 *rsh*. P3 = C3H *rsh* v C57 *rsh*

* <0.05. ** <0.01 *** <0.001 BrdU LI = BrdU labelling index

Parameter	C3H WT			C3H *rsh*			C57 WT			C57 *rsh*			P 1	P 2	P 3
	M	SEM	N	M	SEM	N	M	SEM	N	M	SEM	N			
CD45 density P20	69	9	4	230	12	4	59	5	5	378	19	5	***	***	***
CD45 density P30	63	7	4	163	13	4	42	7	4	234	20	5	**	***	*
NG2 density P15	200	13	4	179	14	4	156	7	4	256	25	4	NS	**	*
NG2 density P20	128	9	4	181	24	6	137	10	5	346	39	4	NS	***	***
NG2 density P30	98	14	4	187	25	4	107	17	4	193	14	4	*	*	NS

Significance: P1 = C3H WT v C3H *rsh*. P2 =C57 WT v C57 *rsh*. P3 = C3H *rsh* v C57 *rsh*

* <0.05. ** <0.01 *** <0.001

Parameter	C3H *rsh*			C57 *rsh*			**P 1**	**P 2**	**P 3**
Western blot	**M**	**SEM**	**N**	**M**	**SEM**	**N**			
PLP	8.7	2.1	7	6.0	0.43	7	***	***	NS
DM20	14.7	3.5	7	4.0	0.84	7	***	***	*
MBP	58.2	11.6	5	30.3	6.8	6	*	***	#
CNP	81.2	14.5	7	25.8	2.7	7	NS	***	**
MAG	71.2	6.7	4	32.3	4.8	3	NS	*	**
GFAP (major)	161.6	23.3	4	123	11	5	**	#	NS
GFAP (minor)	784.8	254.3	4	455	227	4	**	*	NS

Significance: P1 = C3H WT v C3H *rsh*. P2 =C57 WT v C57 *rsh*. P3 = C3H *rsh* v C57 *rsh*

#: approaching statistical significance * <0.05 ** <0.01 *** <0.001

Values shown above were expressed as % of respective wild type. Statistical analysis for the blots was performed using Student's two tailed unpaired t-test. The level of statistical significance in P1 and P2 was derived by comparing the densitometric values while P3 was derived by comparing the % alteration in each mutant.

8. Abbreviations

ABC	avidin biotine complex
APC	adenomatous polyposis and somatic mutations
AOI	area of interest
APES	3-aminopropyltriethoxy-silane
BNF	buffered neutral paraformaldehyde
bp	base pair
BrdU	bromodeoxy Uridine
C2	second segment of cervical cord
CD45	leukocyte cell surface glycoprotein
C3H *rsh*	C3H/101 *rumpshaker*
C3H WT	C3H/101 wild type
CNP	2,3, cyclic nucleotide 3-phosphodiesterase
CNS	central nervous system
C57 *rsh*	C57BL/6J *rumpshaker*
C57 WT	C57BL/6J wild type
DAP	3,4,3,4,-teraminobiphenyl hydrochloride
DAPI	4,6-diamidino-2-phenylindole
dH_2O	distilled water
DM20	26.5 kDa protein isoform encoded by *Plp* gene
DNA	deoxyribonucleic acid
dNTP	deoxynucleoside triphosphate

DTT	dithiothreitol
EDTA	ethylene-di-amine-tetra-acetate
EM	electron microscope
F4/80	a 160 kD glycoprotein expressed by murine macrophages
FGF	fibroblast growth factor
FITC	fluorescein isothiocyanate
GC	galactocerebroside
gDNA	genomic deoxyribonucleic acid
GFAP	glial fibrillary acidic protein
H&E	haematoxylin and eosin
HRP	horseradish peroxidase
HSPGs	heparan sulphate proteoglycans
IPL	intraperiod line
IGF	insulin growth factor
KDa	kiloDalton
LI	labelling index
LM	light microscope
M	molar
MAG	myelin-associated glycoprotein
MBP	myelin basic protein
MDL	major dense line
ml	millilitre
μl	micromillilitre
mg	milligram

mM	millimolar
μm	micromillimetre
MOBP	myelin-associated oligodenrocytic basic protein
MOG	myelin/oligodendrocyte glycoprotein
MOSP	myelin oligodendrocyte specific protein
mRNA	messenger ribonucleic acid
NG2	integral membrane chondroitin sulfate proteoglycan
NGS	normal goat serum
OMGP	oligodendrocyte myelin glycoprotein
OSP	oligodendrocyte specific protein
P	postnatal
PAP	peroxidase-anti-peroxidase
PBS	phosphate buffered saline
PCR	polymerase chain reaction
PDGFRα	platelet-derived growth factor A
PLP	proteolipid protein (30kDa protein)
P-L-P	periodate-lysine-paraformaldehyde
PLP	proteolipid protein (human gene)
Plp	proteolipid protein (non-human gene)
Plp^{jp}	*jimpy*
$Plp^{jp\text{-}4j}$	*jimpy-4j*
Plp^{jp}/y	*jimpy* male
$Plp^{jp/+}$	*jimpy* heterozygote
$Plp^{jp\text{-}msd}$	*myelin synthesis deficient*

Plp^{md}	*myelin deficient*
Plp^{pt}	*paralytic tremor*
Plp$^{jp\text{-}rsh}$	*rumpshaker*
Plp$^{jp\text{-}rsh}$/y	*rumpshaker* male
Plp$^{jp\text{-}rsh/+}$	*rumpshaker* heterozygote
Plp$^{jp\text{-}rsh}$/*Plp*$^{jp\text{-}rsh}$	*rumpshaker* homozygote
Plp$^{+/+}$	wild type
PMD	Pelizaeus-Merzbacher disease
PNS	peripheral nervous system
POA	proligodendroblast antigen
PVDF	polyvinylidene fluoride microporous membrane
RA	retinoic acid
RER	rough endoplasmic reticulum
RNA	ribonucleic acid
RNase	ribonuclease
rpm	revolution per minute
rsh	*rumpshaker*
SDS	sodium dodecyl sulphate
SDS-PAGE	sodium dodecyl sulphate polyarylamide gel eletrophoresis
Sec	second
s.e.m	standard error of the mean
SPG2	Spastic Paraplegi Type 2
SrDM20	soma-restricted DM20 protein isoform
SrPLP	soma-restricted PLP protein isoform

TAE	tris acetate ethylene-di-amine-tetra-acetate buffer
Taq	themophilus aquaticus
TBS	tris buffered saline
TEMED	N,N,N,N', tetramethylethylenediamine
TxR	Texas red
U	unit
U1snRNP	U1 small nuclear ribonucleoproteins
UPR	unfolded protein response
UTR	untranslated region
UV	ultraviolet

9. References

Aldskogius,H. (2001) Microglia in neuroregeneration. *Microscopy Research and Technique.* **54:** 40-46.

Alliot,F., Godin,I. and Pessac,B. (1999) Microglia derive from progenitors, originating from the yolk sac, and which proliferate in the brain. *Developmental Brain Research.* **117:** 145-152.

Amur-Umarjee,S.G., Hall,L. and Campagnoni,A.T. (1990) Spatial distribution of mRNAs for myelin proteins in primary cultures of mouse brain. *Developmental Neuroscience.* **12:** 263-272.

Anderson,T.J., Klugmann,M., Thomson,C.E., Schneider,A., Readhead,C., Nave,K.-A. and Griffiths,I.R. (1999) Distinct phenotypes associated with increasing dosage of the Plp gene: implications for CMT1A due to Pmp22 gene duplication. *Annals of the New York Academy of Sciences.* **883:** 234-246.

Arenella,L.S. and Herndon,R.M. (1984) Mature oligodendrocytes. Division following experimental demyelination in adult animals. *Archives of Neurology.* **41:** 1162-1165.

Aruga,J., Okano,H. and Mikoshiba,K. (1991) Identification of the new isoforms of mouse myelin basic protein: the existence of exon 5a. *Journal of Neurochemistry.* **56:** 1222-1226.

Baba,H., Akita,H., Ishibashi,T., Inoue,Y., Nakahira,K. and Ikenaka,K. (1999) Completion of myelin compaction, but not the attachment of oligodendroglial processes triggers K^+ channel clustering. *Journal of Neuroscience Research.* **58:** 752-764.

Bansal,R., Stefansson,K. and Pfeiffer,S.E. (1992) Proligodendroblast antigen (POA), a developmental antigen expressed by A007/O4-positive oligodendrocyte progenitors prior to the appearance of sulfatide and galactocerebroside. *Journal of Neurochemistry.* **58:** 2221-2229.

Baron,P., Shy,M., Kamholz,J., Scarlato,G. and Pleasure,D. (1994) Expression of P0 protein mRNA along rat sciatic nerve during development. *Developmental Brain Research.* **83:** 285-288.

Barres,B.A., Hart,I.K., Coles,H.S.R., Burne,J.F., Voyvodic,J.T., Richardson,W.D. and Raff,M.C. (1992) Cell death and control of cell survival in the oligodendrocyte lineage. *Cell.* **70:** 31-46.

Barres,B.A. and Raff,M.C. (1993) Proliferation of oligodendrocyte precursor cells depends on electrical activity in axons. *Nature.* **361:** 258-260.

Barres,B.A. and Raff,M.C. (1994) Control of oligodendrocyte number in the developing rat optic nerve. *Neuron.* **12:** 935-942.

Barres,B.A. and Raff,M.C. (1999) Axonal control of oligodendrocyte development. *Journal of Cell Biology.* **147:** 1123-1128.

Bartlett,W.P. and Skoff,R.P. (1986) Expression of the jimpy gene in the spinal cords of heterozygous female mice. I. An early myelin deficit followed by compensation. *Journal of Neuroscience.* **6:** 2802-2812.

Bauer,J., Bradl,M., Klein,M., Leisser,M., Deckwerth,T.L., Wekerle,H. and Lassmann,H. (2002) Endoplasmic reticulum stress in PLP-overexpressing transgenic rats: Gray matter oligodendrocytes are more vulnerable than white matter oligodendrocytes. *Journal of Neuropathology and Experimental Neurology.* **61:** 12-22.

Beesley,J.S., Lavy,L., Eraydin,N.B., Siman,R. and Grinspan,J.B. (2001) Caspase-3 activation in oligodendrocytes from the myelin-deficient rat. *Journal of Neuroscience Research.* **64:** 371-379.

Belmont,J.W. (1996) Genetic control of X inactivation and processes leading to X-inactivation skewing. *American Journal of Human Genetics.* **58:** 1101-1108.

Berry,M., Hall,S., Rees,L., Carlile,J. and Wyse,J.P.H. (1992) Regeneration of axons in the optic nerve of the adult Browman- Wyse (BW) mutant rat. *Journal of Neurocytology.* **21:** 426-448.

Bezzi,P. and Volterra,A. (2001) A neuron-glia signalling network in the active brain. *Current Opinion in Neurobiology.* **11:** 387-394.

Bhat,R.V., Axt,K.J., Fosnaugh,J.S., Smith,K.J., Johnson,K.A., Hill,D.E., Kinzler,K.W. and Baraban,J.M. (1996) Expression of the APC tumour suppressor protein in oligodendroglia. *Glia.* **17:** 169-174.

Bhat,S. and Pfeiffer,S.E. (1986) Stimulation of oligodendrocytes by extracts from astrocyte-enriched cultures. *Journal of Neuroscience Research.* **15:** 19-27.

Bignami,A., Eng,L.F. and Uyeda,C.T. (1972) Localization of the glial fibrillary acidic protein in astrocytes by immunofluorescence. *Brain Research.* **43:** 429-435.

Billings-Gagliardi,S., Adcock,L.H., Lamperti,E.D., Schwing-Stanhope,G. and Wolf,M.K. (1983) Myelination of *jp, jp^{msd}* and *qk* axons by normal glia in vitro: ultrastructural and autoradiographic evidence. *Brain Research.* **268:** 255-266.

Billings-Gagliardi,S., Kirschner,D.A., Nadon,N.L., DiBenedetto,L.M., Karthigasan,J., Lane,P., Pearsall,G.B. and Wolf,M.K. (1995) Jimpy 4J: A new X-linked mouse mutation producing severe CNS hypomyelination. *Developmental Neuroscience.* **17:** 300-310.

Billings-Gagliardi,S., Nunnari,J.N., Nadon,N.L. and Wolf,M.K. (1999) Evidence that CNS hypomyelination does not cause death of jimpy-msd mutant mice. *Developmental Neuroscience.* **21:** 473-482.

Bjornson,C.R., Rietze,R.L., Reynolds,B.A., Magli,M.C. and Vescovi,A.L. (1999) Turning brain into blood: A hematopoietic fate adopted by adult neural stem cells in vivo. *Science.* **283:** 534-537.

Boiko,T., Rasband,M.N., Levinson,S.R., Caldwell,J.H., Mandel,G., Trimmer,J.S. and Matthews,G. (2001) Compact myelin dictates the differential targeting of two sodium channel isoforms in the same axon. *Neuron.* **30:** 91-104.

Boison,D., Büssow,H., D'Urso,D., Müller,H.-W. and Stoffel,W. (1995) Adhesive properties of proteolipid protein are responsible for the compaction of CNS myelin sheaths. *Journal of Neuroscience.* **15:** 5502-5513.

Boison,D. and Stoffel,W. (1989) Myelin-deficient rat: a point mutation in exon III (A->C, Thr75->Pro) of the myelin proteolipid protein causes dysmyelination and oligodendrocyte death. *EMBO J.* **8:** 3295-3302.

Boison,D. and Stoffel,W. (1994) Disruption of the compacted myelin sheath of axons of the central nervous system in proteolipid protein-deficient mice. *Proceedings of the National Academy of Sciences USA.* **91:** 11709-11713.

Bolivar,V.J. and Brown,R.E. (1994) The ontogeny of ultrasonic vocalizations and other behaviours in male jimpy (jp/Y) mice and their normal littermates. *Developmental Psychobiology.* **27:** 101-110.

Bongarzone,E.R., Campagnoni,C.W., Kampf,K., Jacobs,E., Handley,V.W., Schonmann,V. and Campagnoni,A.T. (1999) Identification of a new exon in the myelin proteolipid protein gene encoding novel protein isoforms that are restricted

to the somata of oligodendrocytes and neurons. *Journal of Neuroscience.* **19:** 8349-8357.

Bongarzone,E.R., Foster,L.M., Byravan,S., Schonmann,V. and Campagnoni,A.T. (1997) Temperature-dependent regulation of PLP/DM20 and CNP gene expression in two conditionally-immortalized jimpy oligodendrocyte cell lines. *Neurochemical Research.* **22:** 363-372.

Bongarzone,E.R., Jacobs,E., Schonmann,V. and Campagnoni,A.T. (2001) Classic and soma-restricted proteolipids are targeted to different subcellular compartments in oligodendrocytes. *Journal of Neuroscience Research.* **65:** 477-484.

Brady,S.T., Witt,A.S., Kirkpatrick,L.L., De Waegh,S.M., Readhead,C., Tu,P.H. and Lee,V.M.Y. (1999) Formation of compact myelin is required for maturation of the axonal cytoskeleton. *Journal of Neuroscience.* **19:** 7278-7288.

Bray,G.M., Rasminsky,M. and Aguayo,A.J. (1981) Interactions between axons and their sheath cells. *Annual Review of Neuroscience.* **4:** 127-162.

Bronstein,J.M., Popper,P., Micevych,P.E. and Farber,D.B. (1996) Isolation and characterization of a novel oligodendrocyte- specific protein. *Neurology.* **47:** 772-778.

Brown,M.C., Besio Moreno,M., Bongarzone,E.R., Cohen,P.D., Soto,E.F. and Pasquini,J.M. (1993) Vesicular transport of myelin proteolipid and cerebroside sulfates to the myelin membrane. *Journal of Neuroscience Research.* **35:** 402-408.

Butt,A.M., Ibrahim,M., Gregson,N. and Berry,M. (1998) Differential expression of the L- and S-isoforms of myelin associated glycoprotein (MAG) in oligodendrocyte unit phenotypes in the adult rat anterior medullary velum. *Journal of Neurocytology.* **27:** 271-280.

Butt,A.M., Ibrahim,M., Ruge,F.M. and Berry,M. (1995) Biochemical subtypes of oligodendrocyte in the anterior medullary velum of the rat as revealed by the monoclonal antibody Rip. *Glia.* **14:** 185-197.

Calver,A.R., Hall,A.C., Yu,W.P., Walsh,F.S., Heath,J.K., Betsholtz,C. and Richardson,W.D. (1998) Oligodendrocyte population dynamics and the role of PDGF in vivo. *Neuron.* **20:** 869-882.

Cambi,F. and Kamholz,J. (1994) Transcriptional regulation of the rat PLP promoter in primary cultures of oligodendrocytes. *Neurochemical Research.* **19:** 1055-1060.

Cambi,F., Tang,X.M., Cordray,P., Fain,P.R., Keppen,L.D. and Barker,D.F. (1996) Refined genetic mapping and proteolipid protein mutation analysis in X-linked pure hereditary spastic paraplegia. *Neurology.* **46:** 1112-1117.

Campagnoni,A.T. and Hunkeler,M.J. (1980) Synthesis of the Myelin Proteolipid Protein in the Developing Mouse Brain. *Journal of Neurobiology.* **11:** 355-364.

Campagnoni,C.W., Garbay,B., Micevych,P., Pribyl,T., Kampf,K., Handley,V.W. and Campagnoni,A.T. (1992) DM20 mRNA splice product of the myelin proteolipid protein gene is expressed in the murine heart. *Journal of Neuroscience Research.* **33:** 148-155.

Canoll,P.D., Musacchio,J.M., Hardy,R., Reynolds,R., Marchionni,M.A. and Salzer,J.L. (1996) GGF/neuregulin is a neuronal signal that promotes the proliferation and survival and inhibits the differentiation of oligodendrocyte progenitors. *Neuron.* **17:** 229-243.

Casaccia-Bonnefil,P. (2000) Cell death in the oligodendrocyte lineage: A molecular perspective of life/death decisions in development and disease. *Glia.* **29:** 124-135.

Cattanach,B.M. and Beechey,C.V. (1991) Evidence of allelism between rumpshaker and jimpy. *Mouse Genome.* **89:** 271.

Chandross,K.J., Cohen,R.I., Paras,P., Jr., Gravel,M., Braun,P.E. and Hudson,L.D. (1999) Identification and characterization of early glial progenitors using a transgenic selection strategy. *Journal of Neuroscience.* **19:** 759-774.

Chang,A., Nishiyama,A., Peterson,J., Prineas,J. and Trapp,B.D. (2000) NG2-positive oligodendrocyte progenitor cells in adult human brain and multiple sclerosis lesions. *Journal of Neuroscience.* **20:** 6404-6412.

Chen,H., Cabon,F., Sun,P., Parmantier,E., Dupouey,P., Jacque,C. and Zalc,B. (1993) Regional and developmental variations of GFAP and actin mRNA levels in the CNS of jimpy and *shiverer* mutant mice. *Journal of Molecular Neuroscience.* **4:** 89-96.

Chernoff,G.F. (1981) Shiverer: an autosomal recessive mutant mouse with myelin deficiency. *The Journal of Heredity.* **72:** 128.

Cook,J.L., Irias-Donaghey,S. and Deininger,P.L. (1992) Regulation of rodent myelin proteolipid protein gene expression. *Neuroscience Letters.* **137:** 56-60.

Cross,A.K. and Woodroofe,M.N. (2001) Immunoregulation of microglial functional properties. *Microscopy Research and Technique.* **54:** 10-17.

Cuddon,P.A., Lipsitz,D. and Duncan,I.D. (1998) Myelin mosaicism and brain plasticity in heterozygous females of a canine X-linked trait. *Annals of Neurology.* **44:** 771-779.

Del Rio Hortega,P. (1921) Estudios sobre la neuroglia: La glia de escasas radiaciones (oligodendroglia). *Boletin Ral Sociedad Espanola de Histologia Natural.* **21:** 63-92.

Demerens,C., Stankoff,B., Logak,M., Anglade,P., Allinquant,B., Couraud,F., Zalc,B. and Lubetzki,C. (1996) Induction of myelination in the central nervous system by electrical activity. *Proceedings of the National Academy of Sciences USA.* **93:** 9887-9892.

Dentinger,M.P., Barron,K.D. and Csiza,C.K. (1982) Ultrastructure of the central nervous system in a myelin deficient rat. *Journal of Neurocytology.* **11:** 671-691.

Di Bello,I.C., Dawson,M.R.L., Levine,J.M. and Reynolds,R. (1999) Generation of oligodendroglial progenitors in acute inflammatory demyelinating lesions of the rat brain stem is associated with demyelination rather than inflammation. *Journal of Neurocytology.* **28:** 365-381.

Dickinson,P.J., Fanarraga,M.L., Griffiths,I.R., Barrie,J.A., Kyriakides,E. and Montague,P. (1996) Oligodendrocyte progenitors in the embryonic spinal cord express DM-20. *Neuropathology and Applied Neurobiology.* **22:** 188-198.

Dickinson,P.J., Griffiths,I.R., Barrie,J.A., Kyriakides,E., Pollock,G.S., Barnett,S.C., Barrie,J.M. and Pollock,G.F. (1997) Expression of the *dm-20* isoform of the plp gene in olfactory nerve ensheathing cells: evidence from developmental studies. *Journal of Neurocytology.* **26:** 181-189.

Dobretsova,A., Kokorina,N.A. and Wight,P.A. (2000) Functional characterization of a *cis*-acting DNA antisilencer region that modulates myelin proteolipid protein gene expression. *Journal of Neurochemistry.* **75:** 1368-1376.

Dobretsova,A. and Wight,P.A. (1999) Antisilencing: Myelin proteolipid protein gene expression in oligodendrocytes is regulated via derepression. *Journal of Neurochemistry.* **72:** 2227-2237.

Doetsch,F., Caillé,I., Lim,D.A., García-Verdugo,J.M. and Alvarez-Buylla,A. (1999) Subventricular zone astrocytes are neural stem cells in the adult mammalian brain. *Cell.* **97:** 703-716.

Dubois-Dalcq,M. (1987) Characterization of a slowly proliferative cell along the oligodendrocyte differentiation pathway. *EMBO J.* **6:** 2587-2595.

Dubois-Dalcq,M., Behar,T., Hudson,L.D. and Lazzarini,R.A. (1986) Emergence of three myelin proteins in oligodendrocytes cultured without neurons. *Journal of Cell Biology.* **102:** 384-392.

Duncan,I.D. (1990) Dissection of the phenotype and genotype of the X-linked myelin mutants. *Annals of the New York Academy of Sciences.* **605:** 110-121.

Duncan,I.D.(1995) Inherited disorders of myelination of the central nervous system. *Neuroglia.* Kettenmann,H. and Ransom,B.R., editors: Oxford University Press, Oxford, pp. 843-858.

Duncan,I.D., Griffiths,I.R. and Munz,M. (1983) "Shaking pup": a disorder of central myelination in the spaniel dog. III. Quantitative aspects of the glia and myelin in the spinal cord and optic nerve. *Neuropathology and Applied Neurobiology.* **9:** 355-368.

Duncan,I.D., Hammang,J.P., Goda,S. and Quarles,R.H. (1989) Myelination in the jimpy mouse in the absence of proteolipid protein. *Glia.* **2:** 148-154.

Duncan,I.D., Hammang,J.P. and Trapp,B.D. (1987) Abnormal compact myelin in the myelin-deficient rat: absence of proteolipid protein correlates with a defect in the intraperiod line. *Proceedings of the National Academy of Sciences USA.* **84:** 6287-6291.

Dupree,J.L., Coetzee,T., Blight,A., Suzuki,K. and Popko,B. (1998a) Myelin galactolipids are essential for proper node of Ranvier formation in the CNS. *Journal of Neuroscience.* **18:** 1642-1649.

Dupree,J.L., Suzuki,K. and Popko,B. (1998b) Galactolipids in the formation and function of the myelin sheath. *Microscopy Research and Technique.* **41:** 431-440.

Dyer,C.A. (1993) Novel oligodendrocyte transmembrane signaling systems: Investigations utilizing antibodies as ligands. *Molecular Neurobiology.* **7:** 1-22.

Espinosa de los Monteros,A. and Vellis,J. (1990) Oligodendrocyte differentiation: Developmental and functional subpopulations. *NATO ASI Series.* **43:** 33-45.

Fanarraga,M.L., Griffiths,I.R., McCulloch,M.C., Barrie,J.A., Kennedy,P.G.E. and Brophy,P.J. (1992) Rumpshaker: an X-linked mutation causing hypomyelination. Developmental differences in myelination and glial cells between the optic nerve and spinal cord. *Glia.* **5:** 161-170.

Fanarraga,M.L., Griffiths,I.R., Zhao,M. and Duncan,I.D. (1998) Oligodendrocytes are not inherently programmed to myelinate a specific size of axon. *Journal of Comparative Neurology.* **399:** 94-100.

Fanarraga,M.L., Sommer,I., Griffiths,I.R., Montague,P., Groome,N.P., Nave,K.-A., Schneider,A., Brophy,P.J. and Kennedy,P.G.E. (1993) Oligodendrocyte development and differentiation in the rumpshaker mutation. *Glia.* **9:** 146-156.

Fernandez,P.A., Tang,D.G., Cheng,L.L., Prochiantz,A., Mudge,A.W. and Raff,M.C. (2000) Evidence that axon-derived neuregulin promotes oligodendrocyte survival in the developing rat optic nerve. *Neuron.* **28:** 81-90.

Ferra,F.de., Engh,H., Hudson,L., Kamholz,J., Puckett,C., Molineaux,S. and Lazzarini,R.A. (1985) Alternative splicing accounts for the four forms of myelin basic protein. *Cell.* **43:** 721-727.

ffrench-Constant,C., Miller,R.H., Kruse,J., Schachner,M. and Raff,M.C. (1986) Molecular specialization of astrocyte processes at nodes of Ranvier in rat optic nerve. *Journal of Cell Biology.* **102:** 844-852.

Flores,A.I., Mallon,B.S., Matsui,T., Ogawa,W., Rosenzweig,A., Okamoto,T. and Macklin,W.B. (2000) Akt-mediated survival of oligodendrocytes induced by neuregulins. *Journal of Neuroscience.* **20:** 7622-7630.

Frank,M. and Wolburg,H. (1996) Cellular reactions at the lesion site after crushing of the rat optic nerve. *Glia.* **16:** 227-240.

Franzen,R., Tanner,S.L., Dashiell,S.M., Rottkamp,C.A., Hammer,J.A. and Quarles,R.H. (2001) Microtubule-associated protein 1B: a neuronal binding partner for myelin-associated glycoprotein. *Journal of Cell Biology.* **155:** 893-898.

Frisén,J., Johansson,C.B., Lothian,C. and Lendahl,U. (1998) Central nervous system stem cells in the embryo and adult. *Cellular and Molecular Life Sciences.* **54:** 935-945.

Gao,F.B., Durand,B. and Raff,M. (1997) Oligodendrocyte precursor cells count time but not cell divisions before differentiation. *Current Biology.* **7:** 152-155.

Garbern,J., Yool,D.A., Moore,G.J., Wilds,I., Faulk,M., Klugmann,M., Nave,K.-A., Sistermans,E.A., van der Knaap,M.S., Bird,T.D., Shy,M.E., Kamholz,J. and Griffiths,I.R. (2002) Patients lacking the major CNS myelin protein, proteolipid protein 1, develop length-dependent axonal degeneration in the absence of demyelination and inflammation. *Brain.* **125:** 551-561.

Garbern,J.Y., *et al.* (1997) Proteolipid protein is necessary in peripheral as well as central myelin. *Neuron.* **19:** 205-218.

Gardinier,M.V., Macklin,W.B., Diniak,A.J. and Deininger,P.L. (1986) Characterization of myelin proteolipid mRNAs in normal and jimpy mice. *Molecular and Cellular Biology.* **6:** 3755-3762.

Gebicke-Haerter,P.J. (2001) Microglia in neurodegeneration: Molecular aspects. *Microscopy Research and Technique.* **54:** 47-58.

Gencic,S., Abuelo,D., Ambler,M. and Hudson,L.D. (1989) Pelizaeus-Merzbacher disease: An X-linked neurologic disorder of myelin metabolism with a novel mutation in the gene encoding proteolipid protein. *American Journal of Human Genetics.* **45:** 435-442.

Gencic,S. and Hudson,L.D. (1990) Conservative amino acid substitution in the myelin proteolipid protein of jimpy^{msd} mice. *Journal of Neuroscience.* **10:** 117-124.

Ghandour,M.S. and Skoff,R.P. (1988) Expression of galactocerebroside in developing normal and jimpy oligodendrocytes *in situ*. *Journal of Neurocytology.* **17:** 485-498.

Giulian,D.(1995) Microglia and neuronal dysfunction. *Neuroglia.* Kettenmann,H. and Ransom,B.R., editors: Oxford University Press, Oxford, pp. 671-684.

González-Scarano,F. and Baltuch,G. (1999) Microglia as mediators of inflammatory and degenerative diseases. *Annual Review of Neuroscience.* **22:** 219-240.

Gow,A., Friedrich,V.L., Jr. and Lazzarini,R.A. (1994a) Intracellular transport and sorting of the oligodendrocyte transmembrane proteolipid protein. *Journal of Neuroscience Research.* **37:** 563-573.

Gow,A., Friedrich,V.L., Jr. and Lazzarini,R.A. (1994b) Many naturally occurring mutations of myelin proteolipid protein impair its intracellular transport. *Journal of Neuroscience Research.* **37:** 574-583.

Gow,A. and Lazzarini,R.A. (1996) A cellular mechanism governing the severity of Pelizaeus- Merzbacher disease. *Nature Genetics.* **13:** 422-428.

Gow,A., Southwood,C.M. and Lazzarini,R.A. (1998) Disrupted proteolipid protein trafficking results in oligodendrocyte apoptosis in an animal model of Pelizaeus-Merzbacher disease. *Journal of Cell Biology.* **140:** 925-934.

Gow,A., Southwood,C.M., Li,J.S., Pariali,M., Riordan,G.P., Brodie,S.E., Danias,J., Bronstein,J.M., Kachar,B. and Lazzarini,R.A. (1999) CNS myelin and Sertoli cell tight junction strands are absent in *Osp/Claudin-11* null mice. *Cell.* **99:** 649-659.

Griffiths,I.R., Dickinson,P. and Montague,P. (1995) Expression of the proteolipid protein gene in glial cells of the post-natal peripheral nervous system of rodents. *Neuropathology and Applied Neurobiology.* **21:** 97-110.

Griffiths,I.R., Duncan,I.D. and McCulloch,M. (1981) Shaking pup: a disorder of central myelination in the spaniel dog. II. Ultrastructural observations on the white matter of cervical spinal cord. *Journal of Neurocytology.* **10:** 847-858.

Griffiths,I.R., Klugmann,M., Anderson,T.J., Schwab,M.H., Jung,M., Zimmermann,F. andNave,K.-A.(1997) Mouse models of dysmyelinating diseases: axonal degeneration and glial cell death. *Journal of Neurochemistry.* **69:** S257. [Abstract].

Griffiths,I.R., Klugmann,M., Anderson,T.J., Yool,D., Thomson,C.E., Schwab,M.H., Schneider,A., Zimmermann,F., McCulloch,M.C., Nadon,N.L. and Nave,K.-A. (1998) Axonal swellings and degeneration in mice lacking the major proteolipid of myelin. *Science.* **280:** 1610-1613.

Griffiths,I.R., Montague,P. and Dickinson,P. (1995) The proteolipid protein gene. *Neuropathology and Applied Neurobiology.* **21:** 85-96.

Griffiths,I.R., Scott,I., McCulloch,M.C., Barrie,J.A., McPhilemy,K. and Cattanach,B.M. (1990) Rumpshaker mouse: a new X-linked mutation affecting myelination: evidence for a defect in PLP expression. *Journal of Neurocytology.* **19:** 273-283.

Grinspan,J.B., Coulalaglou,M., Beesley,J.S., Carpio,D.F. and Scherer,S.S. (1998) Maturation-dependent apoptotic cell death of oligodendrocytes in myelin-deficient rats. *Journal of Neuroscience Research.* **54:** 623-634.

Hahn,A.F., Chan,Y. and Webster,H.d. (1987) Development of myelinated nerve fibres in the sixth cranial nerve of the rat: A quantitative electron-microscopic study. *Journal of Comparative Neurology.* **260:** 491-500.

Hall,A., Giese,N.A. and Richardson,W.D. (1996) Spinal cord oligodendrocytes develop from ventrally derived progenitor cells that express PDGF alpha-receptors. *Development.* **122:** 4085-4094.

Harding,B., Ellis,D. and Malcolm,S. (1995) A case of Pelizaeus-Merzbacher disease showing increased dosage of the proteolipid protein gene. *Neuropathol.Appl.Neurobiol.* **21:** 111-115.

Hartman,B.K., Agrawal,H.C., Agrawal,D. and Kalmbach,S. (1982) Development and maturation of central nervous system myelin: comparison of immunohistochemical localization of proteolipid protein and basic protein in myelin and oligodendrocytes. *Proceedings of the National Academy of Sciences USA.* **79:** 4217-4220.

He,Y., Appel,S. and Le,W.D. (2001) Minocycline inhibits microglial activation and protects nigral cells after 6-hydroxydopamine injection into mouse striatum. *Brain Research.* **909:** 187-193.

Helynck,G., Luu,B., Nussbaum,J.L., Picken,D., Skalidis,G., Trifilieff,E., Van Dorsselaer,A., Seta,P., Sandeaux,R., Gavach,D., Heitz,F., Simon,D. and Spach,G. (1983) Brain proteolipids, isolation, purification and effects on ionic permeability of membranes. *European Journal of Biochemistry.* **133:** 689-695.

Hildebrand,C., Remahl,S., Persson,H. and Bjartmar,C. (1993) Myelinated nerve fibres in the CNS. *Progress in Neurobiology.* **40:** 319-384.

Hirano,A., Sax,D.S. and Zimmerman,H.M. (1969) The fine structure of the cerebella of jimpy mice and their "normal" litter mates. *Journal of Neuropathology and Experimental Neurology.* **28:** 388-400.

Hirano,M. and Goldman,J.E. (1988) Gliogenesis in rat spinal cord: evidence for origin of astrocytes and oligodendrocytes from radial precursors. *Journal of Neuroscience Research.* **21:** 155-167.

Hirokawa,N. (1993) Axonal transport and the cytoskeleton. *Current Opinion in Neurobiology.* **3:** 724-731.

Hodes,M.E., Blank,C.A., Pratt,V.M., Morales,J., Napier,J. and Dlouhy,S.R. (1997) Nonsense mutation in exon 3 of the proteolipid protein gene (PLP) in a family with

an unusual form of Pelizaeus-Merzbacher disease. *American Journal of Medical Genetics.* **69:** 121-125.

Hodes,M.E., DeMyer,W.E., Pratt,V.M., Edwards,M.K. and Dlouhy,S.R. (1995) Girl with signs of Pelizaeus-Merzbacher disease heterozygous for a mutation in exon 2 of the proteolipid protein gene. *American Journal of Medical Genetics.* **55:** 397-401.

Hodes,M.E. and Dlouhy,S.R. (1996) The proteolipid protein gene: double, double, and trouble. *American Journal of Human Genetics.* **59:** 12-15.

Hodes,M.E., Pratt,V.M. and Dlouhy,S.R. (1993) Genetics of Pelizaeus-Merzbacher disease. *Developmental Neuroscience.* **15:** 383-394.

Hodes,M.E., Woodward,K., Spinner,N.B., Emanuel,B.S., Enrico-Simon,A., Kamholz,J., Stambolian,D., Zackai,E.H., Pratt,V.M., Thomas,I.T., Crandall,K., Dlouhy,S.R. and Malcolm,S. (2000) Additional copies of the proteolipid protein gene causing Pelizaeus-Merzbacher disease arise by separate integration into the X chromosome. *American Journal of Human Genetics.* **67:** 14-22.

Horner,P.J., Power,A.E., Kempermann,G., Kuhn,H.G., Palmer,T.D., Winkler,J., Thal,L.J. and Gage,F.H. (2000) Proliferation and differentiation of progenitor cells throughout the intact adult rat spinal cord. *Journal of Neuroscience.* **20:** 2218-2228.

Hudson,L.D., Berndt,J., Puckett,C., Kozak,C.A. and Lazzarini,R.A. (1987) Aberrant splicing of proteolipid protein and mRNA in the dysmyelinating jimpy mutant mouse. *Proceedings of the National Academy of Sciences USA.* **84:** 1454-1458.

Hudson,L.D., Ko,N. and Kim,J.G.(1996) Control of myelin gene expression. *Glial Cell Development: basic principles and clinical relevance.* Jessen,K.R. and Richardson,W.D., editors: Bios Scientific Publishers, Oxford, pp. 101-121.

Hudson,L.D., Puckett,C., Berndt,J., Chan,J. and Gencic,S. (1989) Mutation of the proteolipid protein gene PLP in a human X chromosome-linked myelin disorder. *Proceedings of the National Academy of Sciences USA.* **86:** 8128-8131.

Inoue,K., Osaka,H., Kawanishi,C., Sugiyama,N., Ishii,M., Sugita,K., Yamada,Y. and Kosaka,K. (1997) Mutations in the proteolipid protein gene in Japanese families with Pelizaeus-Merzbacher disease. *Neurology.* **48:** 283-285.

Inoue,Y., Kagawa,T., Matsumura,Y., Ikenaka,K. and Mikoshiba,K. (1996) Cell death of oligodendrocytes or demyelination induced by overexpression of

proteolipid protein depending on expressed gene dosage. *Neuroscience Research.* **25:** 161-172.

Jackson,K.F. and Duncan,I.D. (1988) Cell kinetics and cell death in the optic nerve of the myelin deficient rat. *Journal of Neurocytology.* **17:** 657-670.

Jacque,C., Rolland,B., Caldani,M., Fages,Ch. and Tardy,M. (1986) Absence of correlations between glutamine-synthetase activity and dysmyelination-associated modifications of astroglia in the brain of murine mutants. *Neurochemical Research.* **11:** 527-533.

Jenkins,S.M. and Bennett,V. (2002) Developing nodes of Ranvier are defined by ankyrin-G clustering and are independent of paranodal axoglial adhesion. *Proceedings of the National Academy of Sciences of the United States of America.* **99:** 2303-2308.

Jones,L.L., Yamaguchi,Y., Stallcup,W.B. and Tuszynski,M.H. (2002) NG2 is a major chondroitin sulfate proteoglycan produced after spinal cord injury and is expressed by macrophages and oligodendrocyte progenitors. *Journal of Neuroscience.* **22:** 2792-2803.

Jung,M., Sommer,I., Schachner,M. and Nave,K.-A. (1996) Monoclonal antibody O10 defines a conformationally sensitive cell-surface epitope of proteolipid protein (PLP): evidence that PLP misfolding underlies dysmyelination in mutant mice. *Journal of Neuroscience.* **16:** 7920-7929.

Kagawa,T., Nakao,J., Yamada,M., Shimizu,K., Hayakawa,T., Mikoshiba,K. and Ikenaka,K. (1994) Fate of jimpy-type oligodendrocytes in jimpy heterozygote. *Journal of Neurochemistry.* **62:** 1887-1893.

Kanfer,J., Parenty,M., Goujet-Zalc,C., Monge,M., Bernier,L., Campagnoni,A.T., Dautigny,A. and Zalc,B. (1989) Developmental expression of myelin proteolipid, basic protein and 2', 3'-cyclic nucleotide 3'-phosphodiesterase transcripts in different rat brain regions. *Journal of Molecular Neuroscience.* **1:** 39-46.

Kaplan,M.R., Cho,M.H., Ullian,E.M., Isom,L.L., Levinson,S.R. and Barres,B.A. (2001) Differential control of clustering of the sodium channels $Na_v1.2$ and $Na_v1.6$ at developing CNS nodes of ranvier. *Neuron.* **30:** 105-119.

Kaplan,M.R., Meyer-Franke,A., Lamber,S., Bennett,V., Duncan,I.D., Levinson,S.R. and Barres,B.A. (1997) Induction of sodium channel clustering by oligodendrocytes. *Nature.* **386:** 724-728.

Karthigasan,J., Evans,E.L., Vouyiouklis,D.A., Inouye,H., Borenshteyn,N., Ramamurthy,G.V. and Kirschner,D.A. (1996) Effects of rumpshaker mutation on CNS myelin composition and structure. *Journal of Neurochemistry.* **66:** 338-345.

Kaufman,R.J. (1999) Stress signaling from the lumen of the endoplasmic reticulum: coordination of gene transcriptional and translational controls. *Genes and Development.* **13:** 1211-1233.

Kaur,C., Hao,A.J., Wu,C.H. and Ling,E.A. (2001) Origin of microglia. *Microscopy Research and Technique.* **54:** 2-9.

Keirstead,H.S., Levine,J.M. and Blakemore,W.F. (1998) Response of the oligodendrocyte progenitor cell population (defined by NG2 labelling) to demyelination of the adult spinal cord. *Glia.* **22:** 161-170.

Kidd,G.J., Hauer,P.E. and Trapp,B.D. (1990) Axons modulate myelin protein messenger RNA levels during central nervous system myelination in vivo. *Journal of Neuroscience Research.* **26:** 409-418.

Kirkpatrick,L.L., Witt,A.S., Payne,H.R., Shine,H.D. and Brady,S.T. (2001) Changes in microtubule stability and density in myelin-deficient *shiverer* mouse CNS axons. *Journal of Neuroscience.* **21:** 2288-2297.

Kitagawa,K., Sinoway,M.P., Yang,C., Gould,R.M. and Colman,D.R. (1993) A proteolipid protein gene family: Expression in sharks and rays and possible evolution from an ancestral gene encoding a pore-forming polypeptide. *Neuron.* **11:** 433-448.

Klugmann,M., Schwab,M.H., Pühlhofer,A., Schneider,A., Zimmermann,F., Griffiths,I.R. and Nave,K.-A. (1997) Assembly of CNS myelin in the absence of proteolipid protein. *Neuron.* **18:** 59-70.

Knapp,P.E. (1996) Proteolipid protein: Is it more than just a structural component of myelin. *Developmental Neuroscience.* **18:** 297-308.

Knapp,P.E., Bartlett,W.P. and Skoff,R.P. (1987) Cultured oligodendrocytes mimic *in vivo* phenotypic characteristics: cell shape, expression of myelin-specific antigens and membrane production. *Developmental Biology.* **120:** 356-365.

Knapp,P.E., Bartlett,W.P., Williams,L.A., Yamada,M., Ikenaka,K. and Skoff,R.P. (1999) Programmed cell death without DNA fragmentation in the jimpy mouse: secreted factors can enhance survival. *Cell Death & Differentiation.* **6:** 136-145.

Knapp,P.E., Booth,C.S. and Skoff,R.P. (1993) The pH of jimpy glia is increased: Intracellular measurements using fluorescent laser cytometry. *Int.J.Dev.Neurosci.* **11:** 215-226.

Knapp,P.E., Dutta,S. and Skoff,R.P. (1990) Differences in levels of neuroglial cell death in jimpy male mice and carrier females. *Developmental Neuroscience.* **12:** 145-152.

Knapp,P.E. and Skoff,R.P. (1993) Jimpy mutation affects astrocytes: Lengthening of the cell cycle in vitro. *Developmental Neuroscience.* **15:** 31-36.

Knapp,P.E., Skoff,R.P. and Redstone,D.W. (1986) Oligodendroglial cell death in jimpy mice: an explanation for the myelin deficit. *Journal of Neuroscience.* **6:** 2813-2822.

Knapp,P.E., Skoff,R.P. and Sprinkle,T.J. (1988) Differential expression of galactocerebroside, myelin basic protein and 2',3'-cyclicnucleotide 3'-phosphohydrolase during development of oligodendrocytes in vitro. *Journal of Neuroscience Research.* **21249:** 249-259.

Koeppen,A.H., Csiza,C.K., Willey,A.M., Ronne,M., Barron,K.D., Dearborn,R.E. and Hurwitz,C.G. (1992) Myelin deficiency in female rats due to a mutation in the PLP gene. *Journal of the Neurological Sciences.* **107:** 78-86.

Kondo,T. and Raff,M. (2000) Oligodendrocyte precursor cells reprogrammed to become multipotential CNS stem cells. *Science.* **289:** 1754-1757.

Konola,J.T., Tyler,B.M., Yamamura,T. and Lees,M.B. (1991) Distribution of proteolipid protein and myelin basic protein in cultured mouse oligodendrocytes: primary vs. secondary cultures. *Journal of Neuroscience Research.* **28:** 49-64.

Kuhlmann-Krieg,S., Sommer,I. and Schachner,M. (1988) Ultrastructural features of cultured oligodendrocytes expressing stage-specific cell-surface antigens. *Developmental Brain Research.* **39:** 269-280.

Kurihara,T., Monoh,K., Takahashi,Y., Goto,K. and Kondo,H. (1992) 2',3'-Cyclic-nucleotide 3'-phosphodiesterase: Complementary DNA and gene cloning for mouse enzyme and *in situ* hybridization of the messenger RNA in mouse brain. *Adv.Second Messenger Phosphoprotein Res.* **25:** 101-110.

Lachapelle,F., Lapie,P., Campagnoni,A.T. and Gumpel,M. (1991) Oligodendrocytes of the jimpy phenotype can be partially restored by environmental factors in vivo. *Journal of Neuroscience Research.* **29:** 235-243.

Laywell,E.D., Rakic,P., Kukekov,V.G., Holland,E.C. and Steindler,D.A. (2000) Identification of a multipotent astrocytic stem cell in the immature and adult mouse brain. *Proceedings of the National Academy of Sciences USA.* **97:** 13883-13888.

Leber,S.M., Breedlove,S.M. and Sanes,J.R. (1990) Linkage, arrangement and death of clonally related motorneurons in chick spinal cord. *Journal of Neuroscience.* **10:** 2451-2462.

Leber,S.M. and Sanes,J.R. (1995) Migratory paths of neurons and glia in the embryonic chick spinal cord. *Journal of Neuroscience.* **15:** 1236-1248.

Lee,J.C., Mayer-Proschel,M. and Rao,M.S. (2000) Gliogenesis in the central nervous system. *Glia.* **30:** 105-121.

Lemke,G. (1988) Unwrapping the genes of myelin. *Neuron.* **1:** 535-543.

Leroy,K., Duyckaerts,C., Bovekamp,L., Müller,O., Anderton,B.H. and Brion,J.P. (2001) Increase of adenomatous polyposis coli immunoreactivity is a marker of reactive astrocytes in Alzheimer's disease and in other pathological conditions. *Acta Neuropathologica.* **102:** 1-10.

Levine,J.M., Reynolds,R. and Fawcett,J.W. (2001) The oligodendrocyte precursor cell in health and disease. *Trends in Neurosciences.* **24:** 39-47.

Levison,S.W., Chuang,C., Abramson,B.J. and Goldman,J.E. (1993) The migrational patterns and developmental fates of glial precursors in the rat subventricular zone are temporally regulated. *Development.* **119:** 611-622.

Levison,S.W. and Goldman,J.E. (1993) Both oligodendrocytes and astrocytes develop from progenitors in the subventricular zone of postnatal rat forebrain. *Neuron.* **10:** 201-212.

Li,C., Tropak,M.B., Gerlai,R., Clapoff,S., Abramow-Newerly,W., Trapp,B., Peterson,A. and Roder,J. (1994) Myelination in the absence of myelin-associated glycoprotein. *Nature.* **369:** 747-750.

Linington,C., Webb,M. and Woodhams,P.L. (1984) A novel myelin-associated glycoprotein defined by a mouse monoclonal antibody. *Journal of Neuroimmunology.* **6:** 387-396.

Lipsitz,D., Goetz,B.D. and Duncan,I.D. (1998) Apoptotic glial cell death and kinetics in the spinal cord of the myelin-deficient rat. *Journal of Neuroscience Research.* **51:** 497-507.

Lord,K.E. and Duncan,I.D. (1987) Early postnatal development of glial cells in the canine cervical spinal cord. *Journal of Comparative Neurology.* **265:** 34-46.

Ludwin,S.K. (1990) Oligodendrocyte survival in Wallerian degeneration. *Acta Neuropathologica (Berlin).* **80:** 184-191.

Macklin,W.B., Campagnoni,A.T., Deininger,P.L. and Gardinier,M.V. (1987) Structure and expression of the mouse proteolipid protein gene. *Journal of Neuroscience Research.* **18:** 383-394.

Macklin,W.B., Gardinier,M.V., Obeso,Z.O., King,K.D. and Wight,P.A. (1991) Mutations in the myelin proteolipid protein gene alter oligodendrocyte gene expression in jimpy and jimpy^{msd} mice. *Journal of Neurochemistry.* **56:** 163-171.

Magaud,J.-P., Sargent,I., Clarke,P.J., Ffrench,M., Rimokh,R. and Mason,D.Y. (1989) Double immunocytochemical labeling of cell and tissue samples with monoclonal anti-bromodeoxyuridine. *Journal of Histochemistry and Cytochemistry.* **37:** 1517-1527.

Mallon,B.S., Shick,H.E., Kidd,G.J. and Macklin,W.B. (2002) Proteolipid promoter activity distinguishes two populations of NG2-positive cells throughout neonatal cortical development. *Journal of Neuroscience.* **22:** 876-885.

Mattei,M.G., Alliel,P.M., Dautigny,A., Passage,E., Pham-Dinh,D., Mattei,J.F. and Jolles,P. (1986) The gene encoding for the major brain proteolipid (PLP) maps on the q-22 band of the human X chromosome. *Human Genetics.* **72:** 352-353.

Mays,K.N. (1999) Assessing the specificity of APC CC-1 labeling *in vivo* and *in vitro*. Internet Communication: http://www.nslc.wustl.edu/Research/prefreshmen/1999/mays.html

McKinnon,R.D., Smith,C., Behar,T., Smith,T. and Dubois-Dalcq,M. (1993) Distinct effects of bFGF and PDGF on oligodendrocyte progenitor cells. *Glia.* **7:** 245-254.

McLean,I.W. and Nakane,P.K. (1974) Periodate-lysine-paraformaldehyde fixative. A new fixation for immunoelectron microscopy. *Journal of Histochemistry and Cytochemistry.* **12:** 1077-1083.

McMorris,F.A. and Dubois-Dalcq,M. (1988) Insulin-like growth factor I promotes cell proliferation and oligodendroglial commitment in rat glial progenitor cells developing in vitro. *Journal of Neuroscience Research.* **21:** 199-209.

McMorris,F.A., Mozell,R.L., Carson,M.J., Shinar,Y., Meyer,R.D. and Marchetti,N. (1993) Regulation of oligodendrocyte development and central nervous system myelination by insulin-like growth factors. *Ann.NY Acad.Sci.* **692:** 321-334.

McPhilemy,K., Griffiths,I.R., Mitchell,L.S. and Kennedy,P.G.E. (1991) Loss of axonal contact causes down-regulation of the PLP gene in oligodendrocytes: evidence from partial lesions of the optic nerve. *Neuropathology and Applied Neurobiology.* **17:** 275-287.

McPhilemy,K., Mitchell,L.S., Griffiths,I.R., Morrison,S., Deary,A.W., Sommer,I. and Kennedy,P.G.E. (1990) Effect of optic nerve transection upon myelin protein gene expression by oligodendrocytes: evidence for axonal influences on gene expression. *Journal of Neurocytology.* **19:** 494-503.

McTigue,D.M., Wei,P. and Stokes,B.T. (2001) Proliferation of NG2-positive cells and altered oligodendrocyte numbers in the contused rat spinal cord. *Journal of Neuroscience.* **21:** 3392-3400.

Meier,C. and Bischoff,A. (1975) Oligodendroglial cell development in jimpy mice and controls. An electron microscopic study in the optic nerve. *Journal of the Neurological Sciences.* **26:** 517-528.

Meyer-Franke,A., Shen,S.L. and Barres,B.A. (1999) Astrocytes induce oligodendrocyte processes to align with and adhere to axons. *Molecular and Cellular Neuroscience.* **14:** 385-397.

Mi,Z.P., Weng,W., Hankin,M.H., Narayanan,V. and Lagenaur,C.F. (1998) Maturational changes in cell surface antigen expression in the mouse retina and optic pathway. *Developmental Brain Research.* **106:** 145-154.

Mikol,D.D., Rongnoparut,P., Allwardt,B.A., Marton,L.S. and Stefansson,K. (1993) The oligodendrocyte-myelin glycoprotein of mouse: Primary structure and gene structure. *Genomics.* **17:** 604-610.

Miller,R.H., ffrench-Constant,C. and Raff,M.C. (1989) The macroglial cells of the rat optic nerve. *Annual Review of Neuroscience.* **12:** 517-534.

Miller,R.H., Payne,J., Milner,L., Zhang,H. and Orentas,D.M. (1997) Spinal cord oligodendrocytes develop from a limited number of migratory, highly proliferative precursors. *Journal of Neuroscience Research.* **50:** 157-168.

Miller,R.H. and Raff,M.C. (1984) Fibrous and protoplasmic astrocytes are biochemically and developmentally distinct. *Journal of Neuroscience.* **4:** 585-592.

Milner,R.J., Lai,C., Nave,K.-A., Lenoir,D., Ogata,J. and Sutcliffe,J.G. (1985) Nucleotide sequence of two mRNAs for rat brain myelin proteolipid protein. *Cell.* **42:** 931-939.

Mitchell,L.S., Gillespie,C.S., McAllister,F., Fanarraga,M.L., Kirkham,D., Kelly,B., Brophy,P.J., Griffiths,I.R., Montague,P. and Kennedy,P.G.E. (1992) Developmental expression of the major myelin protein genes in the CNS of the X-linked hypomyelinating mutant rumpshaker. *Journal of Neuroscience Research.* **33:** 205-217.

Montag,D., Giese,K.P., Bartsch,U., Martini,R., Lang,Y., Blüthmann,H., Karthigasan,J., Kirschner,D.A., Wintergerst,E.S., Nave,K.-A., Zielasek,J., Toyka,K.V., Lipp,H.-P. and Schachner,M. (1994) Mice deficient for the myelin-associated glycoprotein show subtle abnormalities in myelin. *Neuron.* **13:** 229-246.

Montague,P., Dickinson,P.J., McCallion,A.S., Stewart,G.J., Savioz,A., Davies,R.W., Kennedy,P.G.E. and Griffiths,I.R. (1997) Developmental expression of the murine *Mobp* gene. *Journal of Neuroscience Research.* **49:** 133-143.

Montague,P., Griffiths,I.R.(1997) Molecular biology of the glia: components of myelin-PLP and minor myelin proteins. *Molecular Biology of Multiple Sclerosis.* Russell,W.C., editor: J.Wiley & Sons, Chichester, pp. 55-69.

Mori,S. and Leblond,C.P. (1970) Electron microscopic identification of three classes of oligodendrocytes and a preliminary study of their proliferative activity in the corpus callosum of young rats. *Journal of Comparative Neurology.* **139:** 1-30.

Morita,K., Sasaki,H., Fujimoto,K., Furuse,M. and Tsukita,S. (1999) Claudin-11/OSP-based tight junctions of myelin sheaths in brain and Sertoli cells in testis. *Journal of Cell Biology.* **145:** 579-588.

Nadon,N.L. and Duncan,I.D. (1996) Molecular analysis of glial cell development in the canine 'shaking pup' mutant. *Developmental Neuroscience.* **18:** 174-184.

Nadon,N.L., Duncan,I.D. and Hudson,L.D. (1990) A point mutation in the proteolipid protein gene of the "shaking pup" interrupts oligodendrocyte development. *Development.* **110:** 529-537.

Nagara,H. and Suzuki,K. (1982) Radial component of the central myelin in neurological mutant mice. *Laboratory Investigation.* **47:** 51-59.

Nance,M.A., Boyadjiev,S., Pratt,V.M., Taylor,S., Hodes,M.E. and Dlouhy,S.R. (1996) Adult-onset neurodegenerative disorder due to proteolipid protein gene

mutation in the mother of a man with Pelizaeus- Merzbacher disease. *Neurology.* **47:** 1333-1335.

Nave,K.-A., Bloom,F.E. and Milner,R.J. (1987) A single nucleotide difference in the gene for myelin proteolipid protein defines the *jimpy* mutation in mouse. *Journal of Neurochemistry.* **49:** 1873-1877.

Nave,K.-A. and Lemke,G. (1991) Induction of the myelin proteolipid protein (PLP) gene in C6 glioblastoma cells: Functional analysis of the PLP promoter. *Journal of Neuroscience.* **11:** 3060-3069.

Nishiyama,A., Chang,A.S. and Trapp,B.D. (1999) NG2+glial cells: A novel glial cell population in the adult brain. *Journal of Neuropathology and Experimental Neurology.* **58:** 1113-1124.

Nishiyama,A., Lin,X.H., Giese,N., Heldin,C.H. and Stallcup,W.B. (1996) Co-localization of NG2 proteoglycan and PDGF α-receptor on O2A progenitor cells in the developing rat brain. *Journal of Neuroscience Research.* **43:** 299-314.

Nishiyama,A., Yu,M., Drazba,J.A. and Tuohy,V.K. (1997) Normal and reactive NG2+ glial cells are distinct from resting and activated microglia. *Journal of Neuroscience Research.* **48:** 299-312.

Noble,M., Murray,K., Stroobant,P., Waterfield,M.D. and Riddle,P. (1988) Platelet-derived growth factor promotes division and motility and inhibits premature differentiation of the oligodendrocyte/type-2 astrocyte progenitor cell. *Nature.* **333:** 560-562.

Noll,E. and Miller,R.H. (1993) Oligodendrocyte precursors originate at the ventral ventricular zone dorsal to the ventral midline region in the embryonic rat spinal cord. *Development.* **118:** 563-573.

Noll,E. and Miller,R.H. (1994) Regulation of oligodendrocyte differentiation: A role for retinoic acid in the spinal cord. *Development.* **120:** 649-660.

Norton,W.T., Cammer,W.(1984) Isolation and characterization of myelin. *Myelin.* Morell,P., editor: Plenum Press, New York and London, pp. 147-196.

Nussbaum,J.L. and Roussel,G. (1983) Immunocytochemical demonstration of the transport of myelin proteolipids through the Golgi apparatus. *Cell and Tissue Research.* **234:** 547-559.

Oldfield,B.J. and Bray,G.M. (1982) Differentiation of the nodal and internodal axolemma in the optic nerves of neonatal rats. *Journal of Neurocytology.* **11:** 627-640.

Omlin,F.X., Webster,H.d., Palkovitz,C.G. and Cohen,S.R. (1982) Immunocytochemical localization of basic protein in major dense line regions of central and peripheral myelin. *Journal of Cell Biology.* **95:** 242-248.

Osaka,H., Inoue,K., Kawanishi,C., Sugiyama,N., Onishi,H., Suzuki,K., Kimura,S., Miyakawa,N., Hanihara,T., Yamada,Y. andKosaka,K.(1996) Proteolipid protein gene analysis in Pelizaeus-Merzbacher disease. *American Journal of Human Genetics.* **10:** A276. [Abstract].

Parnavelas,J.G. (1999) Glial cell lineages in the rat cerebral cortex. *Experimental Neurology.* **156:** 418-429.

Pearsall,G.B., Nadon,N.L., Wolf,M.K. and Billings-Gagliardi,S. (1997) Jimpy-4J mouse has a missense mutation in exon 2 of the *Plp* gene. *Developmental Neuroscience.* **19:** 337-341.

Pedraza,L., Huang,J.K. and Colman,D.R. (2001) Organizing principles of the axoglial apparatus. *Neuron.* **30:** 335-344.

Perry,V.H.(1996) Microglia in the developing and mature central nervous system. *Glial Cell Development: basic principles and clinical relevance.* Jessen,K.R. and Richardson,W.D., editors: BIOS Scientific Publishing, Oxford, pp. 123-140.

Perry,V.H. and Gordon,S. (1988) Macrophages and microglia in the nervous system. *Trends in Neurosciences.* **11:** 273-277.

Perry,V.H., Hume,D.A. and Gordon,S. (1985) Immunohistochemical localization of macrophages and microglia in the adult and developing mouse brain. *Neuroscience.* **15:** 313-326.

Peters A, Palay SL, Webster Hd. Saunders WB, editor.The fine structure of the nervous system. Philadelphia: W.B.Saunders; 1976;

Pfeiffer,S.E., Warrington,A.E. and Bansal,R. (1993) The oligodendrocyte and its many cellular processes. *Trends in Cell Biology.* **3:** 191-197.

Pham-Dinh,D., Popot,J.-L., Boespflug-Tanguy,O., Landrieu,P., Deleuze,J.-F., Boué,J., Jollès,P. and Dautigny,A. (1991) Pelizaeus-Merzbacher disease: A valine

to phenylalanine point mutation in a putative extracellular loop of myelin proteolipid. *Proceedings of the National Academy of Sciences USA.* **88:** 7562-7566.

Phillips,D.E. (1973) An electron microscopic study of macroglia and microglia in the lateral funiculus of the developing spinal cord in the fetal monkey. *Zeitschrift Zellforschung Microskopische Anatomie.* **140:** 145-167.

Popko,B. (2000) Myelin galactolipids: Mediators of axon-glial interactions? *Glia.* **29:** 149-153.

Prayoonwiwat,N. and Rodriguez,M. (1993) The potential for oligodendrocyte proliferation during demyelinating disease. *J.Neuropathol.Exp.Neurol.* **52:** 55-63.

Pringle,N.P., Nadon,N.L., Rhode,D.M., Richardson,W.D. and Duncan,I.D. (1997) Normal temporal and spatial distribution of oligodendrocyte progenitors in the myelin-deficient (md) rat. *Journal of Neuroscience Research.* **47:** 264-270.

Pringle,N.P. and Richardson,W.D. (1993) A singularity of PDGF alpha-receptor expression in the dorsoventral axis of the neural tube may define the origin of the oligodendrocyte lineage. *Development.* **117:** 525-533.

Privat,A., Valat,J., Lachapelle,F., Baumann,N. and Fulcrand,J. (1982) Radioautographic evidence for the protracted proliferation of glial cells in the central nervous system of jimpy mice. *Developmental Brain Research.* **2:** 411-416.

Qiu,J., Cai,D.M. and Filbin,M.T. (2000) Glial inhibition of nerve regeneration in the mature mammalian CNS. *Glia.* **29:** 166-174.

Quarles,R.H., Colman,D.R., Salzer,J.L. and Trapp,B.D.(1992) Myelin-associated glycoprotein:structure-function relationships and involvement in neurological diesases. *Myelin: biology and chemistry.* Martenson,R.E., editor: CRC Press Inc., Boca Ranton, pp. 413-448.

Raff,M.C., Miller,R.H. and Noble,M. (1983) A glial progenitor that develops *in vitro* into an astrocyte or an oligodendrocyte depending on culture medium. *Nature.* **303:** 390-396.

Raff,M.C., Mirsky,R., Fields,K.L., Lisak,R.P., Dorfman,S.H., Silberberg,D.H., Gregson,N.A., Liebowitz,S. and Kennedy,M.C. (1978) Galactocerebroside is a specific marker for oligodendrocytes in culture. *Nature.* **274:** 813-816.

Ransom,B.R., Yamate,C.L., Black,J.A. and Waxman,S.G. (1985) Rat optic nerve: disruption of gliogenesis with 5-azacytidine during early postnatal development. *Brain Research.* **337:** 41-49.

Rao,R.V., Hermel,E., Castro-Obregon,S., Del Rio,G., Ellerby,L.M., Ellerby,H.M. and Bredesen,D.E. (2001) Coupling endoplasmic reticulum stress to the cell death program - Mechanism of caspase activation. *Journal of Biological Chemistry.* **276:** 33869-33874.

Rasband,M.N., Peles,E., Trimmer,J.S., Levinson,S.R., Lux,S.E. and Shrager,P. (1999a) Dependence of nodal sodium channel clustering on paranodal axoglial contact in the developing CNS. *Journal of Neuroscience.* **19:** 7516-7528.

Rasband,M.N. and Trimmer,J.S. (2001) Developmental clustering of ion channels at and near the node of Ranvier. *Developmental Biology.* **236:** 5-16.

Rasband,M.N., Trimmer,J.S., Peles,E., Levinson,S.R. and Shrager,P. (1999b) K^+ channel distribution and clustering in developing and hypomyelinated axons of the optic nerve. *Journal of Neurocytology.* **28:** 319-331.

Raskind,W.H., Williams,C.A., Hudson,L.D. and Bird,T.D. (1991) Complete deletion of the proteolipid protein gene (PLP) in a family with X-linked Pelizaeus-Merzbacher disease. *American Journal of Human Genetics.* **49:** 1355-1360.

Readhead,C., Popko,B., Takahashi,N., Shine,H.D., Saavedra,R.A., Sidman,R.L. and Hood,L. (1987) Expression of a myelin basic protein gene in transgenic *shiverer* mice: correction of the dysmyelinating phenotype. *Cell.* **48:** 703-712.

Readhead,C., Schneider,A., Griffiths,I.R. and Nave,K.-A. (1994) Premature arrest of myelin formation in transgenic mice with increased proteolipid protein gene dosage. *Neuron.* **12:** 583-595.

Remahl,S. and Hildebrand,C. (1990) Relation between axons and oligodendroglial cells during initial myelination. I. The glial unit. *Journal of Neurocytology.* **19:** 313-328.

Reynolds,R. and Hardy,R. (1997) Oligodendroglial progenitors labeled with the O4 antibody persist in the adult rat cerebral cortex in vivo. *Journal of Neuroscience Research.* **47:** 455-470.

Richardson,W.D., Pringle,N., Mosley,M.J., Westermark,B. and Dubois-Dalcq,M. (1988) A role for platelet-derived growth factor in normal gliogenesis in the central nervous system. *Cell.* **53:** 309-319.

Richardson,W.D., Pringle,N.P., Yu,W.P. and Hall,A.C. (1997) Origins of spinal cord oligodendrocytes: Possible developmental and evolutionary relationships with motor neurons. *Developmental Neuroscience.* **19:** 58-68.

Rodríguez-Peña,A. (1999) Oligodendrocyte development and thyroid hormone. *Journal of Neurobiology.* **40:** 497-512.

Rosen,C.L., Bunge,R.P., Ard,M.D. and Wood,P.M. (1989) Type 1 astrocytes inhibit myelination by adult rat oligodendrocytes *in vitro*. *Journal of Neuroscience.* **9:** 3371-3379.

Rosenbluth,J., Stoffel,W. and Schiff,R. (1996) Myelin structure in proteolipid protein (PLP)-null mouse spinal cord. *Journal of Comparative Neurology.* **371:** 336-344.

Roth,H.J., Kronquist,K., Pretorius,P.J., Crandall,B.F. and Campagnoni,A.T. (1986) Isolation and characterization of a cDNA coding for a novel human 17.3K myelin basic protein (MBP) varient. *Journal of Neuroscience Research.* **16:** 227-238.

Roussel,G., Neskovic,N.M., Trifilieff,E., Artault,J.-C. and Nussbaum,J.L. (1987) Arrest of proteolipid transport through the Golgi apparatus in jimpy brain. *Journal of Neurocytology.* **16:** 195-204.

Saugier-Veber,P., Munnich,A., Bonneau,D., Rozet,J.-M., Le Merrer,M., Gil,R. and Boespflug-Tanguy,O. (1994) X-linked spastic paraplegia and Pelizaeus-Merzbacher disease are allelic disorders at the proteolipid protein locus. *Nature Genetics.* **6:** 257-262.

Sánchez,I., Hassinger,L., Paskevich,P.A., Shine,H.D. and Nixon,R.A. (1996) Oligodendroglia regulate the regional expansion of axon caliber and local accumulation of neurofilaments during development independently of myelin formation. *Journal of Neuroscience.* **16:** 5095-5105.

Sánchez,I., Hassinger,L., Sihag,R.K., Cleveland,D.W., Mohan,P. and Nixon,R.A. (2000) Local control of neurofilament accumulation during radial growth of myelinating axons in vivo: Selective role of site-specific phosphorylation. *Journal of Cell Biology.* **151:** 1013-1024.

Scarlato,M., Beesley,J. and Pleasure,D. (2000) Analysis of oligodendroglial differentiation using cDNA arrays. *Journal of Neuroscience Research.* **59:** 430-435.

Scherer,S.S., Braun,P.E., Grinspan,J., Collarini,E., Wang,D. and Kamholz,J. (1994) Differential regulation of the 2',3'-cyclic nucleotide 3'- phosphodiesterase gene during oligodendrocyte development. *Neuron.* **12:** 1363-1375.

Scherer,S.S., Vogelbacker,H.H. and Kamholz,J. (1992) Axons modulate the expression of proteolipid protein in the CNS. *Journal of Neuroscience Research.* **32:** 138-148.

Schneider,A., Montague,P., Griffiths,I.R., Fanarraga,M.L., Kennedy,P.G.E., Brophy,P.J. and Nave,K.-A. (1992) Uncoupling of hypomyelination and glial cell death by a mutation in the proteolipid protein gene. *Nature.* **358:** 758-761.

Schwab,M.E. and Schnell,L. (1989) Region-specific appearance of myelin constituents in the developing rat spinal cord. *Journal of Neurocytology.* **18:** 161-169.

Seitelberger,F. (1995) Neuropathology and genetics of Pelizaeus-Merzbacher disease. *Brain Pathology.* **5:** 267-273.

Seitelberger,F., Urbanits,S. and Nave,K.-A.(1996) Pelizaeus-Merzbacher disease. *Neurodystrophies and Neurolipidoses.* Moser,H.W., editor: Elsevier Science, Amsterdam, pp. 559-579.

Sidman,R.L., Dickie,M.M. and Appel,S.H. (1964) Mutant mice (quaking and jimpy) with deficient myelination in the central nervous system. *Science.* **144:** 309-311.

Sinoway,M.P., Kitagawa,K., Timsit,S., Hashim,G.A. and Colman,D.R. (1994) Proteolipid protein interactions in transfectants: Implications for myelin assembly. *Journal of Neuroscience Research.* **37:** 551-562.

Sistermans,E.A., De Coo,R.F., De Wijs,I.J. and Van Oost,B.A. (1998) Duplication of the proteolipid protein gene is the major cause of Pelizaeus-Merzbacher disease. *Neurology.* **50:** 1749-1754.

Sistermans,E.A., De Wijs,I.J., De Coo,I.F.M. andVan Oost,B.A.(1996) Duplication of the proteolipid protein gene (PLP) is a frequent cause of Pelizaeus Merzbacher disease. *American Journal of Human Genetics.* **10:** A10. [Abstract].

Skoff,R.P. (1976) Myelin deficit in the jimpy mouse may be due to cellular abnormalities in astroglia. *Nature.* **264:** 560-562.

Skoff,R.P. (1982) Increased proliferation of oligodendrocytes in the hypomyelinated mouse mutant-jimpy. *Brain Research.* **248:** 19-31.

Skoff,R.P. (1995) Programmed cell death in the dysmyelinating mutants. *Brain Pathology.* **5:** 283-288.

Skoff,R.P. and Ghandour,M.S. (1995) Oligodendrocytes in female carriers of the jimpy gene make more myelin than normal oligodendrocytes. *Journal of Comparative Neurology.* **355:** 124-133.

Skoff,R.P. and Knapp,P.E. (1990) Expression of the jimpy phenotype in relation to proteolipid protein appearance. *Annals of the New York Academy of Sciences.* **605:** 122-134.

Small,R.K., Riddle,P. and Noble,M. (1987) Evidence for migration of oligodendrocyte-type-2 astrocyte progenitor cells into the developing rat optic nerve. *Nature.* **328:** 155-157.

Sommer,I. and Schachner,M. (1981) Monoclonal antibodies (O1-O4) to oligodendrocyte cell surfaces: an immunocytological study in the central nervous system. *Developmental Biology.* **83:** 311-327.

Sorg,B.A., Agrawal,D., Agrawal,H.C. and Campagnoni,A.T. (1986) Expression of myelin proteolipid protein and basic protein in normal and dysmyelinating mutant mice. *Journal of Neurochemistry.* **46:** 379-387.

Sorg,B.A., Smith,M.M. and Campagnoni,A.T. (1987) Developmental expression of the myelin proteolipid protein and basic protein mRNA in normal and dysmyelinating mutant mice. *Journal of Neurochemistry.* **49:** 1146-1154.

Southwood,C. and Gow,A. (2001) Molecular pathways of oligodendrocyte apoptosis revealed by mutations in the proteolipid protein gene. *Microscopy Research and Technique.* **52:** 700-708.

Spassky,N., Goujet-Zalc,C., Parmantier,E., Olivier,C., Martinez,S., Ivanova,A., Ikenaka,K., Macklin,W., Cerruti,I., Zalc,B. and Thomas,J.L. (1998) Multiple restricted origin of oligodendrocytes. *Journal of Neuroscience.* **18:** 8331-8343.

Spassky,N., Olivier,C., Perez-Villegas,E., Goujet-Zalc,C., Martinez,S., Thomas,J.L. and Zalc,B. (2000) Single or multiple oligodendroglial lineages: A controversy. *Glia.* **29:** 143-148.

Stallcup,W.B. and Beasley,L. (1987) Bipotential glial precursor cells of the optic nerve express the NG2 proteoglycan. *Journal of Neuroscience.* **7:** 2737-2744.

Sternberger,N.H., Itoyama,Y., Kies,M.W. and Webster,H.d. (1978) Immunocytochemical method to identify basic protein in myelin-forming oligodendrocytes of newborn rat C.N.S. *Journal of Neurocytology.* **7:** 251-263.

Stoll,G. and Jander,S. (1999) The role of microglia and macrophages in the pathophysiology of the CNS. *Progress in Neurobiology.* **58:** 233-247.

Strenge,K., Schauer,R., Bovin,N., Hasegawa,A., Ishida,H., Kiso,M. and Kelm,S. (1998) Glycan specificity of myelin-associated glycoprotein and sialoadhesin deduced from interactions with synthetic oligosaccharides. *European Journal of Biochemistry.* **258:** 677-685.

Sturrock,R.R.(1983) Problems of glial identification and quantification in the ageing central nervous system. *Brain Ageing: Neuropathology and Neuropharmacology.* Cervos-Navarro,J. and Sarkander,H.-I., editors: Raven Press, New York, pp. 179-209.

Szuchet,S., Watanabe,K. and Yamaguchi,Y. (2000) Differentiation/regeneration of oligodendrocytes entails the assembly of a cell-associated matrix. *International Journal of Developmental Neuroscience.* **18:** 705-720.

Tait,S., Gunn-Moore,F., Collinson,J.M., Huang,J., Lubetzki,C., Pedraza,L., Sherman,D.L., Colman,D.R. and Brophy,P.J. (2000) An oligodendrocyte cell adhesion molecule at the site of assembly of the paranodal axo-glial junction. *Journal of Cell Biology.* **150:** 657-666.

Tang,S., Shen,Y.J., DeBellard,M.E., Mukhopadhyay,G., Salzer,J.L., Crocker,P.R. and Filbin,M.T. (1997) Myelin-associated glycoprotein interacts with neurons via a sialic acid binding site at ARG118 and a distinct neurite inhibition site. *Journal of Cell Biology.* **138:** 1355-1366.

Taraszewska,A. (1988) Ultrastructure of axons in disturbed CNS myelination in *pt* rabbit. *Neuropat.Pol.* **26:** 387-402.

Taraszewska,A. and Zelman,I.B. (1987) Electron microscopic study of glia in pt rabbit during myelination. *Neuropat.Pol.* **25:** 352-368.

Thomson,C.E., Anderson,T.J., McCulloch,M.C., Dickinson,P.J., Vouyiouklis,D.A. and Griffiths,I.R. (1999) The early phenotype associated with the jimpy mutation of the proteolipid protein gene. *Journal of Neurocytology.* **28:** 207-221.

Tikka,T., Fiebich,B.L., Goldsteins,G., Keinänen,R. and Koistinaho,J. (2001) Minocycline, a tetracycline derivative, is neuroprotective against excitotoxicity by inhibiting activation and proliferation of microglia. *Journal of Neuroscience.* **21:** 2580-2588.

Tikka,T.M. and Koistinaho,J.E. (2001) Minocycline provides neuroprotection against *N*-methyl-D-aspartate neurotoxicity by inhibiting microglia. *Journal of Immunology.* **166:** 7527-7533.

Timsit,S., Martinez,S., Allinquant,B., Peyron,F., Puelles,L. and Zalc,B. (1995) Oligodendrocytes originate in a restricted zone of the embryonic ventral neural tube defined by DM-20 mRNA expression. *Journal of Neuroscience.* **15:** 1012-1024.

Timsit,S.G., Bally-Cuif,L., Colman,D.R. and Zalc,B. (1992) DM-20 mRNA is expressed during the embryonic development of the nervous system of the mouse. *Journal of Neurochemistry.* **58:** 1172-1175.

Tosic,M., Dolivo,M., Domanska-Janik,K. and Matthieu,J.-M. (1994) Paralytic tremor (*pt*): A new allele of the proteolipid protein gene in rabbits. *Journal of Neurochemistry.* **63:** 2210-2216.

Tosic,M., Gow,A., Dolivo,M., Domanska-Janik,K., Lazzarini,R.A. and Matthieu,J.M. (1996) Proteolipid/DM-20 proteins bearing the paralytic tremor mutation in peripheral nerves and transfected Cos-7 cells. *Neurochemical Research.* **21:** 423-430.

Tosic,M., Matthey,B., Gow,A., Lazzarini,R.A. and Matthieu,J.M. (1997) Intracellular transport of the DM-20 bearing shaking pup (*shp*) mutation and its possible phenotypic consequences. *Journal of Neuroscience Research.* **50:** 844-852.

Trapp,B.D.(1990) Distribution of myelin protein gene products in actively-myelinating oligodendrocytes. *Cellular and Molecular Biology of Myelination.* Jeserich,G., Althaus,H.A. and Waehneldt,T.V., editors: Springer-Verlag, Berlin, pp. 59-79.

Trapp,B.D., Bernier,L., Andrews,B. and Colman,D.R. (1988) Cellular and subcellular distribution of 2',3'-cyclic nucleotide 3'-phosphodiesterase and its mRNA in the rat central nervous system. *Journal of Neurochemistry.* **51:** 859-868.

Trapp,B.D. and Kidd,G.J. (2000) Axo-glial septate junctions: The maestro of nodal formation and myelination? *Journal of Cell Biology.* **150:** F97-F99.

Trapp,B.D. and Quarles,R.H. (1984) Immunocytochemical localization of the myelin-associated glycoprotein. Fact or artifact? *Journal of Neuroimmunology.* **6:** 231-249.

Trofatter,J.A., Dlouhy,S.R., DeMyer,W., Conneally,P.J. and Hodes,M.E. (1989) Pelizaeus-Merzbacher disease: tight linkage to proteolipid protein gene exon variant. *Proceedings of the National Academy of Sciences USA.* **86:** 9427-9430.

Tsuneishi,S., Takada,S., Motoike,T., Ohashi,T., Sano,K. and Nakamura,H. (1991) Effects of dexamethasone on the expression of myelin basic protein, proteolipid protein, and glial fibrillary acidic protein genes in developing rat brain. *Developmental Brain Research.* **61:** 117-123.

Vela,J.M., Dalmau,I., Acarín,L., González,B. and Castellano,B. (1995) Microglial cell reaction in the gray and white matter in spinal cords from jimpy mice. An enzyme histochemical study at the light and electron microscope level. *Brain Research.* **694:** 287-298.

Vela,J.M., Dalmau,I., González,B. and Castellano,B. (1996) The microglial reaction in spinal cords of jimpy mice is related to apoptotic oligodendrocytes. *Brain Research.* **712:** 134-142.

Vela,J.M., González,B. and Castellano,B. (1998) Understanding glial abnormalities associated with myelin deficiency in the jimpy mutant mouse. *Brain Research Reviews.* **26:** 29-42.

Verity,A.N. and Campagnoni,A.T. (1988) Regional expression of myelin protein genes in the developing mouse brain: in situ hybridization studies. *Journal of Neuroscience Research.* **21:** 238-248.

Vermeesch,M.K., Knapp,P.E., Skoff,R.P., Studzinski,D.M. and Benjamins,J.A. (1990) Death of individual oligodendrocytes in *jimpy* precedes expression of proteolipid protein. *Developmental Neuroscience.* **12:** 303-315.

Wang,H., Allen,M.L., Grigg,J.J., Noebels,J.L. and Tempel,B.L. (1995) Hypomyelination alters K^+ channel expression in mouse mutants *shiverer* and *Trembler. Neuron.* **15:** 1337-1347.

Wang,S.L., Sdrulla,A.D., DiSibio,G., Bush,G., Nofziger,D., Hicks,C., Weinmaster,G. and Barres,B.A. (1998) Notch receptor activation inhibits oligodendrocyte differentiation. *Neuron.* **21:** 63-75.

Wegner,M. (2000) Transcriptional control in myelinating glia: The basic recipe. *Glia.* **29:** 118-123.

Wegner,M. (2001) Expression of transcription factors during oligodendroglial development. *Microscopy Research and Technique.* **52:** 746-752.

Weimbs,T. and Stoffel,W. (1992) Proteolipid protein (PLP) of CNS myelin: Positions of free, disulfide-bonded, and fatty acid thioester-linked cysteine residues and implications for the membrane topology of PLP. *Biochemistry.* **31:** 12289-12296.

Wight,P.A. and Dobretsova,A. (1997) The first intron of the myelin proteolipid protein gene confers cell type-specific expression by a transcriptional repression mechanism in non-expressing cell types. *Gene.* **201:** 111-117.

Willard,H.F.(1995) The sex chromosomes and X inactivation. *The metabolic and inherited basis of inherited disease.* Scriver,C.R., Beaudet,A.L. and Sly,W.S., editors: McGraw-Hill, New York, pp. 719-737.

Willard,H.F. and Riordan,J.R. (1985) Assignment of the gene for myelin proteolipid protein to the X chromosome: implications for X-linked myelin disorders. *Science.* **230:** 940-942.

Williams,M.A.(1977) Stereological techniques. *Practical Methods in Electron Microscopy. Vol. 6. Quantitative Methods in Biology.* Glauert,A.M., editor: North Holland, Amsterdam, pp. 5-84.

Williams,W.C., II and Gard,A.L. (1997) In vitro death of jimpy oligodendrocytes: Correlation with onset of DM-20/PLP expression and resistance to oligodendrogliotrophic factors. *Journal of Neuroscience Research.* **50:** 177-189.

Witt,A. and Brady,S.T. (2000) Unwrapping new layers of complexity in axon/glial relationships. *Glia.* **29:** 112-117.

Wolf,M.K., Nunnari,J.N. and Billings-Gagliardi,S. (1999) Quaking*shiverer double-mutant mice survive for at least 100 days with no CNS myelin. *Developmental Neuroscience.* **21:** 483-490.

Wolswijk,G. and Noble,M. (1989) Identification of an adult-specific glial progenitor cell. *Development.* **105:** 387-400.

Wolswijk,G., Riddle,P.N. and Noble,M. (1990) Coexistence of perinatal and adult forms of a glial progenitor cell during development of the rat optic nerve. *Development.* **109:** 691-698.

Woodruff,R.H., Tekki-Kessaris,N., Stiles,C.D., Rowitch,D.H. and Richardson,W.D. (2001) Oligodendrocyte development in the spinal cord and telencephalon: common themes and new perspectives. *International Journal of Developmental Neuroscience.* **19:** 379-385.

Woodward,K., Kirtland,K., Dlouhy,S., Raskind,W., Bird,T., Malcolm,S. and Abeliovich,D. (2000) X inactivation phenotype in carriers of Pelizaeus-Merzbacher disease: skewed in carriers of a duplication and random in carriers of point mutations. *European Journal of Human Genetics.* **8:** 449-454.

Woodward,K., Palmer,R., Rao,K. and Malcolm,S. (1999) Prenatal diagnosis by FISH in a family with Pelizaeus-Merzbacher disease caused by duplication of the PLP gene. *Prenatal Diagnosis.* **19:** 266-268.

Wren,D., Wolswijk,G. and Noble,M. (1992) In vitro analysis of the origin and maintenance of O-2A^{adult} progenitor cells. *Journal of Cell Biology.* **116:** 167-176.

Wu,Q., Miller,R.H., Ransohoff,R.M., Robinson,S., Bu,J. and Nishiyama,A. (2000) Elevated levels of the chemokine GRO-1 correlate with elevated oligodendrocyte progenitor proliferation in the *jimpy* mutant. *Journal of Neuroscience.* **20:** 2609-2617.

Xu,X.H., Cai,J., Fu,H., Wu,R., Qi,Y.C., Modderman,G., Liu,R.G. and Qiu,M.S. (2000) Selective expression of *Nkx-2.2* transcription factor in chicken oligodendrocyte progenitors and implications for the embryonic origin of oligodendrocytes. *Molecular and Cellular Neuroscience.* **16:** 740-753.

Yamada,M., Ivanova,A., Yamaguchi,Y., Lees,M.B. and Ikenaka,K. (1999) Proteolipid protein gene product can be secreted and exhibit biological activity during early development. *Journal of Neuroscience.* **19:** 2143-2151.

Yamada,M., Jung,M., Tetsushi,K., Ivanova,A., Nave,K.A. and Ikenaka,K. (2001) Mutant PLP/DM20 cannot be processed to secrete PLP-related oligodendrocyte differentiation/survival factor. *Neurochemical Research.* **26:** 639-645.

Yamamoto,Y., Mizuno,R., Nishimura,T., Ogawa,Y., Yoshikawa,H., Fujimura,H., Adachi,E., Kishimoto,T., Yanagihara,T. and Sakoda,S. (1994) Cloning and expression of myelin-associated oligodendrocytic basic protein. A novel basic

protein constituting the central nervous system myelin. *Journal of Biological Chemistry.* **269:** 31725-31730.

Yan,Y., Lagenaur,C. and Narayanan,V. (1993) Molecular cloning of M6: Identification of a PLP/DM20 gene family. *Neuron.* **11:** 423-431.

Yan,Y.M., Narayanan,V. and Lagenaur,C. (1996) Expression of members of the proteolipid protein gene family in the developing murine central nervous system. *Journal of Comparative Neurology.* **370:** 465-478.

Yanagisawa,K. and Quarles,R.H. (1986) Jimpy mice: quantitation of myelin-associated glycoprotein and other proteins. *Journal of Neurochemistry.* **47:** 322-325.

Yasuda,T., Grinspan,J., Stern,J., Franceschini,B., Bannerman,P. and Pleasure,D. (1995) Apoptosis occurs in the oligodendroglial lineage, and is prevented by basic fibroblast growth factor. *Journal of Neuroscience Research.* **40:** 306-317.

Yeh,H.-J., Ruit,K.G., Wang,Y.-X., Parks,W.C., Snider,W.D. and Deuel,T.F. (1991) PDGF A-chain gene is expressed by mammalian neurons during development and in maturity. *Cell.* **64:** 209-216.

Yool,D., Klugmann,M., Barrie,J.A., McCulloch,M.C., Nave,K.-A. and Griffiths,I.R. (2002) Observations on the structure of myelin lacking the major proteolipid protein. *Neuropathology and Applied Neurobiology.* **28:** 75-78.

Yool,D.A., Klugmann,M., McLaughlin,M., Vouyiouklis,D.A., Dimou,L., Barrie,J.A., McCulloch,M.C., Nave,K.-A. and Griffiths,I.R. (2001) Myelin proteolipid proteins promote the interaction of oligodendrocytes and axons. *Journal of Neuroscience Research.* **63:** 151-164.

Yoshida,M. (1997) Oligodendrocyte maturation in *Xenopus laevis*. *Journal of Neuroscience Research.* **50:** 169-176.

Yrjänheikki,J., Tikka,T., Keinänen,R., Goldsteins,G., Chan,P.H. and Koistinaho,J. (1999) A tetracycline derivative, minocycline, reduces inflammation and protects against focal cerebral ischemia with a wide therapeutic window. *Proceedings of the National Academy of Sciences USA.* **96:** 13496-13500.

Yu,W.-P., Collarini,E.J., Pringle,N.P. and Richardson,W.D. (1994) Embryonic expression of myelin genes: Evidence for a focal source of oligodendrocyte precursors in the ventricular zone of the neural tube. *Neuron.* **12:** 1353-1362.

Zahler,A.M. and Roth,M.B. (1995) Distinct functions of SR proteins in recruitment of U1 small nuclear ribonucleoprotein to alternative 5' splice sites. *Proceedings of the National Academy of Sciences USA.* **92:** 2642-2646.

Zalc,B. and Fields,R.D. (2000) Do action potentials regulate myelination? *The Neuroscientist.* **6:** 5-12.

Zhou,Q., Wang,S.L. and Anderson,D.J. (2000) Identification of a novel family of oligodendrocyte lineage-specific basic helix-loop-helix transcription factors. *Neuron.* **25:** 331-343.

Zhu,W., Wiggins,R.C. and Konat,G.W. (1994) Glucocorticoid-induced upregulation of proteolipid protein and myelin-associated glycoprotein genes in C6 cells. *Journal of Neuroscience Research.* **37:** 208-212.